



# "BIOPOLYMERS IN ELASTOMERS: LIGNINS AS BIOFILLER FOR TYRE COMPOUND"



**Paola Frigerio**

Ph.D. School in Material Science-Corimav Pirelli, XXVI cycle  
Thesis presented for the degree of Doctor Europaeus

Supervisors: Prof. M. Orlandi, Dr. L.Castellani  
Dean of the Doctorate: Prof. Gian Paolo Brivio

January 2014

---

<b>LIST OF ABBREVIATIONS .....</b>	<b>1</b>
<b>THE PHD PROJECT .....</b>	<b>4</b>
<b>1 INTRODUCTION .....</b>	<b>7</b>
<b>1.1 Biorefinery .....</b>	<b>7</b>
<b>1.2 Lignocellulosic biomass .....</b>	<b>8</b>
<b>1.3 Lignin .....</b>	<b>10</b>
<i>1.3.1 Lignin types.....</i>	<i>14</i>
1.3.1.1 Botanical origin.....	14
1.3.1.2 Isolation process.....	15
1.3.1.2.1 Lignin from sulfite process.....	15
1.3.1.2.1.1 Kraft process.....	15
1.3.1.2.1.2 Sulfite process.....	16
1.3.1.2.2 Lignin from Sulfur free process.....	16
1.3.1.2.2.1 Soda pulping process.....	17
1.3.1.2.2.2 Organosolv pulping.....	17
1.3.1.2.2.3 Steam explosion process.....	17
<i>1.3.2 Applications of lignin .....</i>	<i>18</i>
1.3.2.1 Rubber-lignin blends .....	19
<b>1.4 Rubber compounds .....</b>	<b>21</b>
<i>1.4.1 Polymer.....</i>	<i>21</i>
1.4.1.1 Natural rubber .....	21
1.4.1.2 Synthetic rubber .....	22
1.4.1.2.1 SBR.....	22
<i>1.4.2 Filler.....</i>	<i>23</i>
1.4.2.1 Carbon black .....	23
1.4.2.2 Silica.....	25
<i>1.4.3 Stabilizer system (Antiozonants) .....</i>	<i>26</i>
<i>1.4.4 Vulcanizing agent.....</i>	<i>27</i>
1.4.4.1 Accelerators .....	27
1.4.4.2 Activators.....	27
<b>1.5 Mixing stage.....</b>	<b>28</b>
<i>1.5.1 Internal mixer.....</i>	<i>28</i>
<i>1.5.2 Two-roll mill.....</i>	<i>29</i>

---

<b>1.6 Vulcanization process.....</b>	<b>29</b>
<b>1.7 The reinforcement of rubber .....</b>	<b>33</b>
<b>2 EXPERIMENTAL SECTION.....</b>	<b>39</b>
<b>2.1 Materials .....</b>	<b>39</b>
<b>2.2 Ionic liquid pretreatment .....</b>	<b>39</b>
2.2.1 Rice husk preparation .....	39
2.2.2 Dissolution of rice husk into ionic liquid and regeneration techniques .....	40
2.2.2.1 Acidic precipitation from ionic liquid .....	40
2.2.2.2 Alkaline precipitation from ionic liquid .....	40
2.2.2.3 Multistep alkaline/acidic precipitation from ionic liquid.....	41
2.2.3 Recovery of soluble rice husk fractions.....	41
2.2.4 Enzymatic hydrolysis.....	42
2.2.5 UV determination of solubilized lignin .....	42
<b>2.3 Lignin characterization .....</b>	<b>43</b>
2.3.1 Lignin content .....	43
2.3.2 Ashes Content.....	43
2.3.3 Lignin extraction.....	44
2.3.4 <sup>31</sup> P NMR Derivatization.....	44
2.3.5 <sup>13</sup> C NMR.....	44
2.3.6 GPC.....	45
2.3.7 Elemental analysis .....	45
2.3.8 Density.....	45
2.3.9 Morphological analysis.....	46
2.3.9.1 Sieve Analysis Methods .....	46
2.3.9.2 Particle size distribution of powders with Laser scattering Particle Size Distribution Analyzer LA-960V2.....	46
2.3.10 Optical microscope.....	47
2.3.11 FT-IR .....	47
2.3.12 Spray drying.....	48
<b>2.4 Lignin modification .....</b>	<b>48</b>
2.4.1 Milling .....	48

2.4.2 Lignin acetylation.....	48
2.4.3 Lignin and biomass acetylation with acetic anhydride and 1-Methylimidazole.....	49
2.4.4 Purification of acetylated biomass.....	49
2.4.5 Lignin benzylation.....	49
2.4.6 Lignin allylation (1 <sup>st</sup> method).....	50
2.4.7 Lignin allylation (2 <sup>nd</sup> method).....	50
2.4.8 Lignin partial allylation.....	50
2.4.9 Allylated lignin acetylation.....	51
2.4.10 Lignin allylation and acetylation (scale up).....	51
2.4.11 Reaction of lignin with Hexamethylenetetramine (HMT)....	52
2.4.12 Reaction of lignin with coupling agent Bis-[ $\gamma$ -(triethoxysilyl)-propyl]-Tetrasulfide (Si69).....	52
2.4.13 Coagulation of NR from latex.....	53
2.4.14 Co-precipitation of NR with lignin from latex.....	53
<b>2.5 Compound preparation.....</b>	<b>53</b>
2.5.1 Mixing process (Haake).....	53
2.5.2 Mixing process (Brabender).....	54
2.5.3 Vulcanization process.....	54
<b>2.6 Compound characterization.....</b>	<b>55</b>
2.6.1 Density.....	55
2.6.2 Viscosity ML.....	55
2.6.3 Kinetics of vulcanization.....	55
2.6.4 Rebound resilience.....	56
2.6.5 The hardness.....	56
2.6.6 Tensile properties.....	56
2.6.7 Compression dynamic mechanical test.....	56
2.6.8 Dispergrader analysis.....	57
2.6.9 SEM.....	58
<b>3 RESULTS AND DISCUSSION.....</b>	<b>59</b>
3.1 Ionic liquids pretreatment of rice husk.....	59

<b>3.2 Steam explosion pretreatment of wheat straw and arundo donax.....</b>	<b>63</b>
3.2.1 <i>Characterization of steam exploded biomass .....</i>	64
<b>3.3 Modification of lignin chemical nature .....</b>	<b>80</b>
3.3.1 <i>Chemical modification of lignin.....</i>	80
3.3.1.1 Acetylation.....	80
3.3.1.2 Allylation .....	85
3.3.1.3 Use of coupling agent.....	102
<b>3.4 Commercial sulfur free lignins .....</b>	<b>106</b>
<b>3.5 Reduction of particle size .....</b>	<b>113</b>
3.5.1 <i>Milling .....</i>	114
3.5.2 <i>Spray drying.....</i>	115
3.5.3 <i>Co-precipitation of latex with lignin .....</i>	119
<b>4 CONCLUSION.....</b>	<b>130</b>
<b>ACKNOWLEDGMENTS.....</b>	<b>132</b>
<b>REFERENCES.....</b>	<b>133</b>

## **LIST OF ABBREVIATIONS**

<b>%RET</b>	Percentage of reversion during the vulcanization stage
<b>[amim]Cl</b>	1-allyl-3-methylimidazolium chloride
<b><sup>13</sup>C NMR</b>	Carbon Nuclear Magnetic Resonance
<b><sup>31</sup>P NMR</b>	Phosphorus Nuclear Magnetic Resonance
<b>6PPD</b>	N-(1,3-dimethylbutyl)-N'-phenyl- <i>p</i> -phenylenediamine
<b>AD</b>	Arundo donax
<b>ATR</b>	Attenuated total reflectance
<b>CB</b>	Carbon black
<b>CBS</b>	N-Cyclohexyl-2-Benzothiazolesulfenamide
<b>COOH</b>	Carboxylic acid functionalities
<b>Eb</b>	Elongation at break (%)
<b>FESEM</b>	Field Emission Scanning Electron Microscope
<b>FT-IR</b>	Fourier Transform Infrared Spectroscopy
<b>G*</b>	Complex shear modulus
<b>G'</b>	Storage modulus
<b>G''</b>	Loss modulus
<b>G-OH</b>	Guaiacyl units
<b>GPC</b>	Gel permeation chromatography
<b>HMT</b>	Hexamethylenetetramine
<b>I</b>	Polydispersity index

*List of abbreviations*

---

<b>IPPD</b>	N-Isopropyl-N'-phenyl- <i>p</i> -phenylenediamine
<b>IRHD</b>	International rubber hardness degree
<b>LCC</b>	Lignin-carbohydrate complexes
<b>M100</b>	Modulus at 100% of elongation
<b>M200</b>	Modulus at 200% of elongation
<b>M300</b>	Modulus at 300% of elongation
<b>M50</b>	Modulus at 50% of elongation
<b>M500</b>	Modulus at 500% of elongation
<b>MH</b>	Highest torque on the vulcanization curve
<b>ML</b>	Lowest torque on the vulcanization curve
<b>Mn</b>	Number-average molecular weight
<b>Mw</b>	Weight-average molecular weight
<b>N375</b>	Carbon black N375
<b>NR</b>	Natural rubber
<b>PDADMAC</b>	Polydiallyldimethylammonium chloride
<b>PhOH</b>	Phenolic units
<b>phr</b>	Parts per hundred rubber
<b>P-OH</b>	<i>p</i> -coumaryl units
<b>Rhenogran HEXA-80<sup>®</sup></b>	Blend of 80% of HMT and 20% of elastomer binder
<b>SBR</b>	Styrene-butadiene rubber
<b>SBR 1500</b>	Emulsion of Styrene butadiene rubber
<b>SEM</b>	Scanning Electron Microscope

*List of abbreviations*

---

<b>Si69</b>	Bis-[ $\gamma$ -(triethoxysilyl)-propyl]-tetrasulfide
<b>S-OH</b>	Syringyl units
<b>STR 20</b>	Natural rubber
<b>t10</b>	the time required for reaching 10% of vulcanization
<b>t100</b>	the time required for reaching 100% of vulcanization
<b>t90</b>	Optimum time of vulcanization, the time required for reaching 90% of vulcanization
<b>t95</b>	the time required for reaching 95% of vulcanization
<b>Tan <math>\delta</math></b>	$\tan \delta = G''/G'$ , Measure of material damping
<b>TBBS</b>	N- <i>t</i> -butyl-2-benzothiazylsulphenamide
<b>TGA</b>	Thermal gravimetric analysis
<b>THF</b>	Tetrahydrofuran
<b>TS</b>	tensile strength
<b>tS2</b>	Scorch time
<b>WS</b>	Wheat straw
<b><math>\delta</math></b>	Phase angle



## **THE PhD PROJECT**

Lignocellulosic biomass is a natural complex composite of cellulose, hemicellulose, lignin, ashes and other soluble substances called extractives.

The significant difficulties related to the separation of lignin-carbohydrates complexes are the major obstacle to overcome for lignocellulosic biomass utilization.

In order to free the locked polysaccharides in cellulose, a number of lignocellulose pretreatment technologies is under intensive investigations, such as steam explosion, organosolv process, chemical treatment with acids or bases (ammonia, NaOH) and ionic liquid pretreatment. The relevance of lignocellulosic biorefinery relies not only on the recovery of carbohydrates, but also on the added value of lignin which is the second most abundant natural polymer, exceeded only by cellulose and hemicellulose.

Lignin's structure is determined by its botanical origin and the adopted isolation process. Depending on the plant source, lignins can be divided into three classes: hardwood (angiosperm), softwood (gymnosperm) and annual plant (graminaceous); on the other hand, according to the isolation process, lignins can be divided into two groups: lignin from sulfite process and sulfur free lignin.

The latter is receiving increasing attentions because it offers a greater versatility than the former and it can be heat-processed avoiding the irritating odor-release commonly associated with commercial kraft lignin. In addition to cost advantages, annual renewability and huge availability are factors that could promote the use of sulfur-free lignin.

Lignin's structure contains a variety of chemical functional groups that affect its reactivity making it able to meet the needs of industry. It's worth noting that lignin can be used for several industrial applications owing to its surface-active

properties. It has also been applied as a filler in many elastomers (butadiene-styrene-butadiene, isoprene-styrene-butadiene (Savel'eva *et al.*, 1983); styrene-butadiene (Kosikova *et al.*, 2003; Kramarova *et al.*, 2007)) or in natural rubber (Kramarova *et al.*, 2007). Moreover, lignin has shown a high antioxidant efficiency both as it is and in combination with commercial antioxidants (Furlan *et al.*, 1985; Gregorová, *et al.*, 2006; Shusheng and Xiansu, 2010).

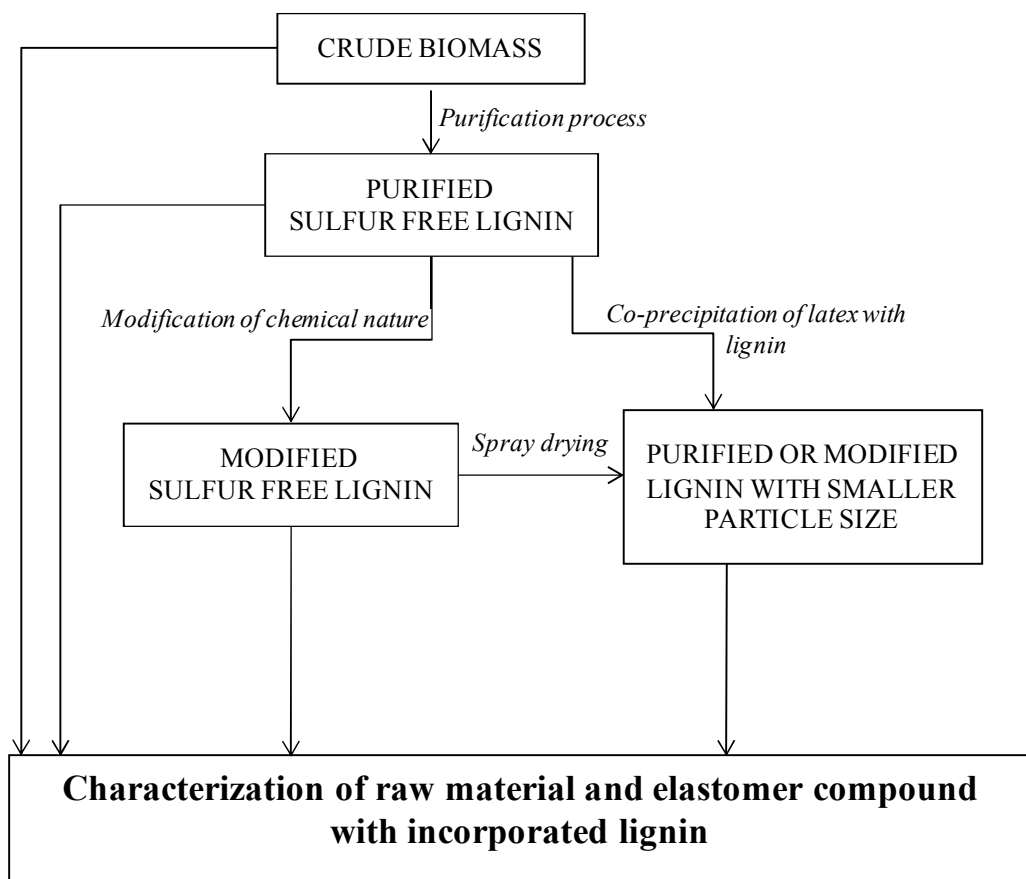
The main purpose of my doctorate has been testing sulfur free lignins (obtained from herbaceous plants as by-products of steam explosion and soda pulping processes) as fillers in rubber compounds in order to evaluate their reinforcement ability and their use as a partial replacement of carbon black. The objective is to realize lighter tyres characterized by a low rolling resistance and a reduced amount of material derived from no renewable sources.

Lignin has some disadvantages that make its application as a rubber-reinforcing filler difficult, such as large particle size, strong polar surface and high tendency of its particles to link together by intermolecular hydrogen bonding arranging agglomerates. To improve the interaction between filler and elastomer, two strategies have been adopted: the chemical modification of lignin and the reduction of the size of its particles.

Concerning the chemical modification, lignin can be functionalized by way of acetylation, allylation, reaction with coupling agents (silane) and with hexamethylenetetramine (HMT), so that also its dispersion in the elastomer is improved. Instead, spray drying and the co-precipitation of latex with lignin have proved to be effective in reducing the particles' size.

All the products obtained have been characterized by IR, <sup>31</sup>P NMR, GPC and microscope analysis and tested in rubber compounds as it is or as partial replacement of carbon black.

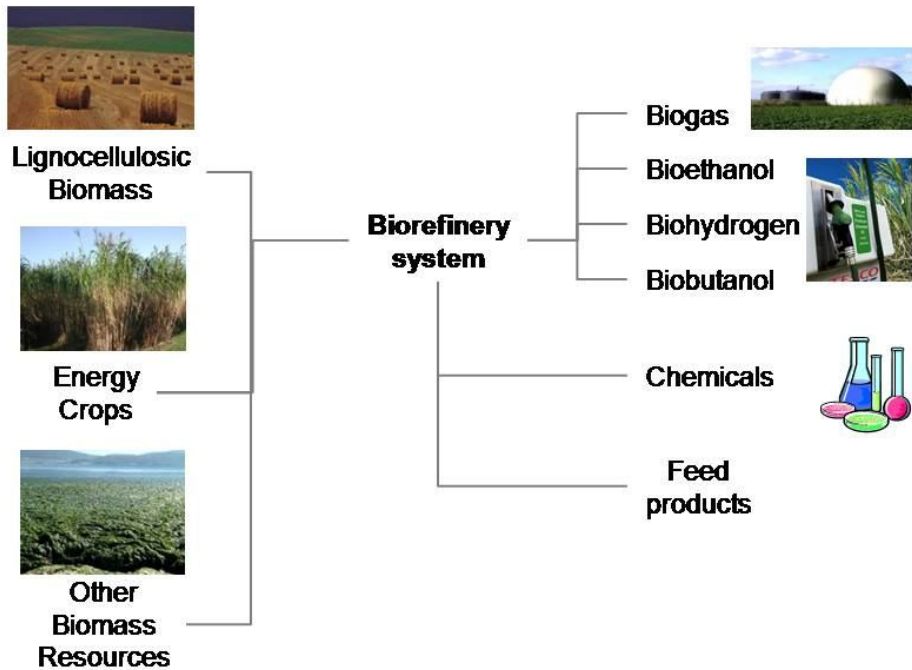
The practical section of my PhD project is described in the following flow chart.



# 1 INTRODUCTION

## 1.1 BIOREFINERY

The International Energy Agency has defined *biorefinery* the sustainable processing of biomass into a spectrum of marketable products, ranging from energy to food, feed, chemicals and materials applications.



Thus a biorefinery arises as the combination of biological, chemical, and physical processes to obtain a range of material products (building block chemicals, nutraceuticals, pharmaceuticals, polymers) and energy (biofuels, heat and power). This kind of bioprocessing clusters will be more competitive with oil refineries when producing high-value (specialty chemicals) as well as low-value (commodities) products because it will not only benefit from increased profitability but will also take advantage from their flexibility to adapt

product mix in response to changing demands. Biorefinery also represents a sustainable and low-pollution system alternative for replacement of petroleum processing. The importance of this renewable feedstock for the processing industry is expected to increase as indicated by the interest of different research institutions, government bodies and companies around the world, especially in the US and Europe.

## **1.2 LIGNOCELLULOSIC BIOMASS**

Lignocellulosic biomass is a natural complex composite of cellulose, hemicellulose, lignin, ashes and other soluble substances called extractives. Thanks to their abundant availability, herbaceous plants can provide a high yield of it multiple times a year; moreover, the chemical nature and low cost make lignocellulosic biomass an excellent feedstock for pulp and paper industry and for the production of bio-fuels.

One of the major priorities for the emerging cellulosic ethanol and bio-based chemical industries is overcoming the uncooperative structure of lignocellulose in order to free the locked polysaccharides of cellulose.

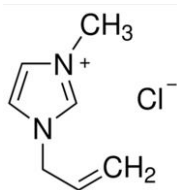
A number of lignocellulose pretreatment technologies are under intensive investigations, such as steam explosion, organosolv process, chemical treatment with acids or bases (ammonia, NaOH). However, most of these processes suffer from relatively low sugar yields, severe reaction conditions and high processing costs. Each of them has pros and cons, in particular:

- the acid pretreatment promotes the hydrolysis of hemicelluloses, but the high content of lignin in the biomass is a disadvantage for the activity of cellulase enzyme; furthermore expensive strategies to face corrosion phenomena in the industrial plant are needed.

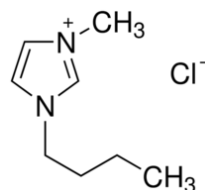
- it has been demonstrated that the alkaline pretreatment is very efficient, but the reaction is very slow and requires additional costs due to regeneration of the base.
- both ammonia and organosolv pretreatments facilitate the hydrolysis of cellulose with high yield of glucose and the latter allows to obtain high purity lignin too. Nevertheless they are also very expensive.

Looking for new approaches for a physico-chemical pretreatment of biomass, ionic liquids (ILs) have been tested. ILs constitute a relatively new class of solvents characterized by low melting points (below 100°C), high polarities, high thermal stabilities and negligible vapor pressures; they entirely consist of ions, typically large organic cations and small inorganic anions.

Among others, 1-allyl-3-methylimidazolium chloride ([amim]Cl) and 1-butyl-3-methylimidazolium chloride ([bmim]Cl) have been recognized as ideal non-derivatizing solvents for lignocellulosic substrates (Kilpelainen *et al.*, 2007; Fort *et al.*, 2007).



*1-allyl-3-methylimidazolium chloride*



*1-butyl-3-methylimidazolium chloride*

In fact, on the one hand the aromatic electron-rich cationic moiety creates strong interactions with polymers which undergo  $\pi$ -stacking (as in the case of lignin) and on the other hand chloride is the most efficient counter-anion in disrupting the extensive inter- and intra-molecular hydrogen bonding interactions present in cellulose. As a result, the ionic liquid deeply diffuses into the material progressively destroying its cell wall structure; the cellulose

fraction can then be recovered by the addition of an anti-solvent, such as water or ethanol (Swatloski *et al.*, 2002).

The regenerated cellulose has almost the same degree of polymerization and polydispersity as the pristine one, but its morphology is significantly changed and its microfibrils are fused into a relatively homogeneous structure. In fact, the regeneration process impacts on the microstructure of cellulose modifying its degree of crystallinity and porosity and its surface area (Zhu *et al.*, 2006). All these chemico-physical modifications contribute to raise the enzymatic digestibility of biomass cellulose.

Another major issue for a green comprehensive exploitation of lignocellulosic materials is the encirclement and the compenetration of cellulose by the complex structure of lignin and hemicellulose (Sun and Cheng, 2002).

### 1.3 LIGNIN

As declared by Ragauskas *et al.* (2006), the relevance of lignocellulosic biorefinery relies not only on the recovery of carbohydrates, but also on the added value of lignin which is the second most abundant natural polymer, exceeded only by cellulose and hemicellulose. The annual production rate of lignin is 20 billion metric tons and its amount on Earth is 300 billion metric tons (Argyropoulos and Menachem, 1998). This molecule is found in the middle lamellae and the secondary cell walls of plants and has the important role of giving the plant rigidity and resistance to environmental stress (Ralph *et al.*, 2007).

The biosynthesis of lignin starts with the conversion of phenylalanine to monolignols by the activity of ten enzyme families via the phenylpropanoid pathway (*Figure 1*).

Once the monolignols (*p*-coumaryl-, sinapyl- and coniferyl-alcohol) are synthesized, they are transferred in the cell wall where the polymerization

process (lignification) starts with the oxidation of the monolignols to phenoxy radicals (Ralph *et al.* 2007; *Figure 2*).

Radicals' coupling leads to specific chemical linkages in a combinatorial way, most of which are ether bonds ( $\beta$ -O-4 structures) and carbon-carbon bonds (resinol ( $\beta$ - $\beta$ ) and phenylcoumaran ( $\beta$ -5) structures), as shown in *Figure 3*.

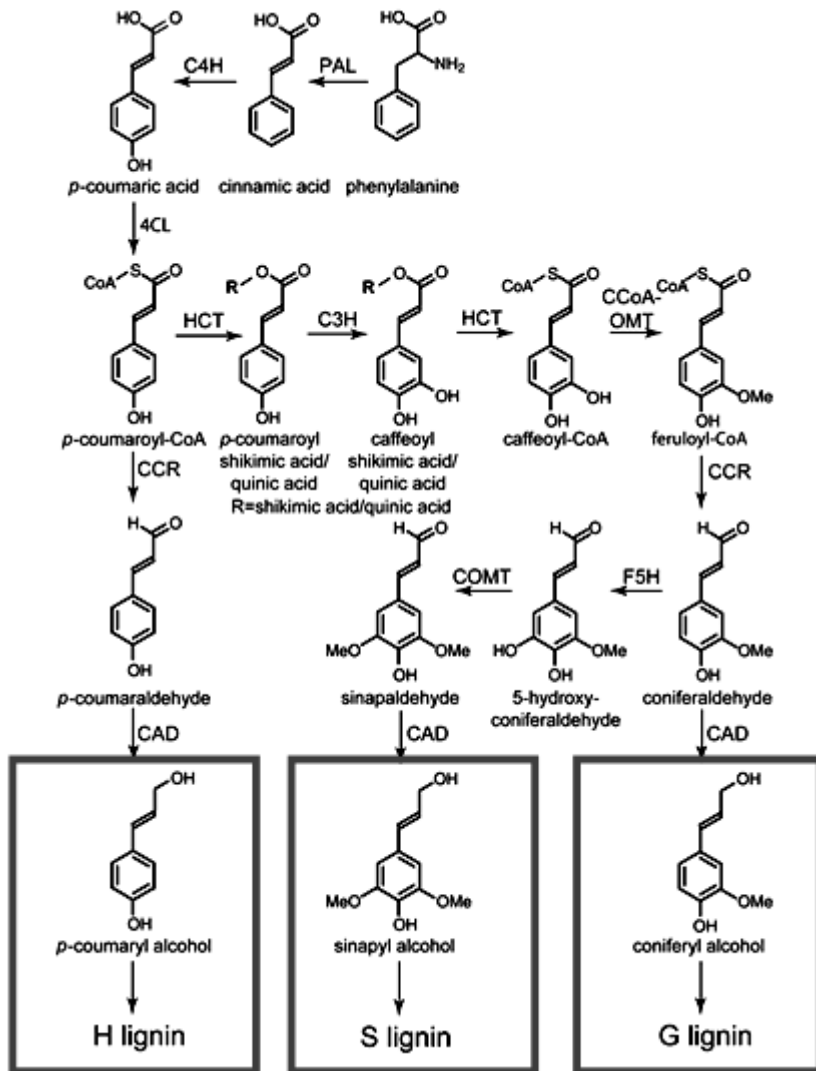


**Figure 1.** Monolignols biosynthetic pathways



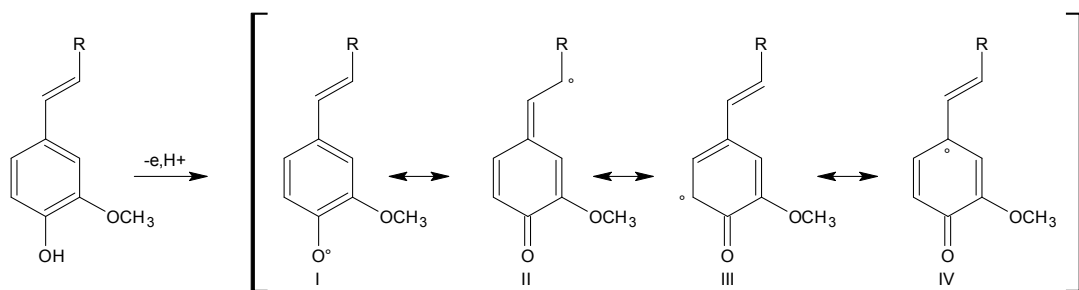


**Figure 2.** Oxidation of the monolignols to phenoxy radicals

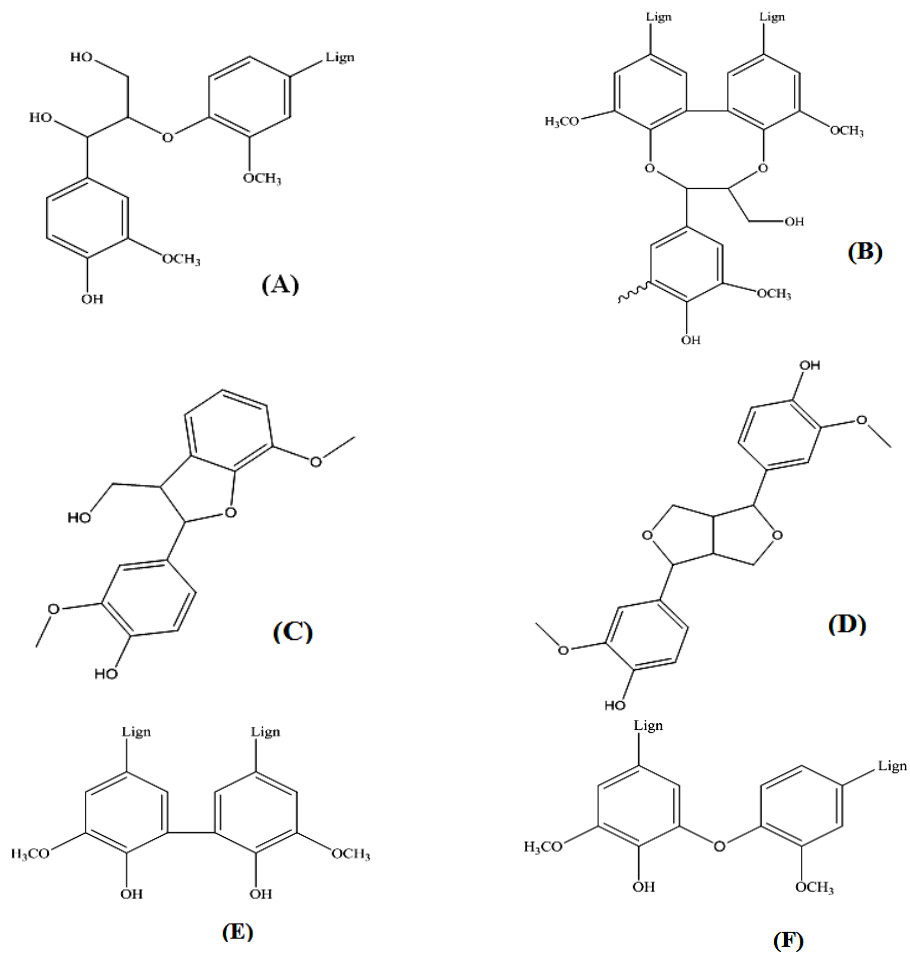


**Figure 3.** Significant lignin linkage structures. (A)  $\beta$ -O-4, (B) 5-5'-O-4, (C)  $\beta$ -5, (D)  $\beta$ - $\beta$ , (E) 5-5' and (F) 4-O-5'.

Lignin's structure contains a variety of chemical functional groups which are partly the result of the adopted extraction method. Hydroxyl, methoxyl, carbonyl and carboxyl moieties linked to aromatic rings or to lateral chains are commonly found and their presence affects lignin's reactivity, as well as confers the molecule a tridimensional structure, as shown in *Figure 4*.

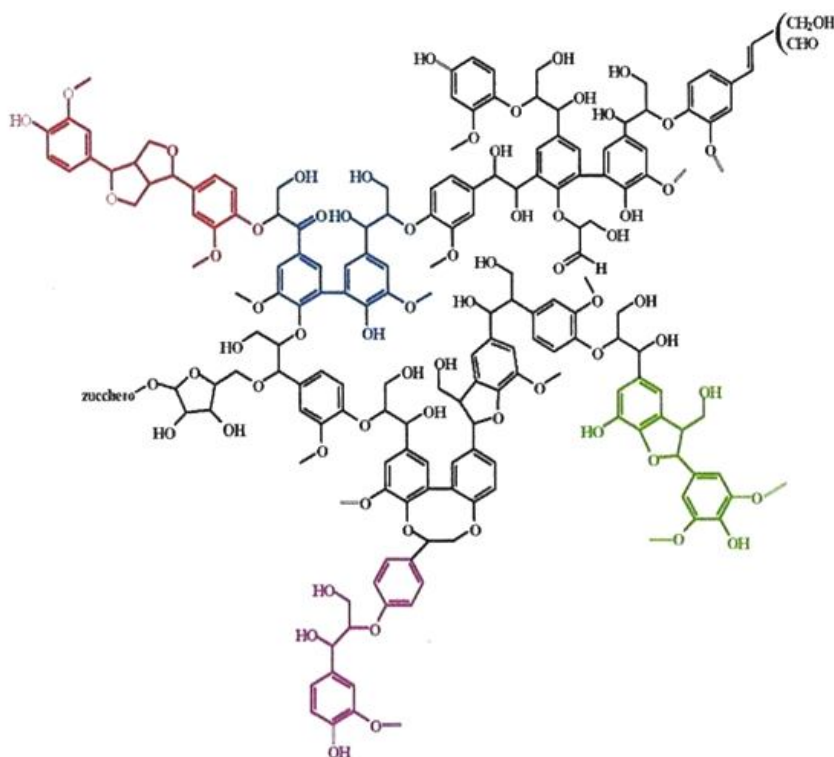


**Figure 4.** Lignin's structure

Lignin doesn't exist as an independent entity in the plants, but it is covalently bonded to other polymers (hemicellulose and cellulose) forming lignin-carbohydrate complexes (LCC) (*Figure 5*). The bonding sites are  $\alpha$ -carbons and C-4 of the aromatic rings. The presence of these covalent bonds prevents from extracting lignin in pure form.

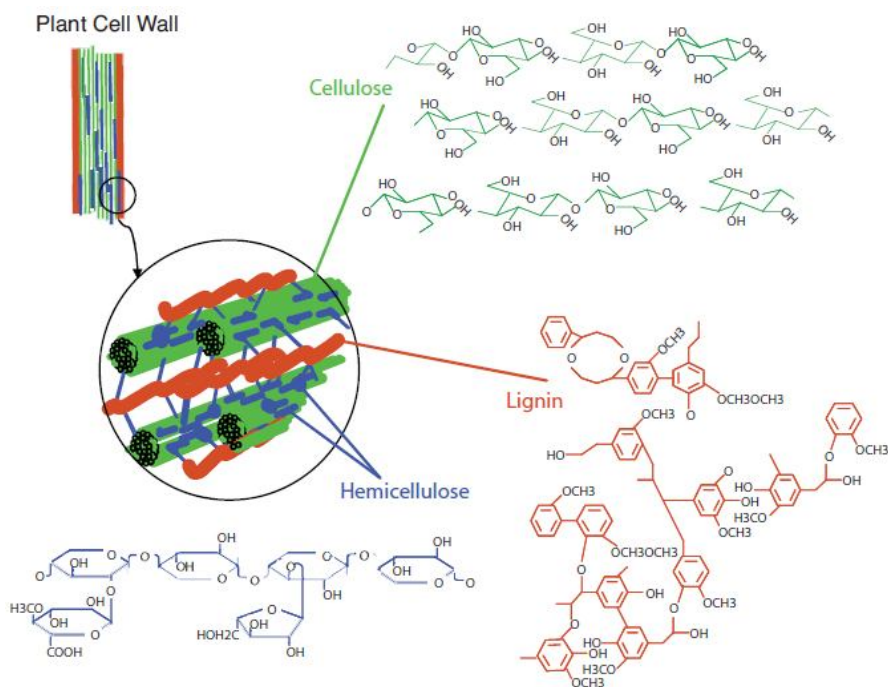


**Figure 5.** Structure of lignocellulosic biomass

### 1.3.1 Lignin types

Lignins have different structures depending on their plant source and their method of extraction (Lora *et al.*, 2008; Lora and Glasser, 2002). The largest differences in lignin's structure derive from the method of isolation.

#### 1.3.1.1 Botanical origin

Depending on the plant source, lignins can be divided in three classes: hardwood (angiosperm), softwood (gymnosperm) and annual plant (graminaceous).

Softwood lignin is composed mainly of guaiacyl units, whereas the hardwood one is composed also of syringyl units; in the end, lignin in herbaceous plants is composed of guaiacyl, syringyl and *p*-hydroxyphenyl units. As a result, wood lignins are more condensed than the herbaceous ones (Billa *et al.*, 1998).

There are also differences related to lignin-carbohydrates complexes between wood and herbaceous lignin: while in woods lignin and carbohydrates are linked via benzyl ether, benzyl ester, glycosidic and acetal bonds, in herbaceous plants they are linked only by way of ferulic bridges (Himmelsbach, 1993; Lapierre and Monties, 1989), as shown in *Figure 6*.

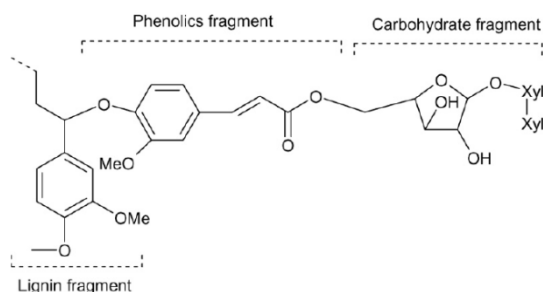


**Figure 6.** Lignin-carbohydrates complexes in herbaceous plant

Furthermore, lignin in herbaceous plants can be naturally acetylated at  $\gamma$ -position on siringyl units (Crestini and Argyropoulos, 1997; Ralph *et al.*, 1999a; Ralph, 1999).

### ***1.3.1.2 Isolation process***

According to the isolation process, lignins can be divided in two groups: lignin from sulfite process and sulfur free lignin.

#### ***1.3.1.2.1 Lignin from sulfite process***

These lignins are obtained in the pulp and paper industry as a by-product. Owing to the conditions adopted during the process, the sulfur content can vary between 1% and 5%.

##### ***1.3.1.2.1.1 Kraft process***

Kraft process (or sulfate process) consists in cooking the lignocellulosic material in NaOH and NaSH and is used for the paper making. The severe

reaction conditions cause the cleavage of  $\beta$ -1,4 bonds in the cellulose allowing the extraction of lignin and the hydrolysis of ether bonds. After the recovery of pulp, lignin is solubilized in a fluid called black liquor and can be retrieved lowering the pH (between 5-7.5) with an acid or carbon dioxide.

Kraft lignin is dark colored, contains 1-2% of sulfur due to the introduction of thiol groups in  $\beta$ -position of propane side chains. This lignin is also soluble in alkaline solutions and insoluble in strongly polar organic solvents.

This process, compared to the other extraction methods available, produces the highest amount of lignin (29-45%) (Smook, 2002).

#### *1.3.1.2.1.2 Sulfite process*

Sulfite process is the most common treatment applied by the paper industry in order to obtain lignin. It consists of treating the lignocellulosic material with a metal sulfite and sulfur dioxide (Smook, 2002).

The reaction is conducted between 140°C and 160°C at pH = 1.5-2 and causes the breaking of  $\alpha$ -ether and  $\beta$ -ether bonds; the cleavage of aryl ethers originates benzyl carbocations, stabilized by resonance, which can lead to condensation reactions.

One of the main reactions is the introduction of sulfonate groups in  $\alpha$ -position of propane side chains and generates water-soluble lignosulfonate derivatives that are thereafter very efficiently separated from impurities. This product contains 5% of sulfur.

#### **1.3.1.2.2 Lignin from Sulfur free process**

Sulfur free lignins are one of the main by-products of processes such as bio-ethanol production and paper making; their structure is similar to the one of native lignin.

#### *1.3.1.2.2.1 Soda pulping process*

The cooking of the lignocellulosic material at 140-170 °C in the presence of 13-16%wt sodium hydroxide aqueous solution is called soda pulping; the product, soda lignin, is isolated by acid precipitation followed by filtration and has a high content of phenols and acid functionalities, the latter derived from the oxidation of aliphatic-OH. It also has a low molecular weight and low hemicelluloses content.

#### *1.3.1.2.2.2 Organosolv pulping*

Organosolv process is more environmentally friendly and inexpensive than kraft and sulfite methods. It consists of the high pressure and high temperature (160-200°C) dissolution of lignocellulosic material in organic solvents and water. In this way, hemicelluloses are hydrolyzed to pentose and hexose sugars and form the liquid portion of the mass with lignin. The desired product is obtained by precipitation after addition of water and regulation of pH and temperature. Organosolv lignin has a low molecular weight and a high degree of purity; it is soluble in organic solvents.

#### *1.3.1.2.2.3 Steam explosion process*

Steam explosion process is the treatment of biomass with saturated steam at high pressure and high temperature and allows the hydrolysis and solubilization of hemicelluloses. The release of the pressure causes the fiber network breaking and the consequent separation of the different components. Treating the mass with alkali and an organic solvent, it is possible to recover water insoluble lignin (Gellerstedt and Henriksson 2008), which has a low content of ashes and a relatively low content of polysaccharides.

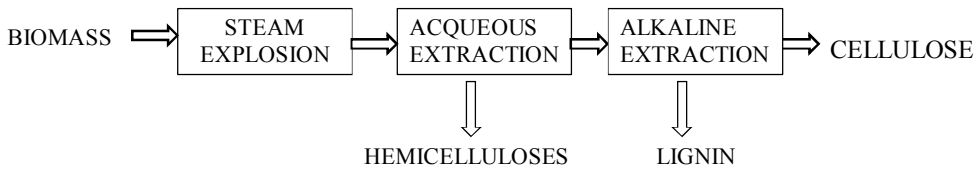


**Figure 7.** Schematic steam explosion process

### 1.3.2 Applications of lignin

Most of lignin is burned as energy source but it can be used for several industrial applications owing to its surface-active properties.

1. Kraft and sulfite lignin have been used as dispersants, binders, additives, in metallic ore processing and as substitutes of phenols in the phenol formaldehyde resins (Gargulak and Lebo, 2000; Stewart, 2008).
2. A variety of added value products has been obtained from liginosulfonates: vanillin, pesticides, pigments, industrial cleaners, dispersants for carbon black and scale inhibitors.
3. Sulfur-free lignin has been used as a partial replacement of phenolic powder resins (PPR, matching or improving their performances) and as a complete replacement of phenols in the epoxy resins.
4. Sulfur-free lignin can be used in many thermoplastic (Bertini *et al.* 2012) and thermosetting applications in conjunction with phenol, epoxy, or isocyanate resins.

Focusing on the incorporation of lignin in natural and synthetic polymers, the increase of the modulus is noteworthy; further, it is also possible to add plasticizers to the composite in order to enhance its mechanical properties by reducing the tendency of lignin particles to link together. Nevertheless, exploitation of lignin in the polymeric matrix could be more intensive if its miscibility could be improved through esterification or coupling reactions.

### **1.3.2.1 Rubber-lignin blends**

A great amount of research (Setua *et al.* 2000; Griffith and MacGregor 1953; Kumaran and De 1978) and patents (Benko *et al.* 2010; Boutsicaris 1984; Davidson and Wunder 1977; Doughty 1967; Doughty and Charlestion 1966) have focused on lignin for its use as a filler that can be added to rubber composites for total or partial carbon black replacement, while achieving similar reinforcement. The first studies done with this aim date back to 1947, when Keilen and Pollak have tested lignin in natural and synthetic latexes. In subsequent years, lignin has been introduced into natural rubber (Kramarova *et al.*, 2007), styrene-butadiene rubber (Košíková *et al.*, 2003; Kramarova *et al.*, 2007), butadiene-styrene-butadiene rubber, isoprene-styrene-butadiene rubber (Savel'eva *et al.*, 1983) and nitrile rubber (Setua *et al.*, 2000). It has been demonstrated that the addition of lignin in blends of natural and synthetic polymers, generally increases the modulus and the cold crystallization temperature but decreases the melt temperature (Feldman *et al.*, 2001).

The combination of lignin with oligomeric polyesters has been applied as modifier of isoprene rubber and methylstyrene-butadiene rubber (Savel'eva *et al.*, 1988). Lignin-phenol formaldehyde resin used as a filler in nitrile rubber has shown good mechanical properties, resistance to environmental oxidation and oil resistance (Wang *et al.*, 1992).

Lignin incorporation can improve the adhesiveness of the material as demonstrated in liginosulfonate-natural rubber blends (Piaskiewicz *et al.*, 1998) and in liginosulfonate-styrene butadiene rubber blends (Lora *et al.*, 1991) whereas the incorporation of modified lignin in natural rubber latex has shown a decrease of the stickiness (Wang *et al.*, 2008).

It has been demonstrated that magnesium, calcium and sodium liginosulfonates act as reinforcing agents in natural rubber (NR) and styrene-butadiene rubber;



in particular in NR they improve the mechanical properties. The addition of glycerol that works as a plasticizer for lignin gives a further enhancement (Alexy *et al.*, 2008). Lignin has also demonstrated a higher tensile strength in natural rubber in comparison to starch or protein (Kramarova *et al.*, 2007).

Sulfur free lignin affects the curing behavior: increasing of lignin loading in the SBR rubber blends slowly decreases the scorch time and significantly improves optimum cure time. This behavior is due to the interaction of lignin with the vulcanization system (Košíková and Gregorová, 2005).

The antioxidant activity of lignin in NR has been proved by several works (Gregorová *et al.*, 2006; Alexy *et al.*, 2000 and Glasser, 1981), for example in the polymer filled with carbon black; indeed its use in combination with commercial antioxidant IPPD has exhibited the highest antioxidant efficiency (Gregorová *et al.*, 2006). Moreover, lignin as it is and in combination with antioxidant D has provided thermal and oxidative protection to styrene-butadiene rubber, ensuring a better performance in comparison to antioxidant only (Sunsheng and Xiansu, 2010). In the end, sugar cane Bagasse-lignin has shown an antioxidant effect in butadiene, natural and styrene-butadiene rubber (Furlan *et al.*, 1985).

The addition of lignin improves the resistance to thermoxidative degradation of NR vulcanizates, thus lignin could be used as thermal stabilizer during thermal degradation of NR vulcanizates (Košíková *et al.*, 2007).

## 1.4 RUBBER COMPOUNDS

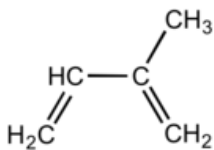
A rubber compound is a combination of different ingredients that assure it required properties; these ingredients, necessary for formulating a tyre, can be divided into four categories: polymer, filler, stabilizer system (antioxidants) and vulcanizing agent. They will be discussed in the following sections.

### 1.4.1 Polymer

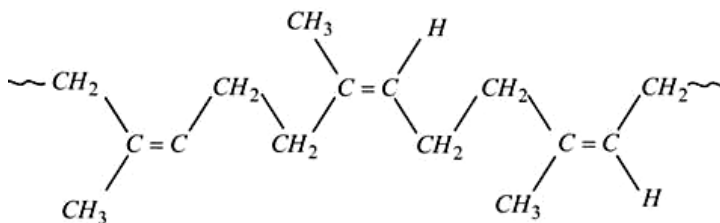
Polymers can be divided in two types: natural and synthetic.

#### 1.4.1.1 Natural rubber

NR is produced from the coagulation of latex of a large variety of plants, but the most common is *Hevea Brasiliensis*. Its monomeric unit is isoprene (2-methyl-1,3-butadiene) that has two double bonds and methylene groups in *cis* configuration. Its specific gravity is 0.915.



*cis-isoprene unit*



*Polymeric structure of NR*

The double bonds and the methylene groups can be used for the sulfur vulcanization, but rubber can also easily react with oxidizing agents and peroxides because of the unsaturation.

NR possesses qualities not shared by synthetic rubber: low heating and ability to return to its original shape. Raw natural rubber has low tensile strength and abrasion resistance. It is insoluble in water, alcohol, acetone, dilute acids and alkalis, but is soluble in ether, carbon disulphide and carbon tetrachloride.

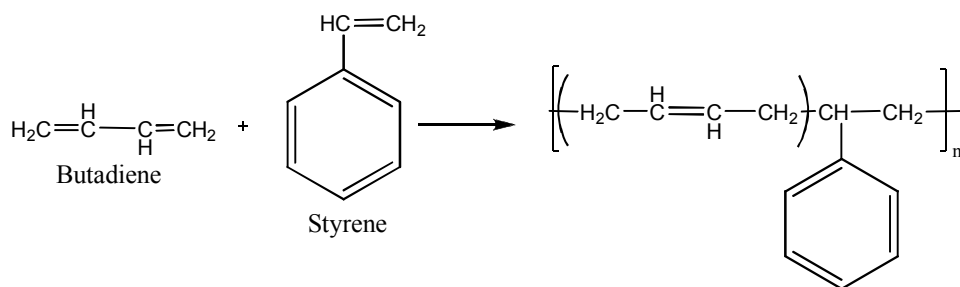
### 1.4.1.2 Synthetic rubber

Any type of artificial elastomer mainly synthesized from raw material derived from petroleum, coal, oil, natural gas and acetylene can be defined as synthetic rubber. Many of them are polymers consisting of different monomeric units. International Institute of Synthetic Rubber Producers (IISRP) has classified the synthetic rubber giving a number according to the properties of the polymer. Styrene-butadiene rubber (SBR) is the most commonly used elastomer, while other general purpose elastomers are *cis*-polybutadiene and *cis*-polyisoprene; each of them has properties similar to natural rubber's.

#### 1.4.1.2.1 SBR

Styrene-butadiene copolymers are among the earliest synthetic rubbers that have been prepared and their properties are very close to those of natural rubber. Their widespread use is due mainly to their low cost and to their good physical properties; it is noteworthy that some characteristics can be modified by simply changing the styrene/butadiene ratio: hardness, for example, increases along with the styrene content. Moreover, SBR shows an excellent abrasion resistance and it is sensitive to oil and ozone.

It is produced through anionic polymerization in solution or through free radical polymerization as an emulsion.



Structural formula of the styrene-butadiene-rubber.

## 1.4.2 Filler

Fillers are materials constituted by insoluble particles that are stable during the mixing process of the compound. They can be used either to reduce cost (inert fillers) or to improve the properties of the material (reinforcing fillers); for example, elastomers may be reinforced by adding a filler, and the most common ones are carbon black and silica.

### 1.4.2.1 Carbon black

Incomplete combustion or thermal decomposition of gaseous and liquid fuels (natural gas, mineral oils etc.) produces what is called carbon black, a particulate matter composed of randomly oriented layers of condensed carbon rings. Organic and mineral impurities (deriving from the production process), oxygenated functions, double carbon bonds and hydrogen are present at its surface.

At the beginning, the interaction between carbon black and natural rubber was attributed to the reactivity of the superficial acidic groups of the former with the basic moieties of the latter. However it seems to be a more complex process since, as demonstrated by Medalia and Kraus (1994), double bonds can react with sulfur (Rivin, 1963 and Lewis *et al.*, 1970), olefins (Rivin *et al.*, 1968) and radicals (Watson, 1955). Moreover, some authors (Hess *et al.*, 1988; Soeda and Kurata, 1995) have proved that the hydrogen content in carbon black is correlated to its reinforcement ability.

There are no clear evidences that functional groups on carbon black's surface are responsible of the interaction filler-polymer. On the other hand, the filler-polymer interaction is attributed to physical phenomena such as the adsorption. The nomenclature used for carbon black, a letter followed by a three digit number, was instituted by the D 24ASTM Committee On Carbon Black in

1968. The letter stands for the type of cure: N for normal and S for slow curing. The first of the three digits indicates a range of average particle size in nanometers, whereas the last two digits are arbitrarily assigned by ASTM. The code numbers are listed in *Table 1*.

<b>ASTM number</b>	<b>Primary particle diameter (nm)</b>
900-999	201 to 500
800-899	101 to 200
700-799	61 to 100
600-699	49 to 60
500-599	40 to 48
400-499	31 to 39
300-399	26 to 30
200-299	20 to 25
100-199	11 to 19
0-99	1 to 10

**Table 1.** ASTM nomenclature of carbon black

The average particle size of carbon blacks commonly available for industrial use is in the range 10-500nm. This parameter in turn affects the size of aggregates, which can have any shape or morphology. Generally, the observed shapes are incomplete spheres of very big dimensions. Herd *et al.* (1991) have classified carbon blacks in four different categories as shown in *figure 8*.

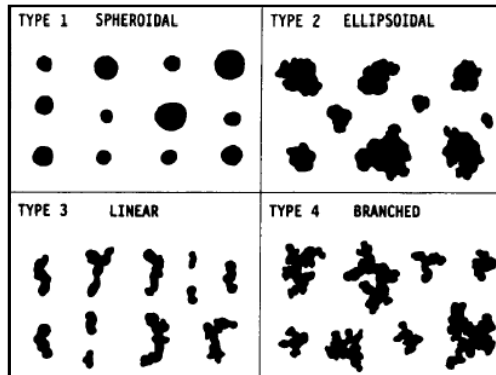


**Figure 8.** Shape categories for carbon black aggregates, (Herd *et al.*, 1991).

### 1.4.2.2 Silica

Silica has been used in rubber composites since the beginning of the 20<sup>th</sup> century (Voet *et al.*, 1977). Silica's surface is composed by silanol groups Si-OH that can be isolated or associated by hydrogen bonds. Precipitated silica can be obtained by precipitation, while fumed silica derives from oxy-decomposition of SiH<sub>4</sub> or other methyl-hydride precursors.

Since this material has a polar character, it results incompatible with rubber and must be used in combination with a specific coupling agent. The reaction can be done directly in the mixing stage or even before; its mechanism is shown here below (*figure 9A*).

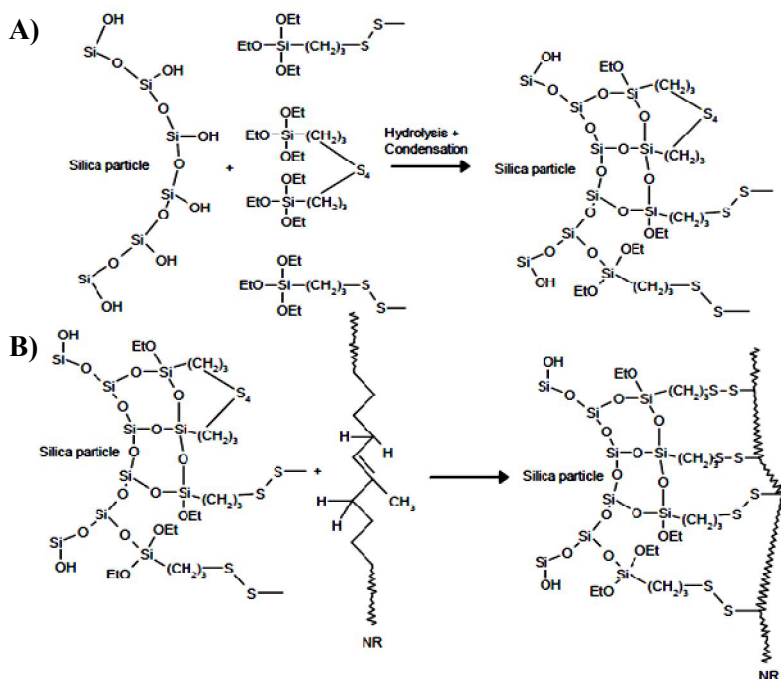


**Figure 9.** Modification reaction of silica with silane Si69 (A) and formation of rubber-to-filler bonds (B).

The addition of silica to rubber leads to many advantages, such as improvement of tear strength, reduction of heat buildup, improvement of rolling resistance and increase in compound adhesion.

Nevertheless, silica presents some disadvantages in comparison to carbon black because it is more difficult to process, it is more expensive and it can abrade the mixing equipment.

### 1.4.3 Stabilizer system (Antiozonants)

The *p*-phenylenediamines form the most common class of antioxidants utilized with rubbers; they protect the rubber from ozone and improve its resistance to fatigue, oxygen, heat and metal ions.

### **1.4.4 Vulcanizing agent**

Vulcanization is a very important process related to rubber; it consists in the formation of a cross-linked molecular network between polymer chains and will be discussed in detail afterwards.

Sulfur, insoluble sulfur and peroxide are used as vulcanizing agents in rubber industry. Sulfur is soluble in natural rubber at levels up to 2 phr (parts per hundred rubber).

#### ***1.4.4.1 Accelerators***

Accelerators are chemicals able to increase the rate of the vulcanization process and the cross-linking degree in the rubber compound. According to their activity, they can be divided in ultra, semiultra, fast, medium system and slow accelerators.

Regarding the chemical classification, accelerators can be sulfonamides (the most widely used), aldehydeamines, thioureas, dithiocarbamates, guanidines, thiurams, thiazoles and xanthates. Thus, the N=C-S functional group is fundamental as well as the presence of one or two sulfur atoms between organic terminal groups.

#### ***1.4.4.2 Activators***

Activators cooperate in increasing the rate of vulcanization by reacting with the accelerators to form rubber soluble complexes. The most common activators are combinations of zinc oxide and stearic acid, weak amines or amino alcohols.

The salt derived from fatty acid and ZnO can subsequently form complexes with the accelerators and the products of accelerators and sulfur.



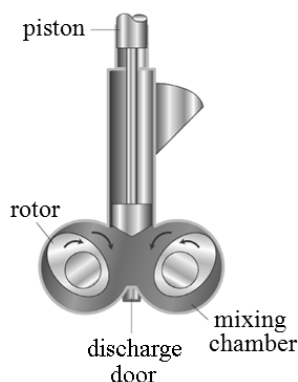
## 1.5 MIXING STAGE

In order to obtain a rubber compound, rubber and other ingredients are mixed together using an internal mixer or a two-roll mill that can ensure good dispersion and high uniformity.

Usually the mixing stage is a two or more step process in which the rubber is re-mixed, once it has become soft, with additional chemicals. The re-mixing can be done in the same instrument or not.

Avoiding vulcanization is essential during the mixing phase, so vulcanizing agents are added to the compound in a second stage at temperatures below 100-110°C.

### 1.5.1 Internal mixer



The most common mixer is an internal one. It is composed by two counter-rotating rotors within a mixing chamber in which a piston drives the materials (*figure 10*). The procedure requires heating the chamber, speeding the rotors and the chamber and finally setting the mixing time. The mixing occurs in the space between the rotors or between the rotor and the chamber.

**Figure 10.** Internal mixer

### 1.5.2 Two-roll mill

The two-roll mill is composed by two coaxial cylindrical rolls that rotate in opposite directions. The gap between the rotors through which the rubber is forced to pass is generally pre-set, but adjustable (*figure 11*).

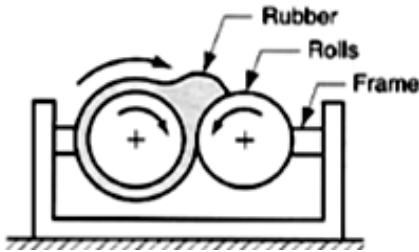


**Figure 11.** Two roll mill operation

The mixing time is longer in comparison to internal mixer because this kind of mixing is strongly dependent on operator intervention; the powders added can drop into and thus be collected in the mill tray, it's the operator's task to put them back

in the mix. The dispersion of filler and chemicals is worse and hard dust can develop during the adding. For these reasons internal mixer is preferred to a two roll mill that can be used in the second stage for the adding of vulcanizing agents.

## 1.6 VULCANIZATION PROCESS

The vulcanization process was discovered by Charles Goodyear in 1841 and consists in the creation of a cross-linked molecular network between polymer chains. Usually it is achieved heating up the rubber and maintaining it at high temperature (140-170°C) after the sulfur incorporation.

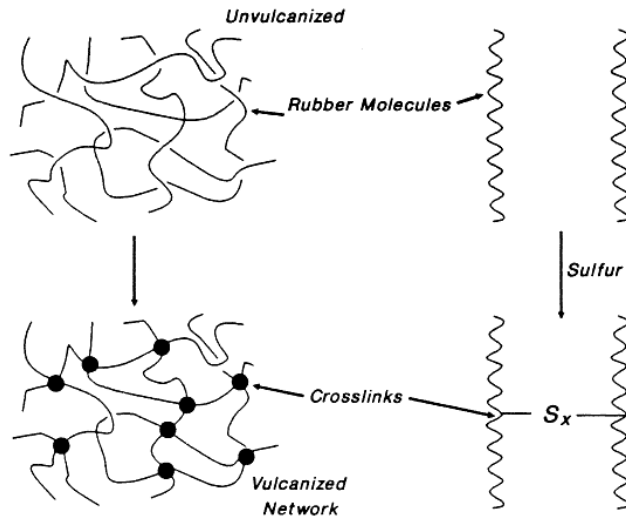
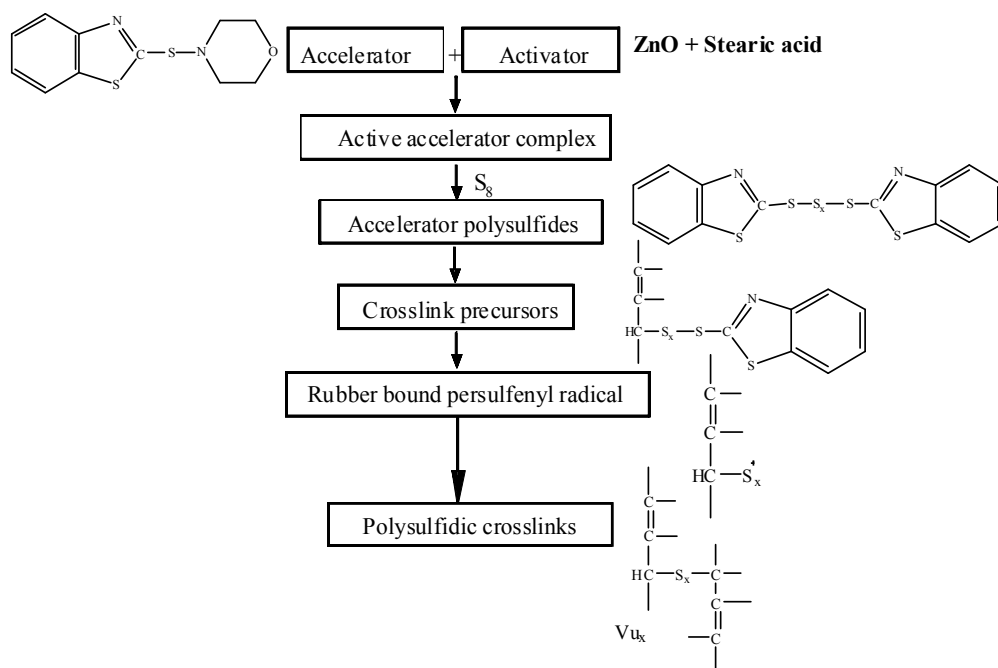


Figure 12. Vulcanization mechanism

As mentioned before, the vulcanization rate can be raised by addition of activators and accelerators.

The vulcanization process begins with the formation of active accelerator complex between accelerator and activators and then continues with the introduction of sulfur to form a polysulfidic species that then reacts with the carbon in the rubber forming a precursor that is terminated with rubber on one end and a benzothiazole group on the other. The precursor forms a radical species that reacts with another chain of rubber to form a cross-linked system (figure 13).



**Figure 13.** Basic mechanism of accelerated sulfur vulcanization

In order to evaluate important characteristics related to vulcanization such as scorch time, optimum cure time and maximum torque, the response of the fluid to applied forces is recorded by means of a rheometer and a curve like the one showed in *figure 14* is recorded. At a given temperature, scorch time ( $t_{S2}$ ) is the time needed by the cross-linking process to begin; maximum torque (MH), instead, is a parameter related to the final level of cross-linking, the quality of the polymer used, the filler used and the compounding process. After the maximum torque has been reached, a crosslink disappearance (reversion) can be observed. The reversion is due to the thermal degradation of unstable polysulfide cross-links formed during vulcanization.

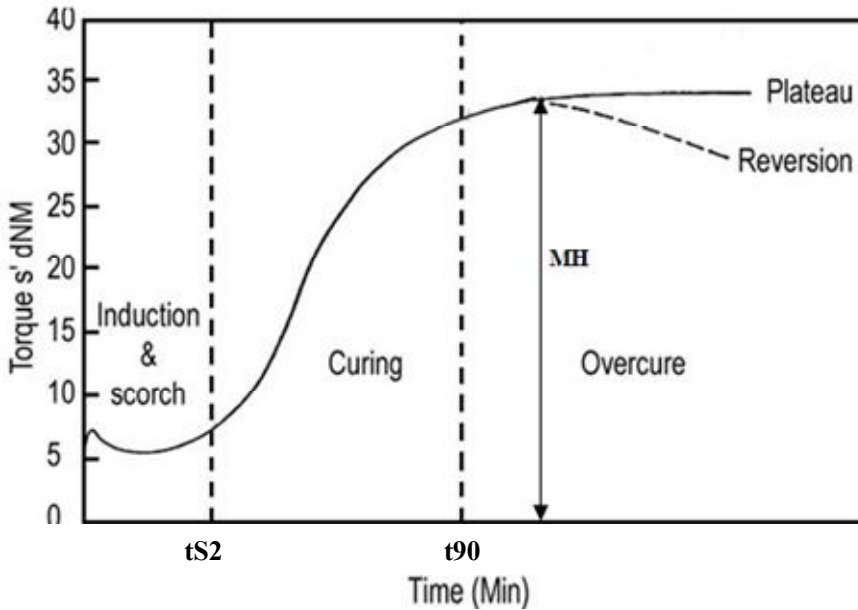


**Figure 14.** Vulcanization curve and determination of vulcanization characteristics

By means of vulcanization, rubber gains an elastic behavior and is able to maintain the shape after a deformation. The effects of this process on several properties are summarized in *figure 15*.

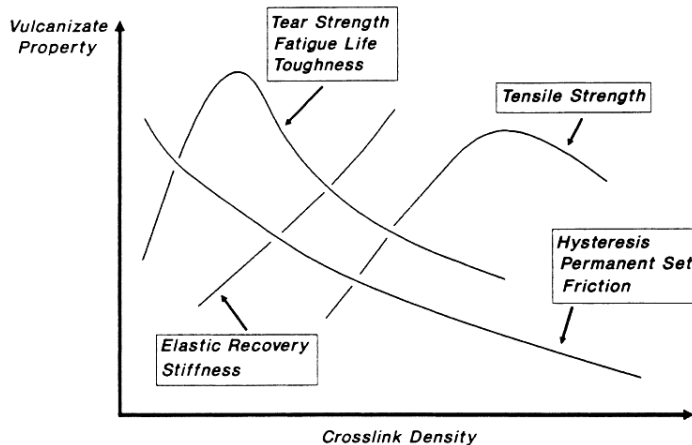


**Figure 15.** Effect of vulcanization on properties

High crosslink density reduces the hysteresis, whereas increases each property related to the energy-to-break.

## 1.7 THE REINFORCEMENT OF RUBBER

Rubbers cannot be used in their pure form because they lack in hardness and strength properties, so the addition of fillers is fundamental to enhance the polymers' properties, as shown in *figure 16*.

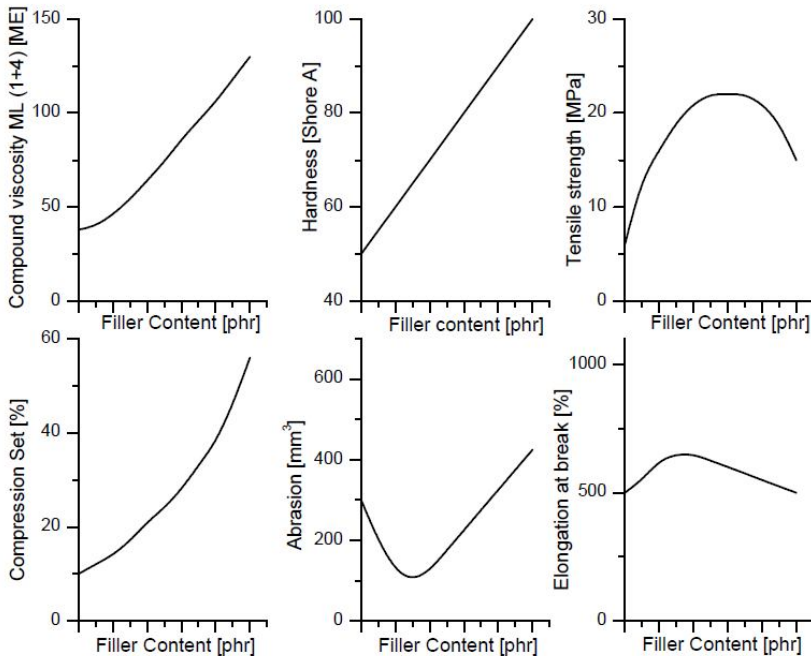


**Figure 16.** The influence of the amount of reinforcing fillers on compound properties

As illustrated and also mentioned before, rubber compound's hardness and viscosity increase and tensile strength improves after the addition of reinforcing filler. The reinforcement's entity depends on many parameters, such as polymeric matrix properties, filler properties (shape, particle size, structure, surface area and chemical nature), loading of polymer, as well as filler-filler and polymer-filler interactions.

Particle size distribution is one of the most important factors and *Table 2* summarizes its effects on the reinforcement (Donnet and Voet, 1976).

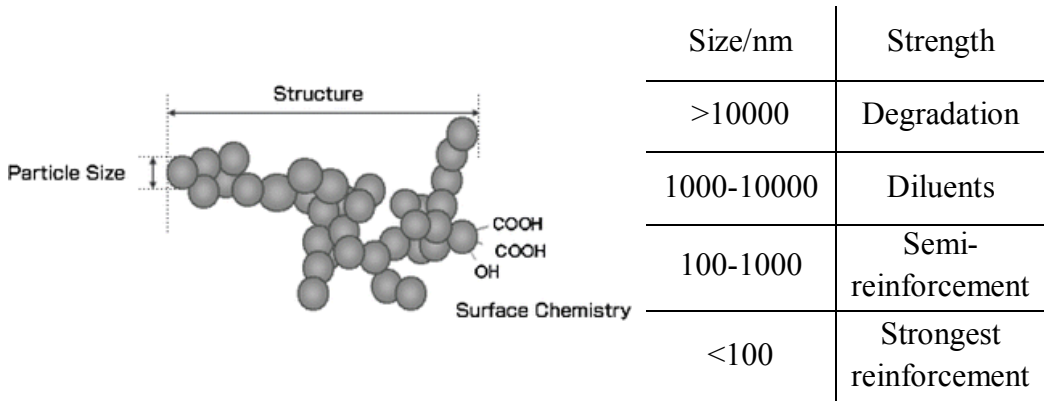


**Table 2.** Effect of particle size on the reinforcement

It comes to light that nanometric particles have the maximum reinforcement effect: in fact, fillers characterized by a too large particle size do not have reinforcement capabilities and facilitate the initiation of fracture phenomena, whereas particles too small can be very difficult to disperse and can form agglomerates that, in the end, act as large particles.

Also the particle shape influences the behavior of the filler: round particles can be dispersed better than fibrous and platy ones.

The filler structure or degree of irregularity depends on the tendency of primary particles to aggregate.

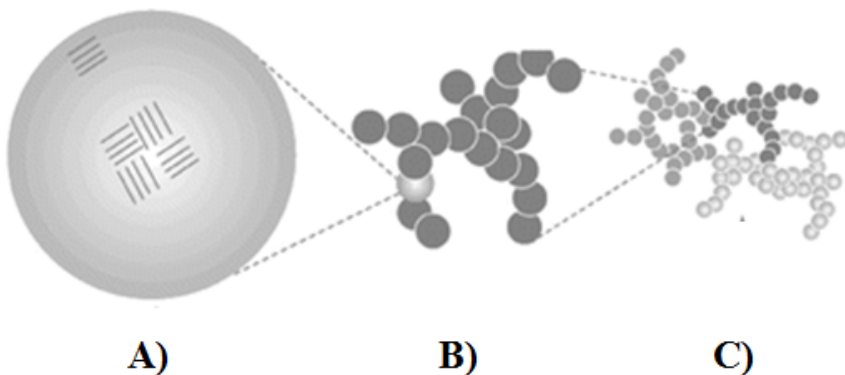


**Figure 17.** Filler primary particle (A), aggregates (B) and agglomerates (C)

Pertaining to *figure 17*, the smallest units that compose the filler are called primary or elementary particles (A); when they strongly bond to each other, they create aggregates (B) that cannot be divided through thermomechanical mixing. Agglomerates (C) are the result of the creation of weak bonds, like Van der Waals interactions, between primary particles and/or aggregates; thus, agglomerates can be separated by mixing.

The interaction between agglomerates and/or aggregates influences also the filler dispersibility. In fact, the higher the interaction strength, the lower the filler dispersion in the polymeric matrix achieved in the mixer.

A highly complex structure usually has branches that form voids which can cause the phenomenon of occluded rubber. The rubber trapped in the filler network does not behave like a rubber, but as an additional filler.

The surface area depends on primary particle size and determines the contacting area between filler and polymer. Reinforcing fillers like carbon black and precipitated silica have a high surface area (40-200 m<sup>2</sup>/g), while inert fillers like calcium carbonate, kaolin and magnesium silicate have a low surface area (1-20 m<sup>2</sup>/g) and are used as diluents in order to reduce costs and increase impermeability.

Surface area also influences the dispersion of filler into rubber. If this parameter is high, generally the filler is characterized by a fine primary particle size and by small aggregates which can easily interact with their neighbors forming a network that disadvantages the dispersion. On the other hand, however, a high surface area is also responsible for effective filler-polymer interactions.

Filler loading can promote the creation of a network too: the higher the loading, the higher the filler-filler interactions because the amount of particles in the same volume unit increases, the distance between them decreases and it is easier for them to aggregate strengthening the filler network.



The filler's chemical nature affects its reinforcement ability. In fact the functional groups on the surface determine the chemical and physical type of bonds that can be formed inside the filler and between the filler and the rubber.

The polymer-filler interaction depends not only on the filler's properties, but also on the mixing stage. At the beginning, before the filler is randomly dispersed, the polymer penetrates in the void space replacing air. After the addition of the filler, if a considerable filler-polymer interaction is established, a further dispersion is difficult because the bound rubber links many primary aggregates together. This phenomenon is responsible for the problems in dispersing fillers which have a simple structure and a high surface area: dense structures and small void spaces create a high concentration of filler and the opportunity for early interactions with the polymer. High structured fillers are more slowly incorporated, but more easily attain a satisfactory degree of dispersion.

A longer mixing step reduces the probability of creating a filler network.

In conclusion the filler reinforcement ability relies on two competitive processes: filler-filler and filler-polymer interaction. The increasing of the latter involves the decreasing of the former. A suitable reinforcing filler should have a good quality of dispersion and favor filler-polymer interactions.

The fillers play a fundamental role in dynamic and static behavior of compounds. *Figure 18* shows the variation of complex shear modulus ( $G^*$ ) versus dynamic shear deformation investigated by performing strain sweep test. The complex shear modulus:  $G^* = G' + iG''$  is a measure of materials overall resistance to deformation, where  $G'$  is the storage modulus that is a measure of elasticity of material and  $G''$  is the loss modulus in other words the ability of the material to dissipate energy.

$G^*$  decreases as strain increases owing to the Payne effect, the breakdown of both the polymer-filler and the filler-filler networks.

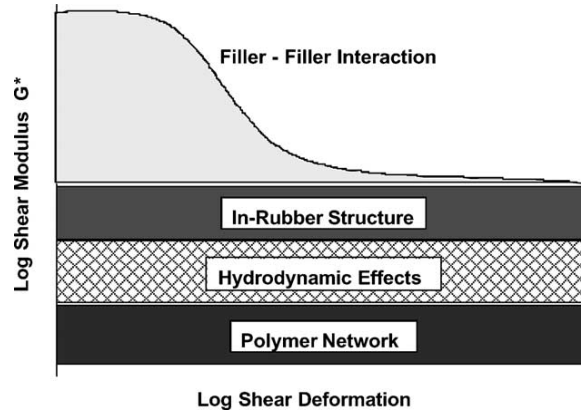


**Figure 18.** Shear modulus versus shear deformation

As shown in *figure 19*, at low strain filled compounds have a greater complex modulus than the rubber itself, but increasing the strain it rapidly diminishes. At low strain, rubber and compounds undergo reversible deformation: stretching of entanglements (A1) and linked polymer chains between filler molecules (C1) while the chains movement and filler-filler interaction do not suffer any deformation.

Increasing the strain, the modulus gradually diminishes due to both reversible responses such as stretching of entanglements (A2) and filler-polymer bonds (C2) and irreversible ones as chain movements (B2) and filler-filler breakdowns (D2). Chain scission, disentanglement or slippage of chain (B3) as well as filler-rubber and filler-filler breakdown take place at high strain. In this region the modulus, which falls gradually at medium strain, reaches its minimum value.

Although the presence of a filler boosts  $G^*$  modulus, filler-filler's breakdown as well as filler-polymer's disturbance take place by increasing the strain.

Modulus can be affected by different parameters as filler loading, particle size, surface area and active surface that are responsible for filler-filler network and filler-polymer interactions. High filler loading, low filler particle size and great surface area cause an increase of modulus  $G^*$ .

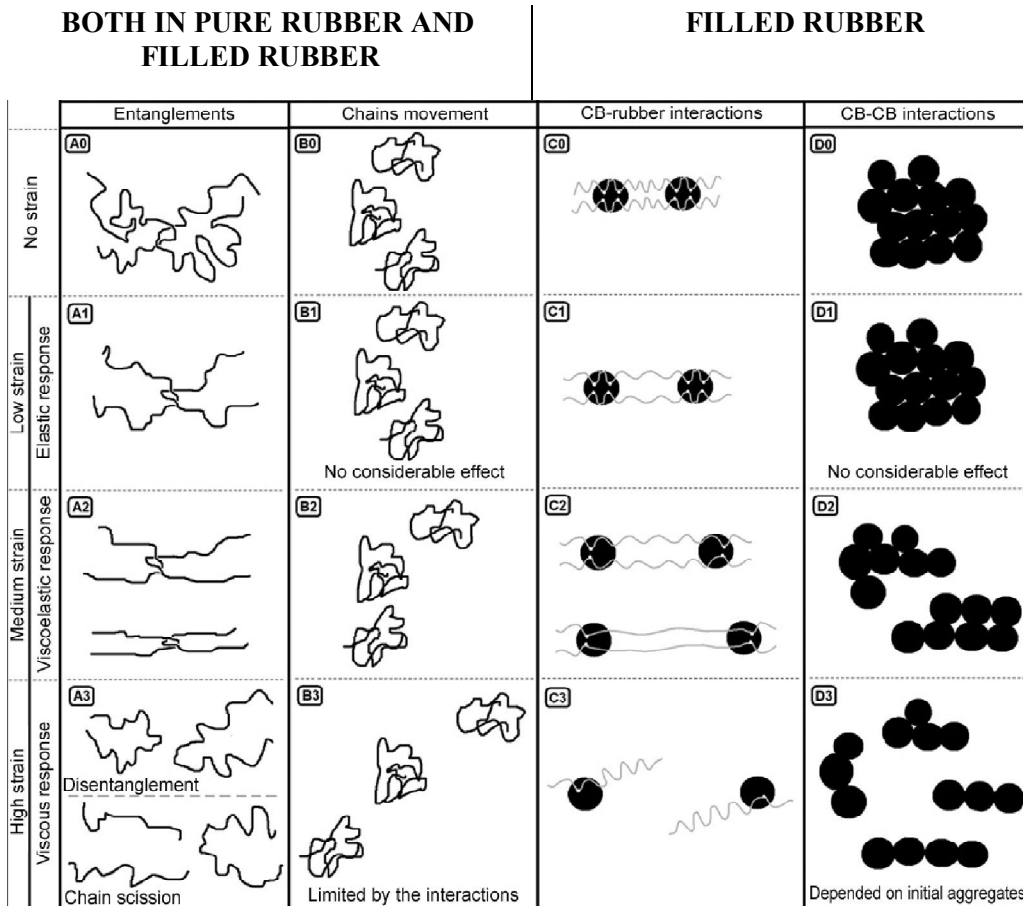


**Figure 19.** Possible responses at various strain regions for rubber and filled rubber (Karrabi *et al.*, 2011).

## 2 EXPERIMENTAL SECTION

### 2.1 MATERIALS

All reagents and solvents (ACS grade) were purchased from Sigma-Aldrich.

Rice husk was kindly provided by a local factory, Gariboldi S.p.A.

*Arundo donax* and *Wheat straw* steam-exploded samples were supplied by a local factory.

Protobind 1000<sup>®</sup>, Protobind 2000<sup>®</sup> and Protobind 3000<sup>®</sup> was purchased from Green Value.

Materials for rubber composite: Natural rubber latex (NR-latex) was latex 60% from Latex Plan-Hevea Ind. (latex from *Hevea brasiliensis* containing 60.0% rubber, 39.3% water, 0.7% ammonia), natural rubber (NR) was STR 20; Styrene butadiene rubber (SBR) was SBR 1500, N-(1,3-dimethylbutyl)-N'-phenyl-*p*-phenylenediamine, 6PPD was Santoflex-6PPD from Flexsys; stearic acid was Stearina TP8 from Undesa; carbon black was N 375 from Cabot; sulfur was from Zolfoindustria; zinc oxide was from Zincol Ossidi; Aromatic oil was MES from ENI SPA; N-*t*-butyl-2-benzothiazylsulphenamide, TBBS was Vulkacit NZ/EG-C from Lanxess; HMT was Rhenogran HEXA-80 that is a blend of 80% of HMT and 20% of elastomer binder and dispersing agents from Rhein Chemie.

### 2.2 IONIC LIQUID PRETREATMENT

#### 2.2.1 Rice husk preparation

Rice husk (50 g) was crushed in a laboratory blender until small enough to pass through a 1 mm screen. The ground material was Soxhlet extracted with c.a. 300 ml of acetone for 24 h. The air-dried, extractives-free blended rice husk was then milled in a planetary ball mill for different periods of time (5, 10, 15, 20, 30, 40 hours, 3 g each) at 300 rpm, using a 100 ml zirconium-grinding bowl

(zirconium dioxide 95%) in the presence of 6 zirconium balls (10 mm in diameter each).

## **2.2.2 Dissolution of rice husk into ionic liquid and regeneration techniques**

250 mg of blended or milled rice husk (5, 10, 15, 20, 30, 40 hours) was added in a screw top, round-bottom flask to 1.750 g of ionic liquid ([amim]Cl) and kept at 80°C overnight under stirring. The dissolution of blended, 5, 10, and 15 hours-milled samples was not complete whereas 20, 30, and 40 hours-milled samples resulted in homogeneous but not perfectly clear solutions due to the large ash content (about 16% w/w) featuring rice husk. After approximately 18 hours, the samples were precipitated from ionic liquid according to the following procedures:

### ***2.2.2.1 Acidic precipitation from ionic liquid***

After approximately 18 hours 20 ml of 0.1 M HCl solution was dropwise added to the ionic liquid dispersions. During the addition, the mixtures were vigorously vortexed and sonicated to prevent the formation of a thick gel. Then the mixtures were filtered on a sintered funnel (grade 3). Each filtrate was basified with NaOH pellets and stored for lignin content UV determination. The solid residues were thoroughly washed with deionized water, ethanol and finally dried with diethyl ether.

### ***2.2.2.2 Alkaline precipitation from ionic liquid***

After approximately 18 hours 20 ml of 0.1 M NaOH solution was added dropwise to the ionic liquid dispersions. During the addition, the mixtures were vigorously vortexed and sonicated to prevent the formation of a thick gel. The mixtures were maintained at 40°C under magnetic stirring for 30 minutes and

then filtered through a sintered funnel (grade 3). Each filtrate was stored for lignin content UV determination. The solid residues were thoroughly washed with deionized water, ethanol and finally dried with diethyl ether.

### ***2.2.2.3 Multistep alkaline/acidic precipitation from ionic liquid***

After approximately 18 hours, 20 ml of 0.1 M NaOH solution was added as described above. After 30 minutes at 40°C under magnetic stirring, the solutions were acidified adding HCl 37% dropwise until pH 2 was reached. The mixtures were then filtered through a sintered funnel (grade 3). Each filtrate was basified with NaOH pellets and stored for lignin content UV determination. The solid residues were thoroughly washed with deionized water, ethanol and finally dried with diethyl ether.

The dried residues were then weighed and submitted for enzymatic hydrolysis.

### **2.2.3 Recovery of soluble rice husk fractions**

The recovery of solubilized rice husk fractions was performed only for the alkaline and the multistep alkaline/acidic precipitation procedures involving 20 hours-milled rice husk samples to benefit of the extensive solubilization of the native material. Both the experimental procedures were performed on 2 g samples, using 12 g of ionic liquid for the dissolution and 60 ml of aqueous solution to precipitate out the insoluble material. The recovered filtrates were acidified with HCl 37% if needed, diluted with 150 ml of ethanol to promote hemicellulose and lignin-carbohydrate complexes (LCCs) precipitation, and stored in a refrigerator at +4°C overnight. The insoluble material was collected by centrifugation (3500 rpm, 15 min), washed with ethanol, and vacuum dried. The precipitation of a solid was noted as the solvent was evaporated in both cases. The phenomena were more pronounced for the alkaline samples. The water-enriched solutions were stored at +4°C overnight to allow for a complete

precipitation of the insoluble substance. The insoluble material was collected by centrifugation (3500 rpm, 15 min), washed with deionized water, and freeze-dried. The ethanol-insoluble and the water-insoluble recovered fractions were then merged together and analyzed by chromatographic and spectroscopic techniques.

#### **2.2.4 Enzymatic hydrolysis**

Approximately 200 mg of differently milled, untreated rice husk samples (blended, 5, 10, 15, 20, 30, 40 hours milled) and insoluble residues collected after regeneration from ionic liquid were dispersed into 35 ml of acetate buffer (pH 4.5) in an Erlenmeyer flask. After the addition of the crude cellulase enzyme (*T. reesei* ATCC 26921, 50 U/g), the flask was covered and placed in a shaker at 40°C for 48 hours. The insoluble material left after the enzymatic hydrolysis was collected by centrifugation (3500 rpm, 15 min), washed with acidified deionized water (pH 2) and freeze-dried. Each supernatant was UV analyzed for lignin content determination.

#### **2.2.5 UV determination of solubilized lignin**

One milliliter of each filtrate (recovered after the regeneration from ionic liquid) and supernatant (collected after the enzymatic hydrolysis) was transferred into a 5 ml vial and diluted with 4 ml of NaOH 0.1 M. The absorbance was measured at 280 nm. If necessary, the solution was diluted to adjust the absorbance into the linear range. A calibration curve was prepared using previously extracted acidolytic lignin from rice husk.

## 2.3 LIGNIN CHARACTERIZATION

### 2.3.1 Lignin content

The lignin content was measured according to the methodology reported by Yeh *et al.* The total amount of lignin is the sum of the acid-insoluble (Klason lignin) and acid soluble lignin.

#### *Acid soluble lignin*

Approximately 100mg of sample was put in a test tube. 2 ml of sulfuric acid solution 72% were added at room temperature for 2 hours with occasional stirring. The solution was diluted with deionized water to a 3% sulfuric acid concentration. The solution was transferred in to a sealed flask and heated at 121°C and 2 atm for 1 hour in a commercial pressure cooker. The solution was filter in crucible size M and washed with deionized water until neutral pH. The crucible was placed in a oven at 105°C over-night. The acid-insoluble lignin was determined gravimetrically.

#### *Acid soluble lignin*

The filtrate was diluted to 100 ml with deionized water.

The acid soluble lignin was calculated from U.V absorbance at 205 nm using an extinction factor of 110 (AU L)/(g cm). (Opt. Abs = 0.2-0.5).

The values reported are the average of 3 analyses  $\pm 1.0\%$  (P=0.05, n=3).

### 2.3.2 Ashes Content

The ashes content of fiber is defined as the residue remaining after ignition at 600°C for 3 hr, or longer if necessary to burn off all the carbon. It is a measure of mineral salts in the fiber.

Accurately weighed and dried samples (100 mg) were put in tared, well desiccated porcelain crucibles and placed in a muffle furnace set at 550°C for 3 hours. The crucibles were then stored in a desiccator until room temperature



was reached. The ash content was determined gravimetrically. The values reported are the average of 3 analyses  $\pm 1.0\%$  ( $P=0.05$ ,  $n=3$ ).

### 2.3.3 Lignin extraction

To produce purified lignin, the starting material was submitted to an alkaline cooking in 1% NaOH aqueous solution under continuous stirring for 30 minutes at 50°C. At the end of extraction, the treated material was centrifuged to separate the liquid and the solid fraction. This procedure was repeated twice. The filtrate was acidified with HCl until pH 1 to allow for the lignin to precipitate. The insoluble matter was then collected by centrifugation (4000 rpm, 15 min), washed with deionized water and air dried. The yield of the reaction was 36% respect to the starting material.

### 2.3.4 $^{31}\text{P}$ NMR Derivatization

Accurately weighted lignin samples (40 mg) were dissolved in a pyridine-deuterated chloroform solution (1.6:1 v/v ml, 800  $\mu\text{l}$ ) containing 1 mg/ml of chromium(III) acetylacetonate,  $[\text{Cr}(\text{acac})_3]$  and 100  $\mu\text{l}$  of *endo*-N-hydroxy-5-norbornene-2,3-dicarboximide (e-HNDI) solution (121.5 mM,  $\text{CDCl}_3/\text{pyridine}$  4.5:0.5). Then 100  $\mu\text{l}$  of 2-chloro-4,4,5,5-tetramethyl-1,3,2-dioxaphospholane as the derivatizing agent was added (Argyropoulos, D.S 1994). The  $^{31}\text{P}$  NMR spectra were recorded at 308 K on 800  $\mu\text{l}$  samples using a Bruker 500 MHz instrument. The  $^{31}\text{P}$  NMR data reported are averages of three experiments. The maximum standard deviation of the reported data was  $2 \times 10^{-2}$  mmol/g, while the maximum standard error was  $1 \times 10^{-2}$  mmol/g.

### 2.3.5 $^{13}\text{C}$ NMR

Accurately weighted acetylated lignin samples (30-50 mg) were dissolved in  $d_6$ -DMSO. The  $^{13}\text{C}$  NMR spectra were recorded at 308 K on 800  $\mu\text{l}$  samples using

a Bruker 500 MHz instrument. A relaxation delay of 10 s was used between the scans. Line broadening of 2-5 Hz was applied to FIDs before Fourier transform. For each spectrum, about 8000 scans were typically accumulated.

### **2.3.6 GPC**

The GPC analyses were performed on a Waters 600 E liquid chromatography connected with an HP1040 ultraviolet diode array (UV) detector set at 280 nm for acetylated samples and at 240 nm in the case of benzoylated samples. The injection port was a 20  $\mu$ l Rheodyne loop valve, the chromatographic system was composed by a sequence of an Agilent PL gel 5  $\mu$ m, 500  $\text{Å}$  column followed by an Agilent PL gel 5  $\mu$ m, 104  $\text{Å}$  column. 220-400 K and the solvent used was tetrahydrofuran (Fluka 99.8%). PL Polymer Standards of Poly Styrene from Polymer Laboratories (Amherst, MA, USA) were used for the calibration Acetylated and benzoylated samples were dissolved in THF (1 mg/ml), filtered through a 0.45  $\mu$ m GHP syringe filter and analyzed at a flow rate of 1 ml/min. The evaluation of the number-average molecular weight ( $M_n$ ), the weight-average molecular weight ( $M_w$ ) and polydispersity index (I) was performed following the methodology reported by Salanti *et al.* 2010.

### **2.3.7 Elemental analysis**

The quantitative determination of carbon, nitrogen and hydrogen in the structure was made with a Perkin Elmer 2400 series II CHNS/O elemental analyzer.

### **2.3.8 Density**

The density of lignin samples was determined with a pycnometer (MicroMeritics AccuPyc 1330) that works by measuring the amount of displaced gas (helium).

### **2.3.9 Morphological analysis**

The particle size is one of the most important characteristic that influence the interaction between filler and polymer and the reinforcement characteristic.

#### ***2.3.9.1 Sieve Analysis Methods***

Sieve analysis was carried out in accordance with ASTM C136-06 procedure. The sieve analysis consists of series of sieves organized in sequence with the openings decreasing going from top to bottom.

Accurately weighted sample was poured into the top sieve and after submitting the sieve column to vibration for 5 minutes, the material in each sieve was weighted and expressed as percentage in respect to the total weight of the sample.

#### ***2.3.9.2 Particle size distribution of powders with Laser scattering***

##### ***Particle Size Distribution Analyzer LA-960V2***

This instrument consists of two light sources that generate two laser beams that pass through a dispersion of particles in water producing diffracted light. The angle of diffraction increases as particle size decreases.

The scattered light over a wide range of angles was detected by an array of high quality photodiodes (3-4). A schematic image of the operation of the analyzer is shown in the *figure 20*.

The software converts the scattered light on the detectors to the particle size distribution of the sample analyzed according to Mie Theory.

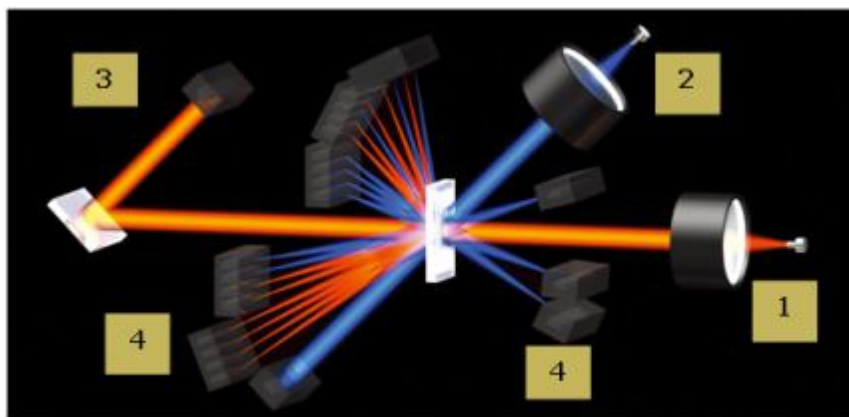


**Figure 20.** Operation of the Laser scattering Particle Size Distribution analyzer  
Two different wavelength light sources are required in order to extend the lower detection limit of the technique.

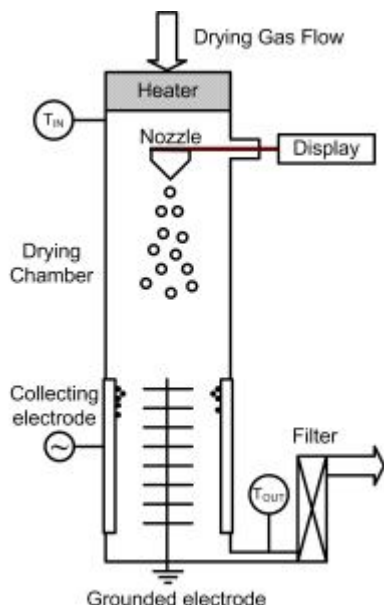
### 2.3.10 Optical microscope

Optical microscope images were carried out by optical microscope Leica DM L.

### 2.3.11 FT-IR

Infrared spectra of the bio polymer were obtained in the attenuated total reflectance (ATR) mode on a Nicolet Is10 FT-IR Spectrometer Thermo Scientific. The spectra were recorded between 400 to 4000  $\text{cm}^{-1}$  at resolution of 2  $\text{cm}^{-1}$ . Thirty-two scans were performed for each sample. The spectra were baseline corrected for further analysis. The wavelength values are expressed in  $\text{cm}^{-1}$ .

### 2.3.12 Spray drying



The sample is composed of 30 g solid material and was solubilized in 300 ml of acetone. The sample was added slowly to acetone and was kept under magnetic stirring until complete solubilization of the material. The experiment was performed using Buchi Mini Spray Dryer B-290 advanced.

In this dryer, pressurized nitrogen (5 bar) was used as spray gas and high-performance cyclone separated the nitrogen-powder mix.

Three different experiments have been done at different inlet temperature. Then 10 ml of sample was diluted 10 times with acetone to obtain a 1 % solution for the experiment with the Nano Spray Dryer B-90.

## 2.4 LIGNIN MODIFICATION

### 2.4.1 Milling

The dry lignins were milled in a planetary ball mill for 20 h at 300 rpm, using a 100 mL zirconium-grinding bowl (zirconium dioxide 95%) in the presence of two zirconium balls (5mm in diameter each), two zirconium balls (10 mm in diameter each) and one zirconium balls (15 mm in diameter).

### 2.4.2 Lignin acetylation

100 mg of lignin was acetylated in 2 ml of an acetic anhydride:pyridine solution (1:1, v/v) kept overnight at 40 °C. At the end of the reaction the solution was stripped with ethanol, toluene and chloroform (20 ml x 3 times each), then the sample was dried in vacuum.

### **2.4.3 Lignin and biomass acetylation with acetic anhydride and 1-Methylimidazole**

The acetylation reaction of lignin was carried out using the following method (Fox and McDonald, 2010): dry lignin (100 mg) was placed in a flat bottom flask and acetic anhydride (1 ml) and 1-methylimidazole (15  $\mu$ l, 0.2 mmol) were added under stirring obtaining a slurry. The flask was dipped into an oil bath set at 120°C and fitted with a reflux condenser for 1h. When the reaction was completed, the flask was removed from the oil bath. The mixture was added drop by drop, under stirring, into an Erlenmeyer flask containing deionized water obtaining a suspension.

The suspension was then stirred to allow the excess acid anhydride to decompose. Once the flask had cooled, the precipitated lignin was filtered with Buchner. The flask was washed several times with deionized water to remove any remaining lignin, and the collected lignin was washed several times with water to remove any carboxylic acid and catalyst traces and then air dried.

### **2.4.4 Purification of acetylated biomass**

Acetylated biomass was dissolved in acetone and kept under stirring for 2 h. The solid was filtered off through a Buchner, washed with further acetone and air dried.

### **2.4.5 Lignin benzylation**

Ionic Liquid, 1-allyl-3-methylimidazolium chloride ([amim]Cl, 950 mg), was added to the pulverized lignocellulose (50 mg) in a 8 ml dried sample bottle equipped with a mechanical stirrer, vortexed and heated at 80°C until the solution was clear (18 hrs, overnight). Pyridine (230  $\mu$ l, 2.6 mmol) was added; the solution was vortexed until it was homogeneous and allowed to cool to room temperature. Then benzoyl chloride (280  $\mu$ l, 2.4 mmol) was added in one

portion and vortexed until a homogeneous paste was formed. The sample was kept under magnetic stirring at room temperature for 2 hours. To precipitate the benzoylated product, a deionized water-ethanol solution (1:3 v/v, 20 ml) was added and the mixture vigorously shaken and vortexed for 5 min. The solid was filtered off through a sintered funnel (grade 3), washed with further ethanol and purified with methanol.

#### **2.4.6 Lignin allylation (1<sup>st</sup> method)**

The allylation reaction was carried out using the following method: dry lignin (100 mg) was placed in a round bottomed flask and potassium carbonate (50 mg, 0.35 mmol), allyl bromide (44  $\mu$ l, 0.5 mmol) and acetone were added. The flask was dipped into an oil bath set at 65°C and fitted with a reflux condenser for 8 h. After cooling, the mixture was poured drop by drop, under stirring, into an Erlenmeyer flask containing acidic water (pH=1), then was filtrated on Buchner and air dried.

#### **2.4.7 Lignin allylation (2<sup>nd</sup> method)**

The allylation reaction was carried out using the following method: dry lignin (100 mg) was solubilized in a acetone and NaOH solution (0.2 M) in a round bottom flask and allyl bromide (44  $\mu$ l, 0.5 mmol) was added. The flask was dipped into an oil bath and fitted with a reflux condenser for 4 h at 70°C. The acetone was distillated off. The water solution was acidified with HCl and the allylated lignin was recovered by filtration.

#### **2.4.8 Lignin partial allylation**

The allylation reaction was carried out using the following method: dry lignin was solubilized in a acetone and NaOH solution (0.2 M) in a round bottom flask and allyl bromide (1.5 mmol/1 g lignin) was added. The flask was dipped

into an oil bath and fitted with a reflux condenser for 4 h at 70°C. The acetone was distilled off. The water solution was acidified with HCl and the allylated lignin was recovered by filtration.

#### **2.4.9 Allylated lignin acetylation**

The acetylation reaction of allylated lignin was carried out using the following method (Fox and McDonald, 2010): dry lignin (100 mg) was placed in a flat bottom flask and acetic anhydride (0.5 ml) and 1-methylimidazole (15  $\mu$ l, 0.2 mmol) were added under stirring obtaining a slurry. The flask was dipped into an oil bath set at 120°C and fitted with a reflux condenser for 1 h. When the reaction was completed, the flask was removed from the oil bath. The mixture was added drop by drop, under stirring, into an Erlenmeyer flask containing deionized water obtaining a suspension.

The suspension was then stirred to allow the excess acid anhydride to decompose. Once the flask had cooled, the precipitated lignin was filtered with Buchner. The flask was washed several times with deionized water to remove any remaining lignin, and the collected lignin was washed several times with water to remove any carboxylic acid and catalyst traces and then air dried.

#### **2.4.10 Lignin allylation and acetylation (scale up)**

The allylation reaction was carried out using the following method: dry lignin (200 g) was placed in a round bottomed flask and potassium carbonate (95 g), allyl bromide (90 ml) and acetone were added. The flask was dipped into a bath set at 65°C and fitted with a reflux condenser for 8 h. At the end of the reaction the acetone was distilled off. Acetic anhydride and 1-methylimidazole were added under stirring obtaining a slurry. The flask was dipped into an oil bath set at 120°C and fitted with a reflux condenser for 1 h.



When the reaction was completed, the flask was removed from the oil bath. The mixture was added drop by drop, under vigorous stirring, into an Erlenmeyer flask containing deionized water obtaining a suspension.

The suspension was then stirred to allow the excess acid anhydride to decompose. Once the flask had cooled, the precipitated lignin was filtered with Buchner. The flask was washed several times with deionized water to remove any remaining lignin, and the collected lignin was washed several times with water to remove any carboxylic acid and catalyst traces and then air dried.

#### **2.4.11 Reaction of lignin with Hexamethylenetetramine (HMT)**

The reaction was carried out using the following method (Falkehag 1970): dry lignin (100mg) was slurred in 5 ml of water. To this slurry 10% NaOH aqueous solution (6 $\mu$ l) and 33% NH<sub>3</sub> aqueous solution (27 $\mu$ l) were added and the mixture stirred for 2 minutes. Then hexamethylenetetramine (10mg) was added. The flask was dipped into an oil bath set at 100°C and fitted with a reflux condenser for 6 h. At the end of the reaction the NH<sub>3</sub> was distilled off; acetic acid was added and the mixture agitated for 2 minutes to form an emulsion and then air dried.

#### **2.4.12 Reaction of lignin with coupling agent Bis-[ $\gamma$ -(triethoxysilyl)-propyl]-Tetrasulfide (Si69)**

The reaction of lignin with Bis-[ $\gamma$ -(triethoxysilyl)-propyl]-tetrasulfide (Si69) was carried out using the following method (Blume 2011): a solution of Si69 in squalene was added to the solution of lignin in squalene and kept for 30 minutes at 120°C. The reacted lignin was recovered by filtration followed by a soxhlet extraction in methanol for 16 h. The yield of the reaction is 10%.

### **2.4.13 Coagulation of NR from latex**

The latex solution was precipitated by means of the adding of sulfuric acid solution. The obtained product was filtered, washed several times with distilled water and then vacuum dried.

### **2.4.14 Co-precipitation of NR with lignin from latex**

NR and lignin was co-precipitated from latex by means of the addition of sulfuric acid solution. The obtained product was filtered, washed several times with distilled water and then vacuum dried.

## **2.5 COMPOUND PREPARATION**

### **2.5.1 Mixing process (Haake)**

All compounds were prepared in two steps: the first step using a Haake at a rotor speed of 60 rpm while the second step in two roll mill according to the composition shown in *Table 3*.

All components, except vulcanization agent, were mixed on Haake Rhecord internal mixer for 6 minutes at 90°C. At time zero the rubber was introduced, after 1 minute half carbon black and biofiller, at 1'30'' half carbon black and oil and after 3 minutes Stearic acid, 6PPD and zinc oxide.

In the second step the rubber compound was mixed in a two roll mill at 40°C for 6 minutes with accelerator and soluble sulfur.

Ingredients	phr
1° step	
STR 20	50
SBR 1500	50
Carbon black	65
Stearic acid	2
Zinc oxide	3
Aromatic oil	10
6PPD	2
2° step	
Sulfur	1.5
TBBS	0.8

Ingredients	phr
1° step	
STR 20	50
SBR 1500	50
Carbon black	50
Biofiller	15
Stearic acid	2
Zinc oxide	3
Aromatic oil	10
6PPD	2
2° step	
Sulfur	1.5
TBBS	0.8

**Table 3.** Formulation of reference compound (on the left) and formulation of compound with the partial replacement of 15 phr of carbon black with the biofiller.

### 2.5.2 Mixing process (Brabender)

All components, shown in *Table 4*, were mixed on Brabender internal mixer for 10 minutes at 90°C. At time zero the rubber was introduced, after 3 minutes Stearic acid and zinc oxide and after 6 minutes CBS and Sulfur.

Ingredients	phr
NR coagulated from latex	100
Stearic acid	2
Zinc oxide	5
CBS	2
Sulfur	2

Ingredients	phr
NR co-precipitated with 7-15 phr purified lignin from latex	107-115
Stearic acid	2
Zinc oxide	5
CBS	2
Sulfur	2

**Table 4.** Formulation of reference compound (on the left) and formulation of compound with the introduction of biofiller

### 2.5.3 Vulcanization process

2 mm thickness rubber sheets were compression molded at 170°C for SBR and 150°C for NR and pressure 4.3 bar for 10 minutes using an electrically heated hydraulic press BM Biraghi while for compounds realized at DIK, the

vulcanization has been done at  $t_{90}$  (optimum cure time) plus two minutes (one minute each millimeter of thickness).

## **2.6 COMPOUND CHARACTERIZATION**

### **2.6.1 Density**

The standard procedure for the measure of density is given in ISO 2781 Method A using water as a reference liquid.

### **2.6.2 Viscosity ML**

The Mooney viscosity was determined on uncured samples by using a Mooney viscometer, Alpha Technologies MV 2000 E at 100°C according to the standard procedure described by ASTM D1646.

Mooney viscosity is expressed as: ML (1+4) 100°C where M is the Mooney viscosity, L indicates the use of large rotor, 1 is the preheating time in minutes, 4 is the reading time in minutes and 100°C is the test temperature.

### **2.6.3 Kinetics of vulcanization**

The standard procedure for kinetics of vulcanization is described by ISO 6502. Vulcanization curves were recorded using a Moving Die Rheometer (RPA2000, Alpha Technologies) operating at 170°C or 150°C, rotor frequency 1Hz and running time 30 minutes.

The curing characteristics of the rubber composite, were expressed in terms of the vulcanization times,  $t_{S2}$  (scorch time) and  $t_{90}$  (optimum cure time), as well as the maximum and minimum values of the torque, MH[dN m] and ML[dN m].

After vulcanization for all tests, 16 h is the minimum time between the forming and the testing of material.

### **2.6.4 Rebound resilience**

The measurement of rebound resilience is standardized in ISO 4662 with Control Systems Instruments model AL/4.

The method verifies the ability to the compound to return to original shape after deformation.

### **2.6.5 The hardness**

The hardness is measured according to the method ISO 48 with the DURATRON of Alpha Technologies for measure at 23°C and with Control Systems Instruments model HRT-48 for other temperatures.

The *IRHD (International Rubber Hardness Degrees)* instrument has a spherical indenter which indents the sample under a minor and a major load. The differential indentation depth is measured and tabulated to read directly in "IRHD" degrees. The internationally accepted standard dead load method is given in ISO 48 which covers rubbers in the range 10 to 100 IRHD.

The hardness is measured according to the method ASTM D2240 for the compounds done at DIK.

### **2.6.6 Tensile properties**

Tensile stress-strain properties, include tensile strength (TS), elongation at break (Eb) and tensile modulus (M50, M100, M200, M300, M500), were performed according to UNI 6065. The tensile test involves stretching standard test pieces to breakage at constant speed using a tension testing machine. The values reported are the average of 3 analyses.

### **2.6.7 Compression dynamic mechanical test**

Shear modulus  $G'$  and  $G''$ , complex shear modulus  $G^*$  and  $\tan \delta$  are measured according to the method ASTM D6204-12 with the Rubber Process Analyzer

(RPA2000, Alpha Technologies). The strain sweep tests were carried out at  $T=70^{\circ}\text{C}$  and 1 Hz from 0.2 to 100% of elongation. In order to evaluate the effect of vulcanization on the dynamic mechanical properties, the samples were heated at  $170^{\circ}\text{C}$  for 10 minutes (corresponding to the vulcanization time and temperature), then cooled down to  $70^{\circ}\text{C}$  for 10 minutes before performing a new strain sweep test. Specimens for the analysis were cut by a Constant Volume Rubber Sample Cutter (CUTTER 2000, Alpha Technologies) from the uncured samples with weight  $5 \pm 0.3$  g.

### **2.6.8 Dispergrader analysis**

The determination of filler dispersion in technical rubber goods and in tyre compounds is of great importance for the industry. The dispersion quality has a direct impact on final product properties and is also often used as parameter of the quality control system.

According to the method described in the ISO/DIS 11345 the Dispergrader 1000-Optigrade works with a light source at an angle of  $30^{\circ}$  with respect to the observation surface (*Figure 21*) and uses a magnification of 100x. The image obtained is transformed by numerical treatment in a black and white image that has been compared with the images in the software to assign X value. The Y value is calculated by an histogram of size distribution. “X” parameter is the best indicator of the filler dispersion. The level of the overall dispersion is expressed with a numerical value ranging from 1 to 10 (1 = worst, 10 = best). The “Y” value must be regarded as an evaluation of the dimension of the largest agglomerates present in the sample.

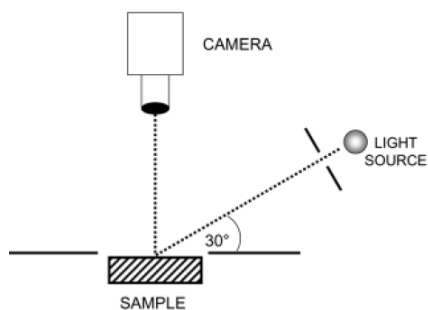


**Figure 21.** Operation of dispergrader

### **2.6.9 SEM**

The lignin powders and compounds were investigated by using Field Emission Scanning Electron Microscope FESEM ULTRA PLUS Zeiss.

### **3 RESULTS AND DISCUSSION**

Lignocellulosic biomass is a complex natural composite of cellulose, hemicellulose, lignin, ashes and other soluble substances called extractives. Overcoming the recalcitrant structure of lignocellulose to release the locked polysaccharides of cellulose is one of the major priorities for the emerging cellulosic ethanol and bio-based chemical industries. A number of lignocellulose pretreatment technologies including steam explosion, hot water/auto-catalyzed pretreatment, dilute acid, aqueous lime or NaOH pretreatment, ammonia, and organosolv pretreatment are under intensive investigation but most of them suffer from relatively low sugar yields, severe reaction conditions, and high processing costs. A new approach on physico-chemical pretreatment of biomass is the use of ionic liquids (ILs).

#### **3.1 IONIC LIQUIDS PRETREATMENT OF RICE HUSK**

Rice is among the most cultivated crops in the world with a global production of about 680 million tons/year ([www.fao.org](http://www.fao.org) FAOSTAT Database, 2008). Rice husk, the outer cover of rice grain accounting for about 20% w/w of rice, it is one of the major agro-industrial side-product produced worldwide. Averagely, rice husk is composed by 4.7% extractives, 26% lignin, 16.8% ashes, and 52.6% carbohydrates (Salanti *et al.*, 2010). Despite its widespread and annual availability, only few works in literature deal with rice husk pretreatment, enzymatic saccharification and fermentation.

Rice husk samples, both milled for different time periods and simply ground, were dispersed overnight in [amim]Cl at 80° C and then regenerated by addition of either an acidic aqueous solution, or an alkaline aqueous solution, or via a multistep (alkaline-acidic) precipitation as described in the experimental section. Acidic and alkaline aqueous solutions are known to readily dissolve



hemicellulose and lignin respectively. The multistep regeneration, involving a first alkaline regeneration directly followed by a second step concerning the acidification of the mixture, was attempted as a viable way to obtain rice husk samples consisting of a physical mixture of the proper water-insoluble material and re-precipitated lignin.

Each solid residue was dried and weighed to calculate the weight loss. Each filtrate was UV analyzed to determine the amount of solubilized lignin. Within a specific regeneration procedures, weight losses become greater as the milling time is raised, reaching a plateau for the more pulverized samples. When equal milling times are considered, an increasing trend of the weight loss percentage was observed going from the acidic, to the alkaline, and finally to the multistep aqueous regeneration technique.

For the acidic regeneration experiments, the weight losses were found to be really low while the weight loss of both the alkaline and the multistep regeneration was much higher and comprised between 10 and 30%.

In the alkaline procedure the solubilized fractions were for the most part represented by lignin while for the multistep alkaline-acidic regeneration procedure, the carbohydrates were found to be the highest solubilized fractions. It is well established that hemicellulose and lignin are covalently associated through LCCs. In particular, in herbaceous plants hydroxycinnamic acids (mostly ferulic and *p*-coumaric acid) are attached to lignin and hemicellulose forming lignin/phenolics-carbohydrate complexes (Buranov and Mazza, 2008). The phenolic bridge is attached to lignin via ether bonds and to carbohydrates via ester bond. In the Gramineae, these alkali-labile ester linkages predominate over alkali-stable bonds such as phenyl glycosidic and benzylether linkages (Ford, 1990) found in wood. Because of this difference, half of the total phenolics in herbaceous plants can be removed with sodium hydroxide at

ambient temperature. Thus, the alkaline regeneration procedure was expected to lixiviate both intact LCCs and unbound (i.e., not linked to polysaccharides) lignin macromers. Such unbound lignin fraction might be represented by both natively free lignin and lignin macromolecules released after alkali-labile bonds cleavage, as described above. In the alkaline-acidic regeneration procedure, the second step involving the neutralization of NaOH resulted in the precipitation of a certain amount of lignin fraction previously alkali-solubilized.

When the outcomes of the enzymatic hydrolysis on the three differently regenerated rice husk were analyzed, it was found that the best results over the whole milling periods tested were achieved using the multistep regeneration procedure. These results were regarded as an evidence of the crucial role played by lignin and, especially, hemicellulose in the inhibition of the enzymatic hydrolytic process.

To confirm the chemical composition of the rice husk fractions solubilized during the aqueous regeneration from ionic liquid, GPC and quantitative  $^{31}\text{P}$ -NMR analyses were performed.

*Figure 22* reports the acetylated chromatograms of the recovered fractions along with molecular weight distributions concerning acetylated native rice husk, acetylated hemicellulose extracted, and acetylated lignin extracted from rice husk, all used as reference signals. The soluble material recovered after alkaline-regeneration procedures contains lignin-carbohydrate complexes, the predominant peak of the molecular weight distribution, and a certain amount of unbound lignin, represented by a shoulder in the low molecular weight region of the chromatogram. Concerning the soluble material collected from the multistep alkaline/acidic regeneration procedure, the molecular weight distribution showed higher molecular weights and a bimodal trend, resembling the distribution observed for rice husk hemicelluloses.

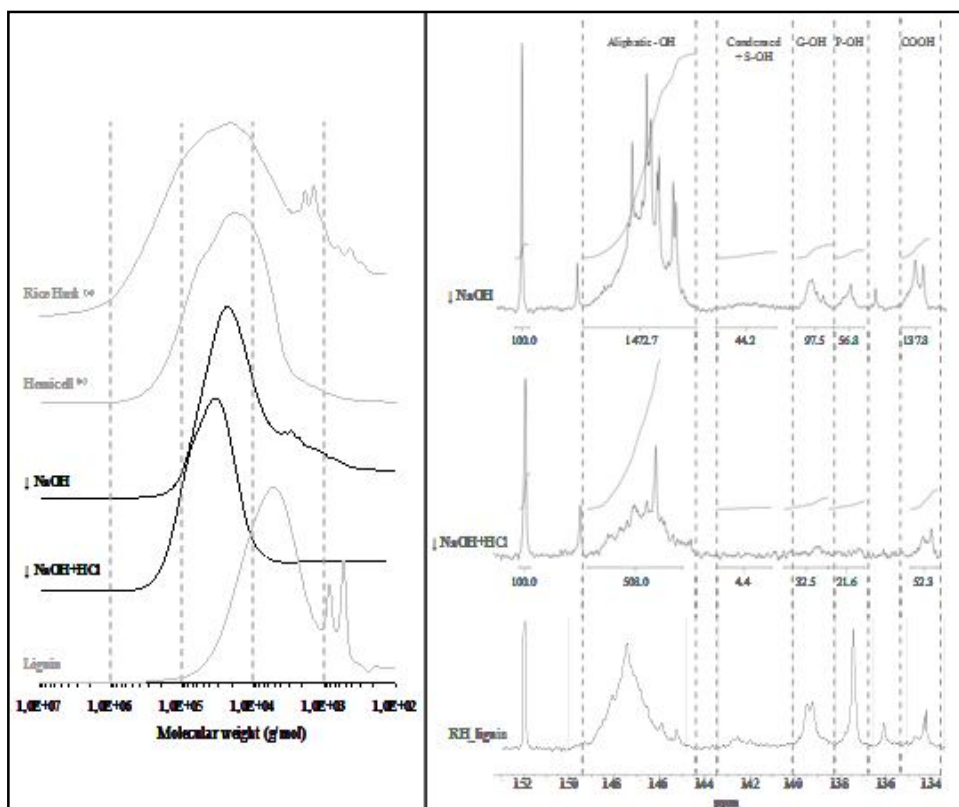


**Figure 22.** GPC profiles of acetylated soluble rice husk fractions (left) and  $^{31}\text{P}$ -NMR spectra (right) of soluble rice husk fractions recovered after ionic liquid dissolution followed by alkaline and multistep (alkaline-acidic) regeneration. GPC profiles of native rice husk acetylated samples, extracted rice husk hemicellulose, and acidolysis rice husk lignin are reported as reference signals (grey lines).  $^{31}\text{P}$ -NMR spectrum of rice husk acidolysis lignin is also reported as reference. (a) Chromatograms reported in a previous work (Salanti *et al.*, 2012).

Figure 22 reports the  $^{31}\text{P}$ -NMR spectra of the alkaline- and the multistep-soluble rice husk fractions, respectively. Comparing the  $^{31}\text{P}$ -NMR spectra of the alkaline-soluble fraction and the acidolysis lignin, taken as reference, the presence of several resolved peaks in the aliphatic region, along with well represented signals related to free phenols was noted for the alkali-soluble fraction. Sharp and resolved peaks in the aliphatic region are diagnostic for the presence of carbohydrate impurities into lignin samples (Salanti *et al.*, 2010). Moreover, the fair amount of condensed and syringyl units detected supported

the hypothesis of a solubilized fraction consisting of the most part of unbound oligomeric/polymeric lignin.

On the contrary, when the multistep-soluble material was examined, a low amount of free phenols was detected, in agreement with the hypothesized exclusive presence of lignin-carbohydrate complexes involving hemicellulose and non-core lignin in this sample. In both cases, the presence of carboxylic acids was consistent with the occurrence of uronic acids into hemicellulose structure.

As reported by Ragauskas *et al.* (2006) the lignocellulosic biorefinery is not important only for the recovery of carbohydrates but also for the added value of lignin. Lignin obtained as by-product after the ionic liquid pretreatment followed by alkaline or multistep regeneration, that gave the best results in terms of cellulose digestibility, presents carbohydrates impurities in both cases. These impurities will be deeply discussed hereinafter in terms of the possible use of lignin as a biofiller.

### **3.2 STEAM EXPLOSION PRETREATMENT OF WHEAT STRAW AND ARUNDO DONAX**

Steam explosion is considered the most effective and least costly pretreatment for biomass. This process allows to break the linkages between cellulose, hemicelluloses and lignin without the use of chemicals but only with high pressurized steam. Cellulose and hemicelluloses are broken down into their monomers by the addition of hydrolytic enzymes. As a by-product of this process, a waste biomass enriched in lignin is obtained.

### 3.2.1 Characterization of steam exploded biomass

The materials are wastes of annual plants (*Arundo donax* and *Wheat straw*) recovered after steam explosion treatment. On these materials a preliminary chemical characterization has been done. After drying the starting materials in oven at 40°C overnight, the lignin and ashes content in them was determined and their composition was ascertained. The amount of polysaccharides has been calculated by mass difference, once known the amount of water, lignin and ash according to the equation: [100% - (water content + lignin content + ash content)].

Moreover, the materials have been characterized by GPC analyses, in order to identify the molecular weight distributions, and by means of quantitative <sup>31</sup>P-NMR spectroscopy to determine the amount of aliphatic hydroxyls, condensed and syringyl phenolic moieties (Cond PhOH + S-OH), guaiacyl units (G-OH), *p*-coumaryl alcohols (P-OH), and carboxylic acid functionalities (COOH). Results relating to compositional evaluation, GPC, and <sup>31</sup>P-NMR characterization are reported in *Table 5*.

	<i>Arundo Donax</i>	<i>Wheat straw</i>
Water (%)	4.8	2.2
Ashes (%)	10.0	16.1
Klason lignin (%)	52.1	56.8
Polysaccharides (%)	33.1	24.9
<b>GPC</b>		
M <sub>n</sub> (g/mol)	3500 <sup>a</sup>	2500 <sup>a</sup>
M <sub>w</sub> (g/mol)	9500 <sup>a</sup>	6900 <sup>a</sup>
I	2.8 <sup>a</sup>	2.8 <sup>a</sup>
<b><sup>31</sup>P NMR</b>		
Aliphatic OH (mmol/g)	3.29 <sup>a</sup>	2.39 <sup>a</sup>
Condensed PhOH + S-OH (mmol/g)	0.48 <sup>a</sup>	0.58 <sup>a</sup>
G-OH (mmol/g)	0.45 <sup>a</sup>	0.46 <sup>a</sup>
P-OH (mmol/g)	0.19 <sup>a</sup>	0.23 <sup>a</sup>
COOH (mmol/g)	0.26 <sup>a</sup>	0.27 <sup>a</sup>

**Table 5.** Chemical characterization of starting materials. The data indicated with <sup>a</sup> are not reliable due to the incomplete solubility of the sample in the analysis solvent.

The analysis have demonstrated that more than a half of the by-products obtained by steam explosion process is composed by lignin but also a high percentage of residual polysaccharides (33% in *Arundo Donax* and 24% in *Wheat Straw*) and ashes has been detected. The former could be attributed to the partial and not complete cleavage of lignin-carbohydrate complexes, naturally present in herbaceous lignocellulosic materials (Salanti *et al.*, 2012), during the steam explosion process.

All samples have been analyzed by quantitative <sup>31</sup>P-NMR spectroscopy. The derivatization mechanism of labile hydroxyl groups of lignin with a suitable derivatizing agent, 2-chloro-4,4,5,5-tetramethyl-1,3,2-dioxaphospholane, is

reported in *figure 23*. By means of this reaction it has been possible to quantify the amount of different OH groups characterized by typical chemical shift values (*figure 24*).

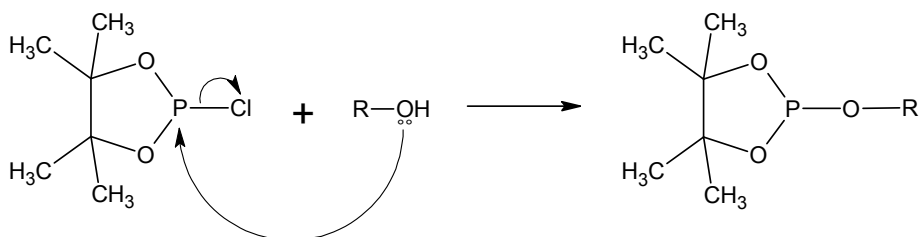


**Figure 23.** Reaction of lignin with 2-chloro-4,4,5,5-tetramethyl-1,3,2-dioxaphospholane

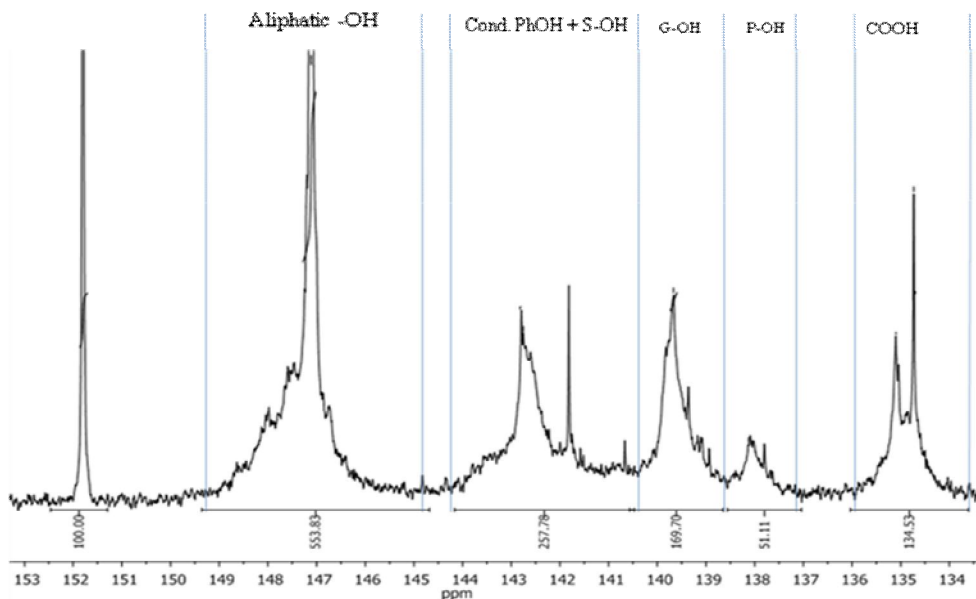


**Figure 24.** Typical  $^{31}\text{P}$ -NMR spectrum of lignin

As observed in *table 5*, three quarters of hydroxyl groups are aliphatic while one quarter is composed by phenolic hydroxyl groups. Moreover, an important amount of carboxylic acids has been detected. The  $^{31}\text{P}$ -NMR analyses have confirmed the presence of the three main typical units of herbaceous plant lignin.

However, the data reported after GPC and  $^{31}\text{P}$ -NMR analysis (indicated with <sup>a</sup> in *table 5*) are not completely reliable, due to the incomplete solubility of the sample in the analysis solvent. This phenomenon is due to the presence of residual polysaccharides and ashes that could not be solubilized in pyridine neither during the acetylation and derivatization reaction used for GPC nor during the NMR analyses. The data obtained are referred only to a fraction of the sample and they are not completely representative for the entire sample.

To overcome this problem, a different derivatization reaction in ionic liquid followed by derivatization with benzoyl chloride in homogenous condition has been explored. The method has already been applied in lignocellulosic materials characterization (Salanti *et al.*, 2012). The overlap of GPC profiles of acetylated (in traditional way) and benzoylated (ionic liquid) materials chromatograms have confirmed the presence of residual polysaccharides: the benzoylated chromatograms indeed have shown to be shifted to higher molecular weight and moreover a shoulder in the higher molecular weight region than the acetylated ones has been detected (*figure 25*). These results confirm the compositional analyses indicating the presence of residual polysaccharides either in form of free residues and in form of lignin-bonded residues as not complete cleavage of lignin-carbohydrate complexes, during the steam explosion process occurred.



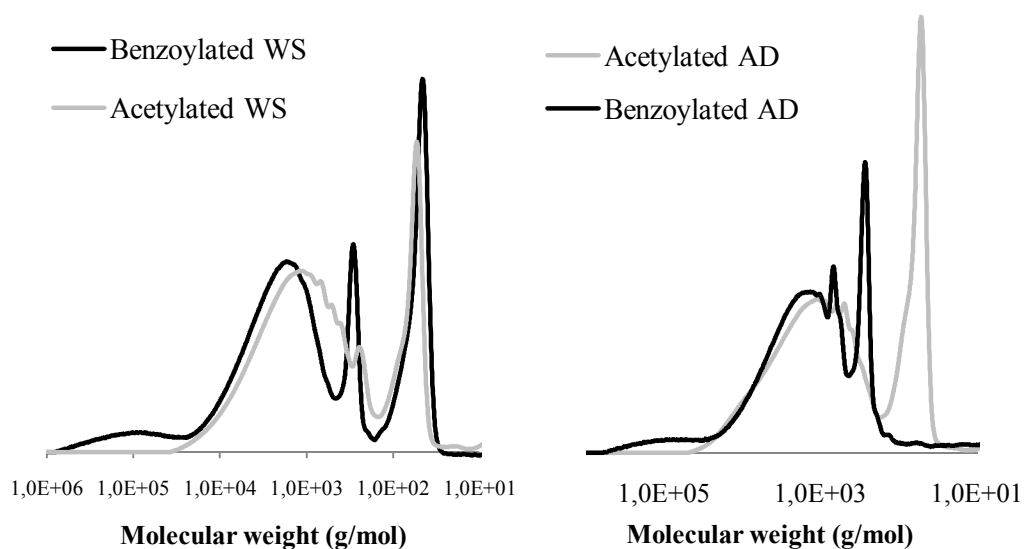


**Figure 25.** Overlapped GPC profiles of *Wheat straw* and *Arundo donax*, acetylated and IL benzoylated.

The materials have been also characterized by optical microscopy; as reported in the *figure 26*, the characterization has highlighted a fibrous aspect of the starting biomass and the presence of large dimension agglomerates.

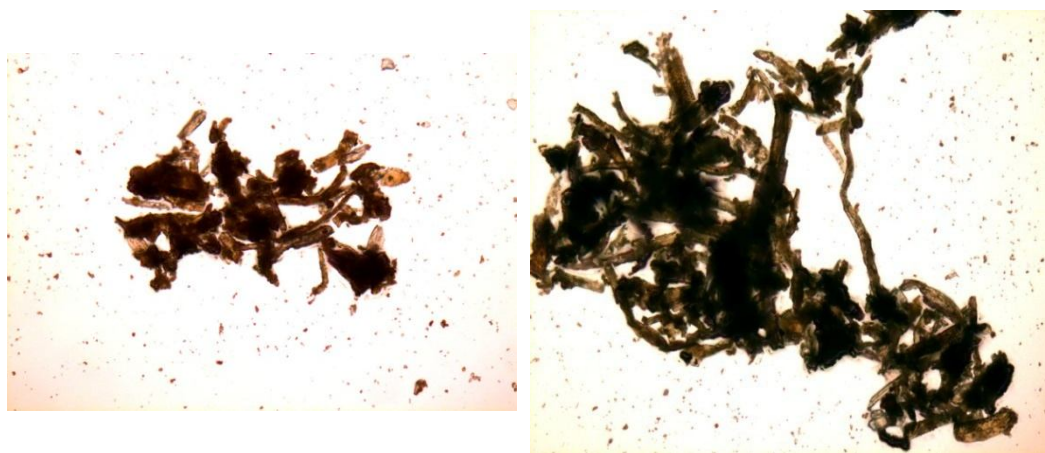


**Figure 26.** Optical microscope images of the starting material

The analyzed materials come from renewable sources and are produced in a steam explosion pilot plant of a factory located in northern Italy; thanks to its abundant availability and its interesting price, steam exploded biomass has been chosen as starting material for the project.

Sulfur-free lignin has been already exploited as a substitute for phenol in phenolic and epoxy resins, or as stabilizer against oxidation, as reported in literature; instead its use as reinforcing filler in rubber composites has been only marginally investigated. In this thesis the lignin's ability to reinforce has been evaluated and the partial replacement of carbon black in tyre composites has been investigated.

First of all, a compound with 65 phr of biomass has been compared to rubber composite with 65 phr of carbon black, used as a reference.

The compounds have been prepared in two steps: the first step using a Haake internal mixer while the second step in a two roll mill according to the composition shown in *table 6*.

Ingredients	Reference carbon black	Biomass
Haake mixing step		
Natural rubber	50	50
Styrene-butadiene rubber	50	50
Carbon black N375	65	
Wheat straw biomass		65
Stearic acid	2	2
Zinc oxide	3	3
Aromatic oil	10	10
6PPD	2	2
Mill mixing step		
Soluble sulfur	1.5	1.5
TBBS	0.8	0.8

**Table 6.** Tyre recipe (phr) of reference compound and biomass compound

The replacement of carbon black with biomass has created some problems during the vulcanization stage. The compound appeared crude and inflated, so it has not been possible to test its mechanical properties.

After that, a compound in which 15 phr of carbon black has been replaced with the biomaterial has been obtained.

		Carbon black Reference	Biomass
		Phr	Phr
NR		50	50
SBR		50	50
N375		65	50
Biomass			15
MDR 20min 170°C	ML[dN m]	2.12	1.45
	MH[dN m]	12.46	9.52
	TS2[min]	2.12	2.29
	T90[min]	6.49	6.84
	T100[min]	11.56	14.80
<b>Curing</b>	<b>10 min 170°C</b>		
DENSITY	Density[g/cm <sup>3</sup> ]	1.141	1.131
RING TENSILE TEST 23°C	M50[MPa]	1.01	0.91
	M100[MPa]	1.60	1.39
	M300[MPa]	8.57	4.98
	TS[MPa]	16.58	12.92
	Eb[%]	533.09	621.88
	Energy[J/cm <sup>3</sup> ]	37.19	33.84
HARDNESS IRHD 23°C	Hardness[IRHD]	61.5	53.6
HARDNESS IRHD 100°C	Hardness[IRHD]	51.2	43.4
DISPERGRADER ANALYSIS	Average (X)[-]	5.2	0.5
	Average (Y)[-]	9.4	0.5

**Table 7.** Curing characteristics and mechanical properties of reference compound with carbon black and the compound with biomass

The partial replacement of carbon black with the biomass, strongly decreased the mechanical properties of rubber composites, like hardness and tensile strength as reported in *table 7*. The dispergrader data showed a not

homogeneous dispersion of filler in the polymeric matrix. X and Y values, a measure of dispersion and the distribution of filler in the polymeric matrix respectively, are even lower than the threshold limit value that is 1. The reason of these expected results is related to the incompatibility between elastomers and biopolymers. High level of impurities (such as carbohydrates and ashes), high content of strongly polarized hydroxyl groups and high particle size have been identified as possible interferences for elastomer-biopolymer interactions. In order to remove all the impurities from the starting material and therefore to obtain pure lignin, a purification process has been developed (*figure 27*). The purification process is based on the dissolution of the biomass in alkaline solution and the recovery by acidification with HCl.

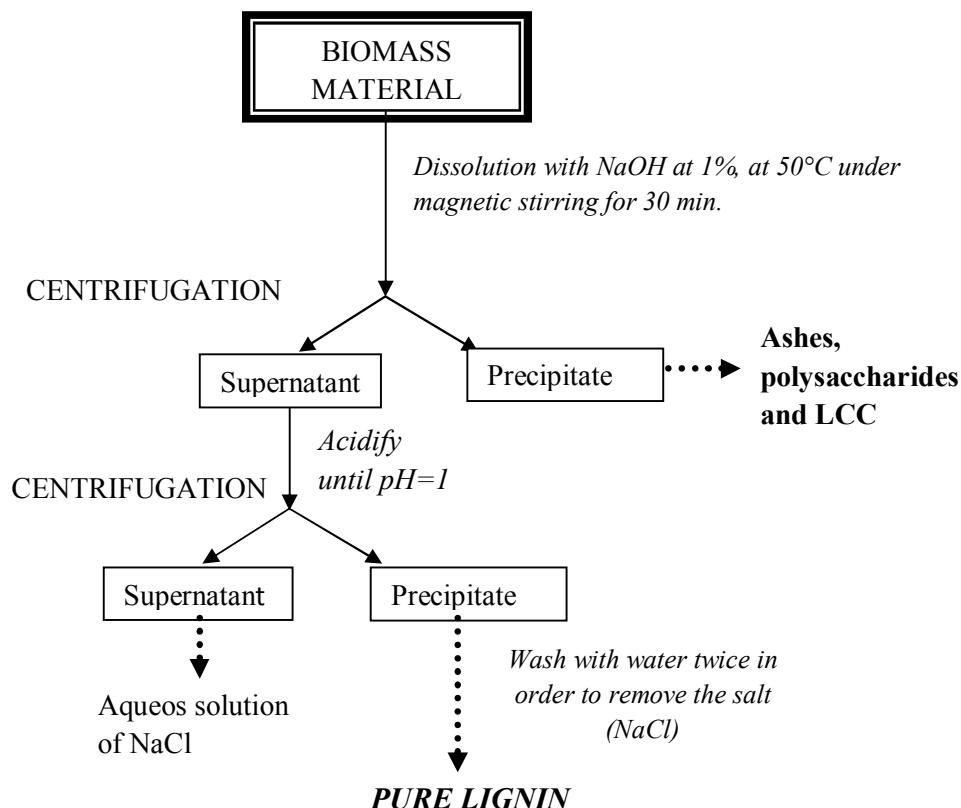
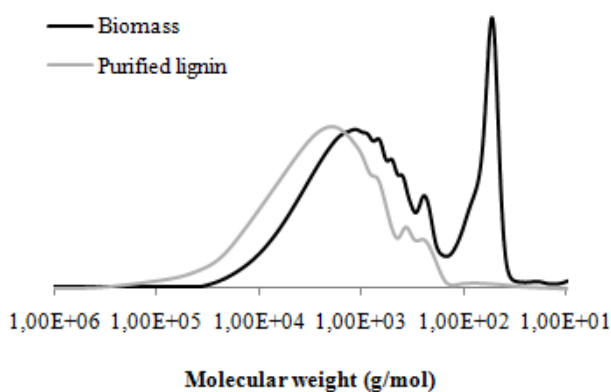


Figure 27. Scheme of purification process of biomass

The yield of purification process is 36%. Lignin does not exist in the herbaceous plant as an independent entity but it is always bonded with polysaccharides forming lignin-carbohydrate complexes (LCC) (Salanti *et al.*, 2012). The only partial break of these complexes makes it difficult to extract all the lignin naturally present in herbaceous lignocellulosic materials nevertheless, the adopted purification strategy has allowed to obtain pure lignin, removing all inorganic impurities and polysaccharides. The molecular weight of purified lignin relatively increased as a consequence of the purification process, in which the lower molecular weight fractions were partially lost (figure 28).



**Figure 28.** Overlapped GPC profiles of biomass (black) and purified lignin (grey)

The removal of polysaccharides during the purification process has been confirmed by the decrease of aliphatic hydroxyls while the phenolic and acid groups relatively increase as shown from the overlap of  $^{31}\text{P}$  NMR spectra (figure 29), as well as from the data reported in table 8.

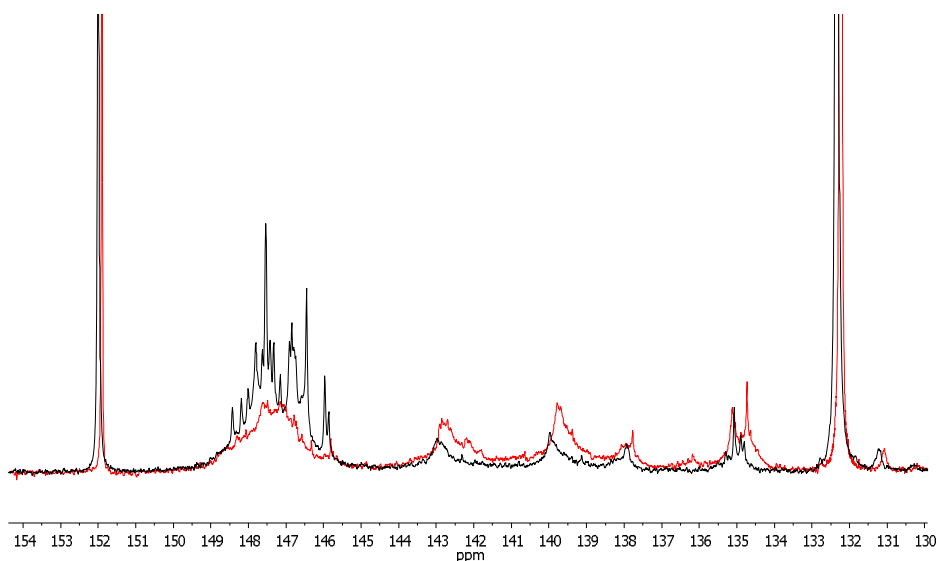


**Figure 29.** Overlapped  $^{31}\text{P}$  NMR spectra of biomass (black) and purified lignin (red).

The occurred purification has been also demonstrated by the intensity decrease of the peaks relative to the C-O bonds, at  $1121$  and  $1032\text{ cm}^{-1}$ , due to the removal of the carbohydrates (*figure 30*).

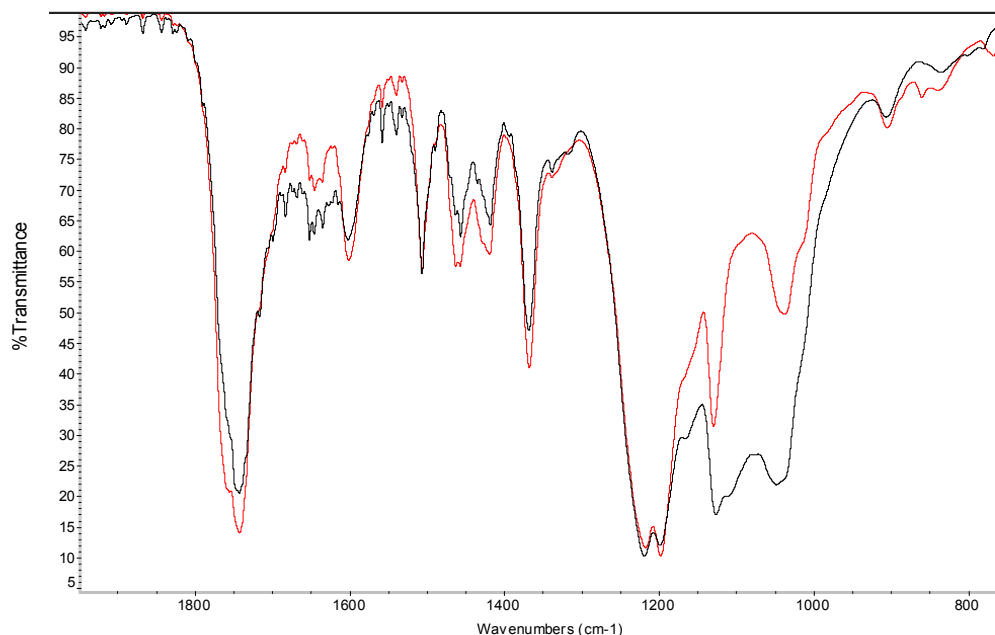


**Figure 30.** Overlapped IR spectra of biomass (black line) and purified lignin (red line).

The best information on lignin structure derived from 2D-HSQC NMR spectra (figure 31). These bidimensional spectra let the identification of the intermonomeric bonds in the aliphatic region and the three principal units in the aromatic region.

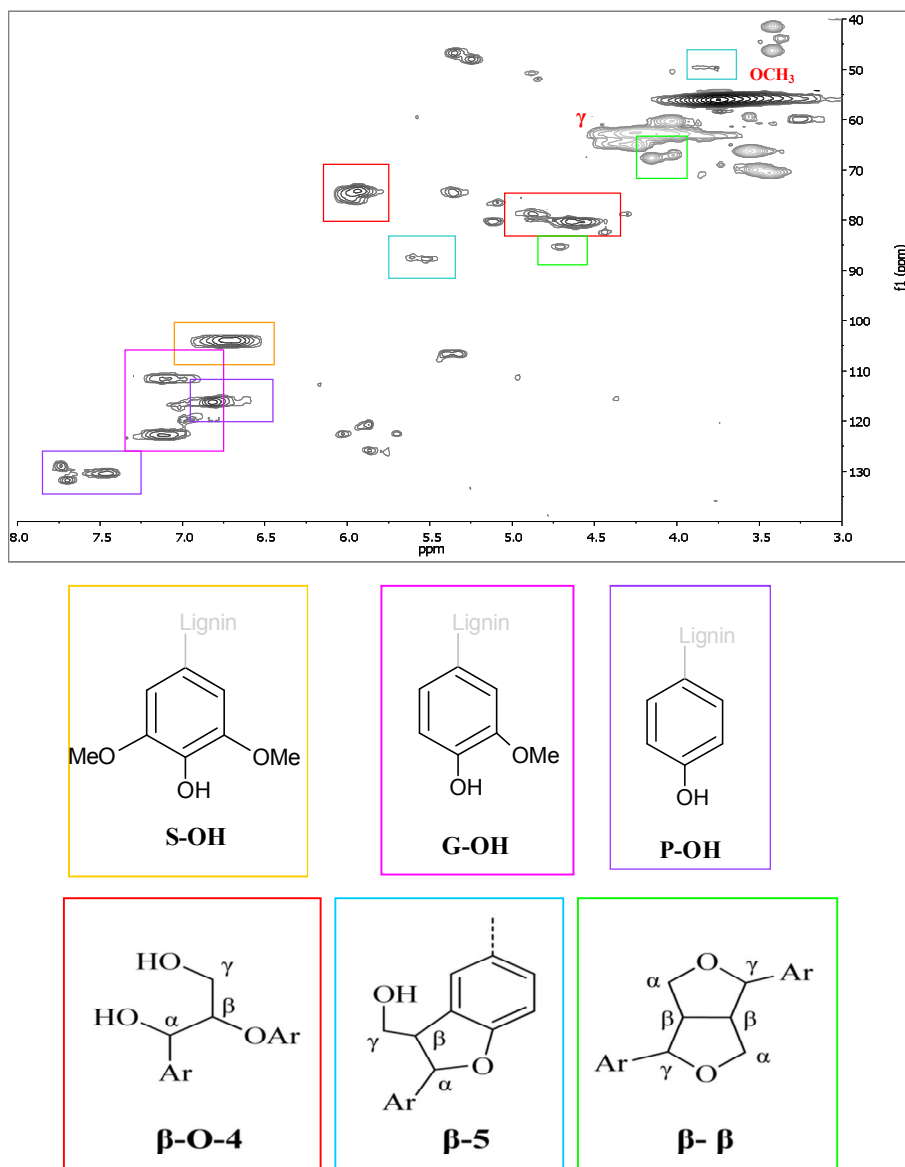


**Figure 31.** 2D-HSQC-NMR spectra of wheat straw. Side chain region  $^{13}\text{C}/^1\text{H}$  correlation area: 40-90/3-6. Aromatic region  $^{13}\text{C}/^1\text{H}$  correlation area: 100-140/6-8. (Salanti *et al.*, 2012)

Purified lignin showed a granular nature, with the particle size of about tenths of micron, as shown in the *figure 32*.

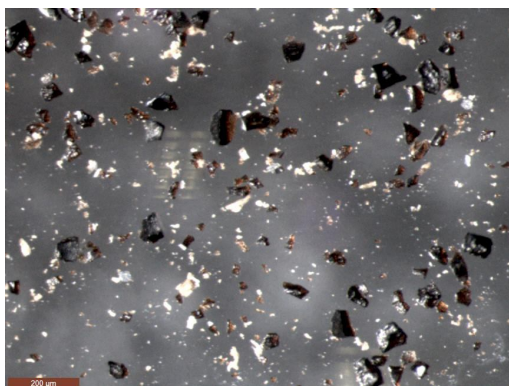


**Figure 32.** Optical microscope images of purified lignin

	<i>Biomass</i>	<i>Purified lignin</i>
Ashes (%)	16.5	0.2
Klason lignin (%)	58.1	99.2
Polysaccharides (%)	25.4	0.6
<b>GPC</b>		
M <sub>n</sub> (g/mol)	2500 <sup>a</sup>	4400
M <sub>w</sub> (g/mol)	7000 <sup>a</sup>	12000
I	2.8 <sup>a</sup>	2.7
<b><sup>31</sup>P NMR</b>		
Aliphatic OH (mmol/g)	2.39 <sup>a</sup>	1.84
Condensed PhOH + S-OH (mmol/g)	0.58 <sup>a</sup>	0.79
G-OH (mmol/g)	0.46 <sup>a</sup>	0.74
P-OH (mmol/g)	0.23 <sup>a</sup>	0.24
COOH (mmol/g)	0.27 <sup>a</sup>	0.51

**Table 8.** Compositional evaluation, GPC, and <sup>31</sup>P-NMR data for starting material and purified lignin. The data indicated with <sup>a</sup> are not reliable due to the incomplete solubility of the sample in the analysis solvent.



In order to understand the reinforcement ability of purified lignin, the behavior of the biofiller in the natural rubber (NR) and Styrene-Butadiene rubber (SBR) has been investigated.

A small amount of lignin (5 phr) has been added in the compound composed by 100 phr of rubber, 10 phr of aromatic oil, 2 phr of stearic acid, 3 phr of zinc oxide, 0.8 phr of TBBS and 1.5 phr of sulfur.

Two only-polymer rubber compounds have been utilized as a reference and have been compared to the compounds obtained after the addition of lignin.

		NR	NR -lignin	SBR	SBR- lignin
		phr	phr	phr	phr
NR		100	100		
SBR				100	100
Purified lignin			5		5
VISCOSITY ML (1+4) 100 C	Mooney ML(1+4) [Mooney Unit]	41.4	24.0	30.3	25.8
MDR 30 min 170°C	ML[dN m]	0.88	0.67	0.43	0.42
	MH[dN m]	5.72	4.67	5.63	4.45
	T10[min]	1.60	2.10	5.66	6.60
	T50[min]	2.70	2.83	8.73	11.37
	T90[min]	3.68	4.28	13.81	20.33
<b>Curing 170°C</b>		<b>10 min</b>	<b>7 min</b>	<b>16 min</b>	<b>22 min</b>
DUMBELL TENSILE TEST 23°C	M50[MPa]	0.4	0.4	0.5	0.4
	M100 [MPa]	0.6	0.5	0.8	0.6
	M200 [MPa]	0.9	0.7	1.3	0.7
	M300[MPa]	1.1	1.0	1.8	0.9
	M500[MPa]	2.1	1.9	-	1.3
	TS[MPa]	14.1	5.7	2.5	1.5
	Eb [%]	555.9	662.8	410.7	580.7
HARDNESS Shore A	Hardness[shore A]	42.3	28.0	35.0	31.6

**Table 9.** Curing characteristics and mechanical properties of pure NR, pure SBR and their composites with lignin

In both cases a decrease of Mooney viscosity has been observed after the introduction of lignin as reported in *table 9*; this is not only an indication of high rate of occluded filler, but also of a poor dispersion of the filler in the compound. For the NR, the microscope analyses (*figure 33*) have confirmed that the filler has not been dispersed in the polymeric matrix pointing out the presence of micrometric lignin particles.

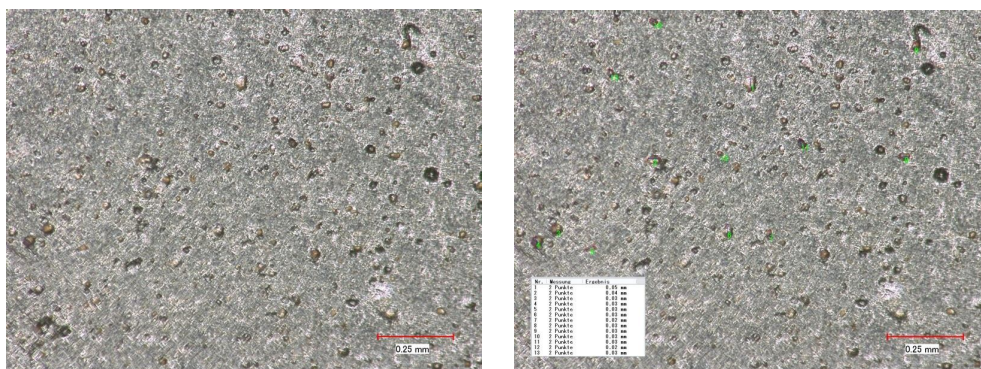


**Figure 33.** Optical microscope images of NR rubber compound with 5 phr of purified lignin

Moreover lignin seems to have an influence on vulcanization process. In general, a decrease of vulcanization rate has been observed. Scorch time as well as optimum of vulcanization increased with the purified lignin. It could be attributed to the fact that phenolic hydroxyl groups of lignin react with curing system to increase optimum cure time because of their acidity (Kumaran and De 1978; Nando and De 1980) and also the presence of free carboxylic acids could play a similar role.

The fillers play a fundamental role in dynamic and static behavior of compounds. In fact the introduction of 5 phr of purified lignin strongly decreased the static modulus.

The influences of the addition of purified lignin have been studied with rubber process analyzer (RPA) that allows to test the strength of filler-filler network and the interaction between filler and elastomer.

In order to evaluate the dynamic behavior of the compound the complex shear modulus has been reported depending on the dynamic shear deformation (*figure 34*). At low strains, the polymer free of filler has a lower  $G^*$  value than the polymer in presence of fillers. The continuous disruption and restoration of the filler network (filler-filler interaction) causes the hysteretic effects in rubber: the decrease of the dynamic modulus with strain causes energy dissipation (Payne effect).

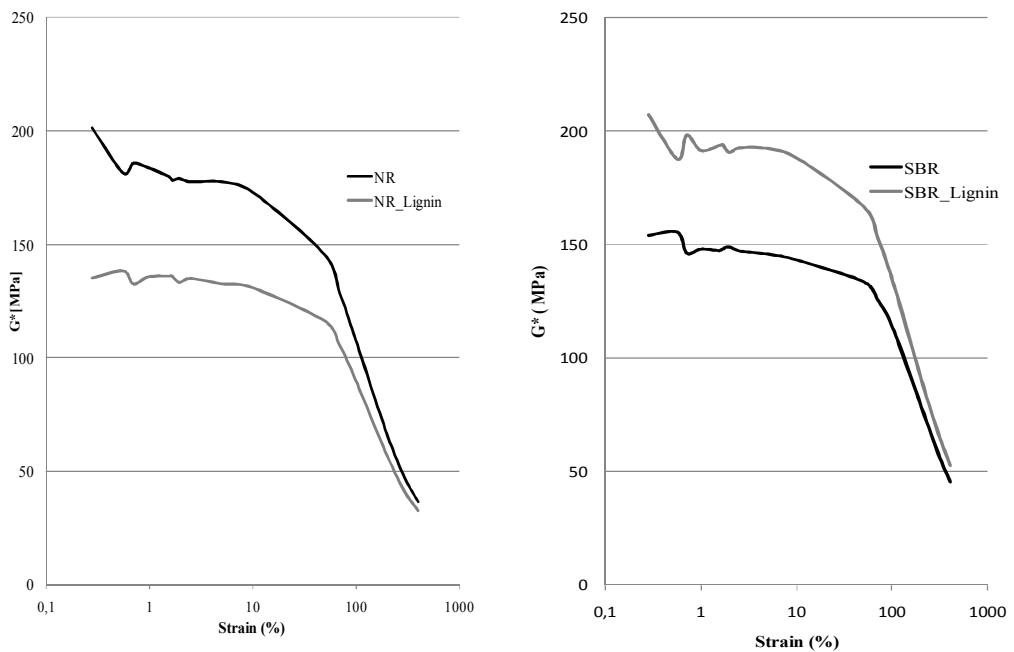


**Figure 34.** Strain amplitude dependence of  $G^*$  of lignin in natural rubber (left) and in styrene butadiene rubber (right).

For Styrene Butadiene rubber the addition of lignin increased the  $G^*$  modulus. At low strains, in addition to the contribution of the filler-filler interaction, occluded rubber phenomena could occur and thus the polymer does not behave

like a rubber, but acts like an additional filler. The lignin-elastomer interaction is better with SBR than NR, probably due to the presence of aromatic rings. The introduction of lignin in NR indeed, has shown an unexpected decreasing of modulus at low strain. This could be attributed to a poor interaction between lignin and elastomer as previously demonstrated by microscope images.

All the data indicated that lignin has some disadvantages for its application as rubber-reinforcing filler, such as its large particle size, strong polar surface and high tendency of lignin particles to form aggregate by intermolecular hydrogen bonds.

Filler particle size, structure, surface area and chemical nature of filler determine the effective interaction between the filler and polymeric matrix. Fillers with particle size larger than 10  $\mu\text{m}$  have no reinforcement capabilities. Fillers with particles between 1 to 10  $\mu\text{m}$  are used as diluents. Semi-reinforcing fillers range from 100 to 1000 nm. Fillers in the range from 10 nm to 100 nm can significantly improve rubber properties.

The average particle sizes of carbon black are in the range from 10 nm to 500 nm while initial lignin particle size is tenths of micron as previously shown. The structure of filler depends on the degree of irregularity: the high tendency of lignin particles to form aggregates by hydrogen bonds that cannot be divided by thermo-mechanical mixing impedes their dispersion during the mixing stage. Moreover the chemical nature and surface area of filler influence its dispersion in the elastomers and the filler-polymer interaction. Carbon black's relatively non-polar surface provides a higher interaction with the non-polar hydrocarbon rubber. Due to the presence of strong polar groups in lignin (mainly hydroxyl groups) a poor interfacial adhesion with nonpolar-hydrophobic matrix is expected. The hydrophilic character of lignin is incompatible with the hydrophobic polymer matrix.

After these preliminary results, in order to make this low-cost and highly-availability material usable as reinforcing filler, two different strategies have been tested: chemical modification of active surface and reduction of particle size.

### **3.3 MODIFICATION OF LIGNIN CHEMICAL NATURE**

#### **3.3.1 Chemical modification of lignin**

In order to modify the active surface of lignin and improve the lignin-elastomers interaction, the hydrophobization of lignin has been explored by the chemical modification of the lignin hydroxyl groups. As a preliminary study, the simple acetylation reaction has been investigated.

##### ***3.3.1.1 Acetylation***

There are several methods that could be applied for the acetylation reaction. The most common is based on the use of acetic anhydride and pyridine. This method is largely used at laboratory scale (Salanti *et al.*, 2010) in lignin sample preparation for characterization, however the excess of pyridine used in this method does not make reliable its use with large amounts of material (around 300 g) or for industrial plants.

A new method has been developed with acetic anhydride, optimizing the following parameters: reaction time, reaction temperature and possible use of catalyst. The best results have been obtained with the method in which acetic anhydride has been used in presence of 1-methylimidazole as a catalyst for 1h at 120°C. The reaction mechanism is reported in *figure 35*.

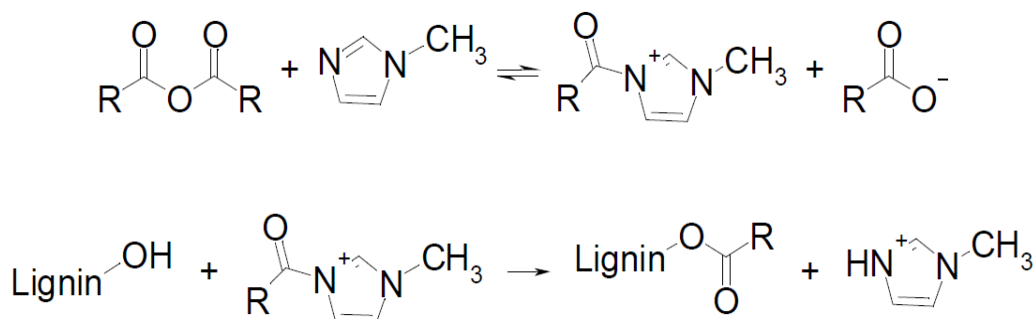


**Figure 35.** Reaction mechanism for lignin acetylation

The occurred acetylation has been demonstrated by the weight increase of the recovered lignin (WPG, weight percent gain, %) as well as by FT-IR analyses. In the FT-IR spectra (*figure 36*), the esterification was revealed by the presence of the ester and ether bond's peaks respectively at  $1734 \text{ cm}^{-1}$  and  $1200 \text{ cm}^{-1}$  and the disappearance of the broad OH band at  $3300 \text{ cm}^{-1}$ .

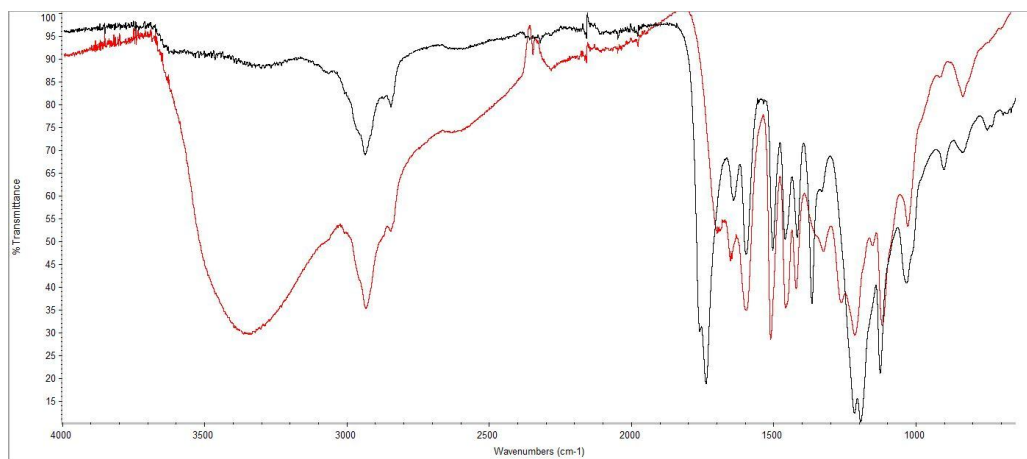


**Figure 36.** Overlapped IR spectra of purified lignin (red line) and acetylated lignin (black line).

In order to improve the yield and the efficiency of lignin acetylation, due to the modified material high amount required, two different strategies have been developed starting from the biomass (*figure 37*).

The first method involves the acetylation of biomass with the method described above. The acetylated biomass, despite the hydrophobization reaction, still showed high incompatibility with the elastomers due to the presence of impurities that interfere in the filler-polymer interaction. It was therefore necessary the purification of the obtained material by acetone extraction. On the other hand, the second method consists of the purification of starting material followed by the acetylation. In either cases it was possible to obtain hydrophobic lignin free of impurities.

The acetylation of purified lignin has a higher efficiency than acetylation of raw material followed by acetone extraction and shorter reaction times are required; for these reasons the first method has been chosen.

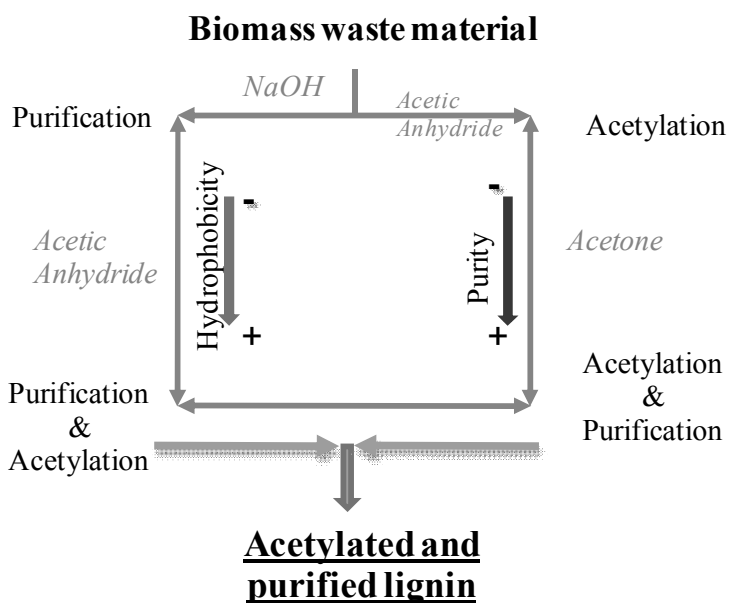


**Figure 37.** Scheme of two strategies for obtaining acetylated and purified lignin.

The behavior of acetylated lignin in natural rubber (NR) and Styrene-Butadiene rubber (SBR) has been investigated. Furthermore, the acetylated purified lignin has been also used as partial replacement of carbon black with the formulations

reported in the *table 10* and compared with a compound in which 15 phr of carbon black was replaced with purified lignin.

The density of the compound decreased due to the introduction of lignin (density 1.3 g/cm<sup>3</sup>) whose density is lower than the current in-use reinforcing fillers', as carbon black (1.8 g/cm<sup>3</sup>) or silica (2.0 g/cm<sup>3</sup>). The decrease of density allows to reduce the weight of the tyre.

As previously demonstrated for the compound with purified lignin, scorch time (tS2) and optimum of vulcanization (t90) measured by rheometer, increased. In particular, in the case of acetylated lignin, as it is or in combinations with carbon black, these two values were higher probably due to the presence of residual acetic acid in the acetylated specimen.

After mixing acetylated lignin with elastomer, a higher tensile strength has been observed compared to the purified lignin, but the performance of carbon black N375 (as reported in *table 10*) has not been achieved yet. The addition of lignin could influence the macromolecular rearrangements during the tension, lowering tensile values.



*Results and discussion*

		Reference carbon black	Reference carbon black	Purified lignin	Acetylated lignin
NR		50	50	50	50
SBR		50	50	50	50
Carbon black N375		65	50	50	50
Purified lignin				15	
Acetylated lignin					15
Stearic acid		2	2	2	2
Zinc oxide		3	3	3	3
Aromatic oil		10	10	10	10
6PPD		2	2	2	2
Soluble sulfur		1.5	1.5	1.5	1.5
TBBS		0.8	0.8	0.8	0.8
MDR 20 min 170°C	ML[dN m]	2.12	1.58	1.64	1.06
	MH[dN m]	12.46	10.61	10.35	9.35
	tS2[min]	2.12	2.13	2.44	2.74
	t90[min]	6.49	6.24	7.59	9.30
	t100[min]	11.65	11.00	14.72	16.98
	%RET[%]	2.61	6.76	1.26	0.60
<b>Curing</b>	<b>10 min 170°C</b>				
DENSITY	Density[g/cm <sup>3</sup> ]	1.141	1.108	1.122	1.116
RING TENSILE TEST 5 23°C	M50[MPa]	1.01	0.85	0.88	0.86
	M100[MPa]	1.60	1.33	1.36	1.22
	M300[MPa]	8.57	6.90	5.50	4.72
	TS[MPa]	16.58	18.42	13.40	14.61
	Eb[%]	533.09	622.76	593.65	723.00
	Energy[J/cm <sup>3</sup> ]	37.19	45.76	32.94	45.44
REBOUND 23°C	R.E.[%]	43.1	46.9	47.4	43.1
HARDNESS IRHD 23°C	Hardness[IRHD]	61.5	50.4	55.6	59.6
HARDNESS IRHD 100°C	Hardness[IRHD]	51.3	47.9	46.3	42.0
DISPERGRADER ANALYSIS	Average (X)[-]	5.2	5.6	0.5	5.0
	Average (Y)[-]	9.4	9.3	2.6	8.7

**Table 10.** Formulation, Curing characteristics and mechanical properties of reference compound, purified lignin compound and acetylated lignin compound.

The hardness measured at 23°C is increased, but increasing the temperature (100°C) the values strongly decreased probably due to the increase of the mobility of lignin molecules with high temperature.

The elongation of break is inversely proportional to the degree of crosslink density (Choi S.S., 2001) therefore a compound with shorter elongation of break has high crosslink density. The partial replacement of carbon black with acetylated lignin has caused an increase of elongation at break thus a lower crosslink density, as confirmed by the lower value of MH. The decrease of cross-linking could be the cause of decreasing of some other mechanical properties.

The microscope analysis of compounds with 5 phr of acetylated lignin, that are not reported, has proved a very poor dispersion of filler in the polymeric matrix; on the other hand the dispergrader data, reported in *table 10*, highlighted a very good dispersion of acetylated lignin in combinations of carbon black, with values really close to the reference. The acetylation makes lignin more hydrophobic and thus more compatible with the elastomers but its complex structure and its particle size prevent its dispersion in the polymeric matrix. Instead the presence of carbon black, probably favors an interaction between lignin and carbon black that leads the filler's dispersion.

### ***3.3.1.2 Allylation***

The second method investigated for lignin functionalization was the allylation reaction that allows to insert a double bond functionality on lignin structure. The acetylation makes lignin more hydrophobic and thus better dispersed in the polymeric matrix but it does not reinforce it; thus the introduction of allyl group, that could be reactive during vulcanization stage, could favorite the formation of a filler-polymer network guaranteeing good mechanical properties.

The lignin allylation is not reported in the literature, so two different strategies has been developed and tested based on phenols allylation. The first method (*figure 38*) consists on the reaction of purified lignin with allyl bromide and potassium carbonate in acetone; the second method (*figure 39*), instead, contemplates the dissolution of purified lignin in acetone and NaOH aqueous solution in the presence of allyl bromide as reported in the experimental part.

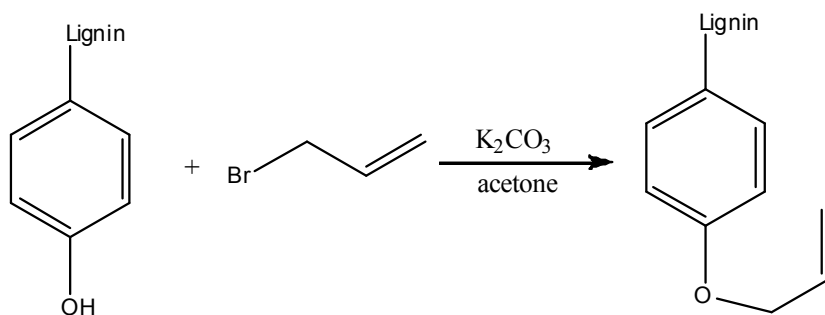


**Figure 38.** Reaction mechanism for lignin allylation (1<sup>st</sup> method)

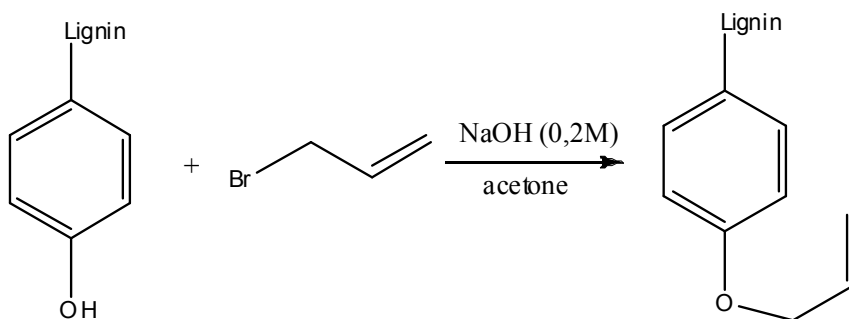


**Figure 39.** Reaction mechanism for lignin allylation (2<sup>nd</sup> method)

FT-IR and <sup>31</sup>P NMR spectroscopy analyses have been used as evidences of occurred allylation. In the IR spectra, the introduction of an allyl group is revealed by the presence of the peaks at 930 cm<sup>-1</sup> and 990 cm<sup>-1</sup> and the intensity decrease of the broad band related to OH groups at 3300 cm<sup>-1</sup> (*figure 40*).

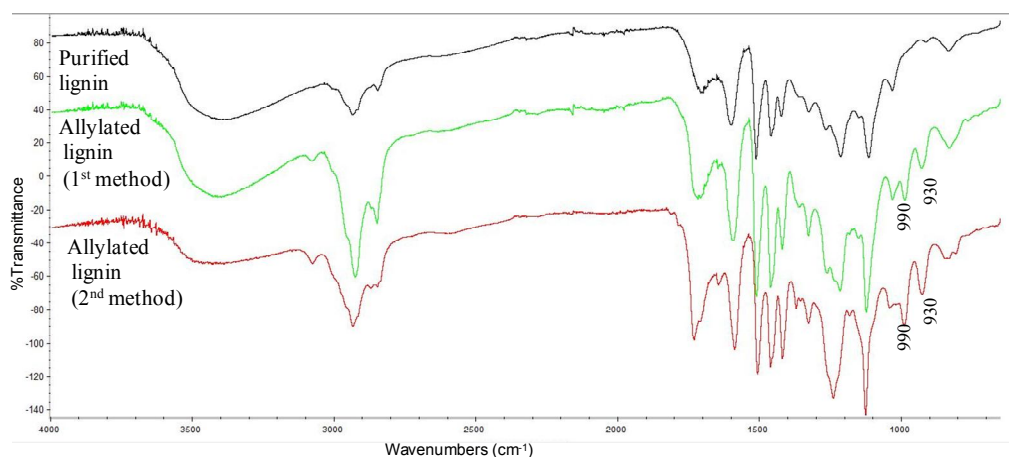


**Figure 40.** IR spectra of purified lignin (black line) and allylated lignin, 1<sup>st</sup> method (green line) 2<sup>nd</sup> method (red line).

Table 11 reports the  $^{31}\text{P}$  NMR quantification of different hydroxyl groups present in purified lignin and in allylated lignin. The aliphatic OH groups remained present in high amount after allylation with both methods, as shown by the peaks in the range 149-146 ppm (figure 41). The first method has allowed the modification of 80% of the phenolic units while for the second reaction method all the available phenols present have been allylated. Acid moieties have totally disappeared in the product obtained by first method, while following the second method they have been modified in a small percentage.

	Purified lignin	Allylated lignin (1 <sup>st</sup> method)	% of modification	Allylated lignin (2 <sup>nd</sup> method)	% of modification
aliph OH	1.69	0.89	47%	1.14	29%
cond PhOH	2.01	0.38	81%	n.d.	100%
G-OH	1.00	0.20	79%	n.d.	100%
P-OH	0.44	0.12	72%	n.d.	100%
COOH	1.07	0.02	98%	0.69	35%

**Table 11.** Quantification of hydroxyl groups by  $^{31}\text{P}$  NMR in purified lignin and allylated lignin.

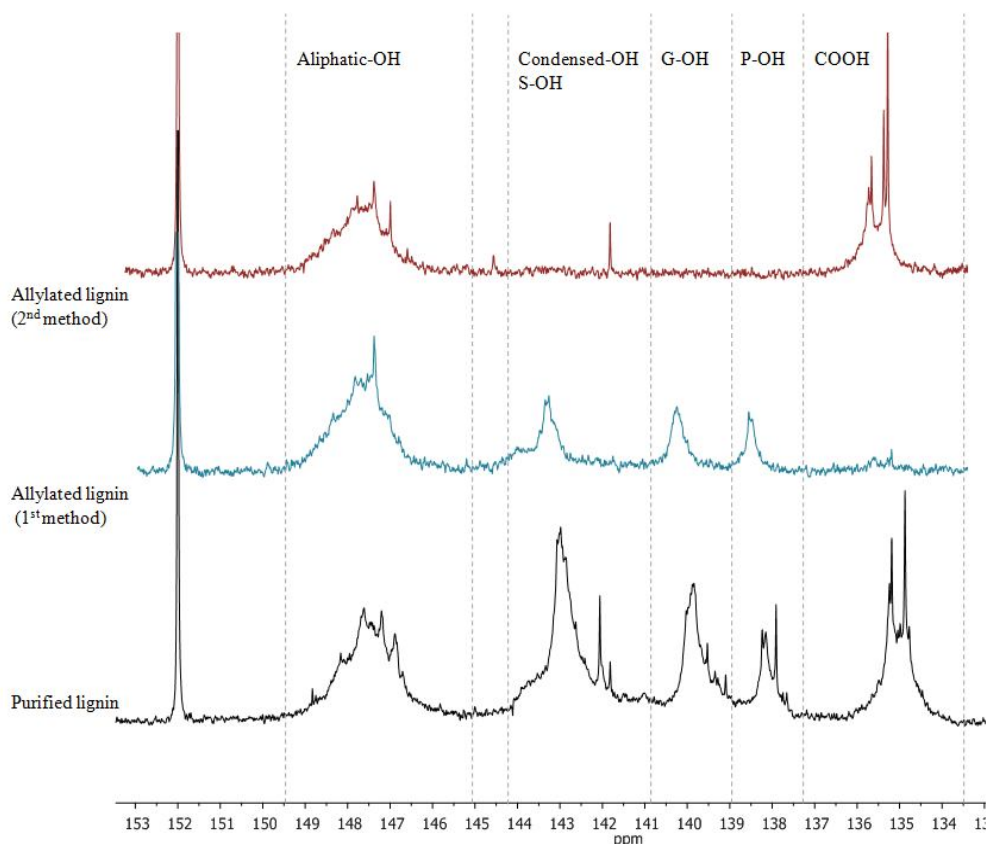


**Figure 41.**  $^{31}\text{P}$  NMR spectra of purified lignin and allylated lignin, 1<sup>st</sup> method and 2<sup>nd</sup> method.

$^{31}\text{P}$  NMR is an indirect method for evaluating the occurred allylation because it allows to quantify the residual hydroxyl groups after the functionalization reaction, while the allylated ones have been calculated by difference.

The direct evidence of the allylation reaction has been obtained by  $^{13}\text{C}$  NMR spectroscopy.  $^{13}\text{C}$  NMR is usually utilized for assigning different structures to various lignins and it can also be used to distinguish the primary, secondary and phenolic hydroxyl groups (Faix *et al.*, 1994, Choi and Faix, 2011) after acetylation. The  $^{13}\text{C}$  NMR spectra of acetylated lignin has been collected and reported in the *figure 42*.

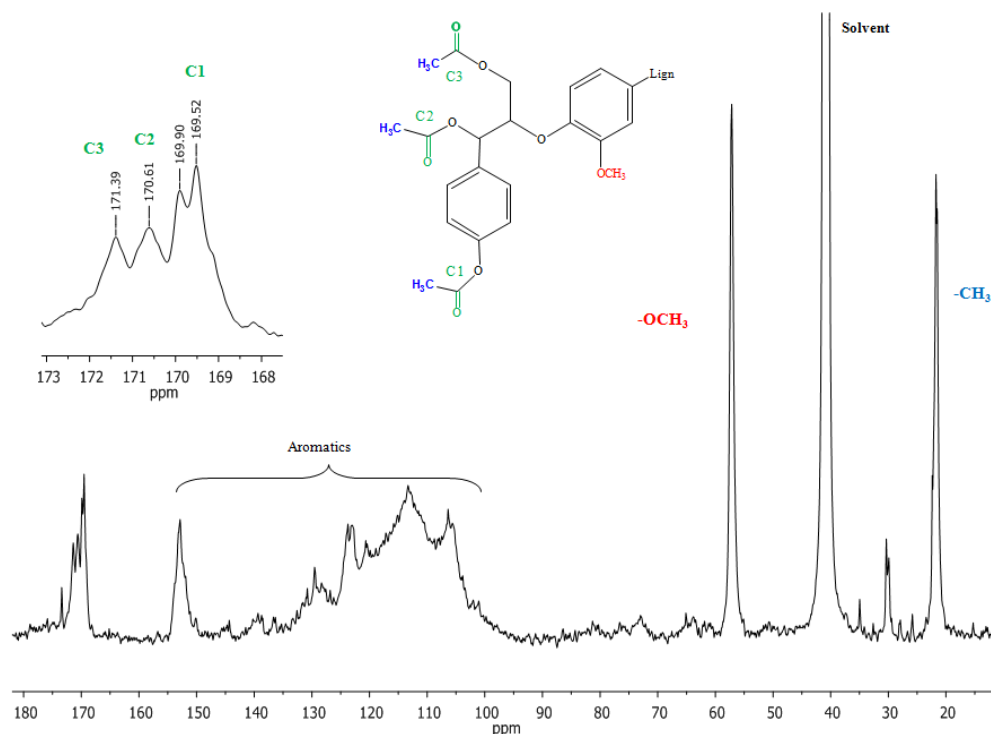


**Figure 42.**  $^{13}\text{C}$  NMR spectrum of acetylated purified lignin and the magnification of the area between 173 and 168 ppm.

The magnification of the area between 173-168 ppm highlights the slight but significant different chemical shifts of the carbonyl C atom of acetyl group bonded to a phenolic or an alcoholic unit (green color). The peak at about 171 ppm is attributed to the carbonyl bonded to a primary alcohol (C3), the peak at 170 ppm is related to a C=O bonded to secondary alcohol (C2) and the one near 169 ppm is attributed to the carbonyl bonded to phenolic unit (C1). The typical aromatic carbons' peaks lie between 150 and 100 ppm, while the methoxy group's (red) and the one related the methyl group present in  $\alpha$ -position to the carbonyl of the acetyl groups (blue) are found at 56 ppm and 21 ppm respectively.

The overlap of  $^{13}\text{C}$  NMR spectra of acetylated lignin and allylated-acetylated lignin, normalized to the methoxy groups at 56 ppm, has demonstrated the presence of new peaks related to the allyl chain ( $\alpha$ ,  $\beta$  and  $\gamma$ ) and the decrease of intensity of other peaks.

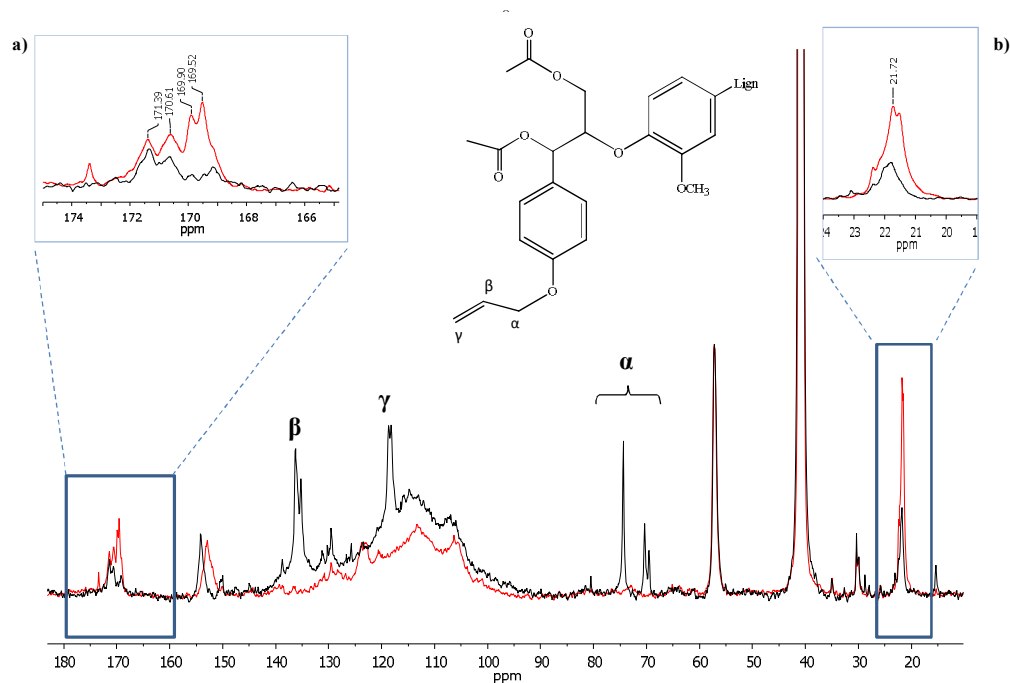


**Figure 43.** Overlapped  $^{13}\text{C}$  NMR spectra of acetylated lignin (red) and allylated acetylated lignin (black).

More specifically, it was possible to observe a decrease in the intensity of the peak related to carbonyl group bonded to the phenolic units (*figure 43a*): this is clearly due to the allylation reaction occurred at these functionalities. A decrease in the intensity of the peak attributed to  $\text{CH}_3$  in  $\alpha$ -position to carbonyl can also be noted (*figure 43b*).

In order to examine the occurred allylation in detail, studies on model compounds have been conducted (*table 12*). The model compounds represent the different phenolic units present in the lignin structure and, after allylation,

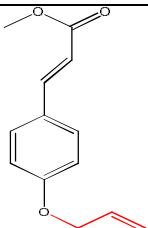
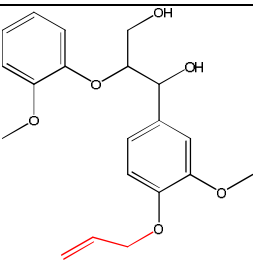
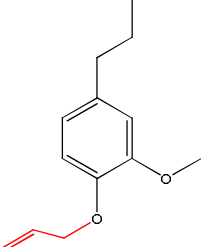
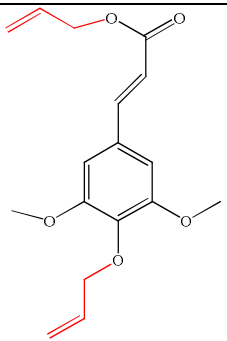
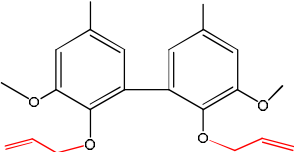
allowed the identification of the carbon chemical shifts of allyl chain in different chemical environment. Their  $^{13}\text{C}$  NMR spectra are not shown here, but the chemical shift values of different allyl chain carbons are collected in the *table 12*. From these data it comes to light that the carbon of the allyl group in  $\alpha$ -position is the most affected by the chemical environment; its peak lie at 64 ppm for acid units, at 68 ppm for *p*-hydroxyphenyl unit, at 70 ppm for guaiacyl unit and at 73 ppm for syringylic and condensed unit.

The chemical shift differences for carbon in  $\beta$ -position are less pronounced in comparison to the carbon directly linked to the oxygen atom, in fact the peak occurs at about 133 ppm, if the allyl unit is connected to a phenol, and at about 138 ppm when bonded to an acid group.

Carbons in  $\gamma$ -position, the most distant from the oxygen atom, are the least affected in term of chemical shift by the kind of hydroxyl group which are bonded to and in fact the related chemical shifts vary between 117-118 ppm.

All these peaks can be found in the  $^{13}\text{C}$  NMR spectra of allylated lignin, as reported in the *figure 43*. It was possible to observe the peaks related to the allyl chain ( $\beta$  at around 138 ppm,  $\gamma$  around 117 ppm and different peaks at 73, 70 and 69 ppm) related to the different kind of phenolic units present in the lignin structure.



Model compound	Chemical structure	$\alpha$	$\beta$	$\gamma$
		ppm	ppm	ppm
Methyl- <i>p</i> -coumarate		68,30	133,42	117,84
Erol		70,05	133,42	118,45
4-propylguaiacol		70,20	133,81	117,80
Sinapic acid (PhOH) Sinapic acid (Acid)		73,16 64,56	134,69 138,11	117,40 117,13
Dihydroanisole		73,01	134,10	117,00

**Table 12.** Model compound structures and chemical shifts of allyl chain carbon.

As previously demonstrated the presence of acid and phenolic units interferes during the vulcanization process, decreasing the vulcanization rate. The first reaction method has allowed to obtain allylated lignin without free acid moieties and only 20% of free phenolic units, for this reason this method has been preferred.

Allylated lignin has been tested as filler in the compound as partial replacement of carbon black. The results of physical and mechanical characterization are reported in *table 13*. No ability to reinforce has been observed for allylated lignin and furthermore the lignin was clearly not well dispersed in the polymeric matrix. The presence of free hydroxyl groups made the material still incompatible with the elastomeric matrix so in order to improve the hydrophobicity of lignin it was necessary to acetylate the material with the same method used for the purified lignin. It is worth noting that the value of MH is quite low compared to compound with pure lignin or CB. Probably part of sulfur is consumed for the reaction with allyl groups reducing the total density of cross-linking.

The behavior of allylated-acetylated lignin in natural rubber (NR) and Styrene-Butadiene rubber (SBR) has been investigated. The characterization of these compounds, that has not been reported here, has shown no improvements in mechanical properties after the addition of lignin. Furthermore, the microscope analysis of compounds with 5 phr of allylated-acetylated lignin has proved a very poor dispersion of filler in the polymeric matrix.

The partial replacement of carbon black with allylated-acetylated lignin, on the contrary, has allowed to ensure superior mechanical properties and reinforcement ability in comparison to the previous compounds with a minimum difference respect to CB. In addition it can reduce the density of final

compound and thus the weight of tyres. Reinforcing effect was observed by increasing of static modulus, tensile strength and hardness (*table 13*).

A higher value of rebound has been observed with allylated-acetylated lignin thus the partial replacement of carbon black with this filler could reduce the hysteresis. Normally carbon black improves rubber properties but increases the hysteresis whereas its partial replacement with allylated-acetylated lignin allowed to reduce the hysteresis and thus the rolling resistance of tyre. Since hysteresis and rolling resistance are related to fuel efficiency of a vehicle, their reduction could reduce the consumption of fuel.

As demonstrated by values of dispergrader analysis and optical microscope images (*Figure 44*), the dispersion of allylated-acetylated lignin in the polymeric matrix (*Figure 44 C*) is certainly better than the purified lignin's (*Figure 44 A*). The dispersion of allylated-acetylated lignin was also better than the dispersion of carbon black (*Figure 44 B*). A better dispersion improves the homogeneity of the elastomeric material and consequently the tyre tear and aging resistance.

		Reference	Reference 50 phr	Purified lignin	Allylated lignin	Allylated Acetylated lignin
NR		50	50	50	50	50
SBR		50	50	50	50	50
N375		65	50	50	50	50
Purified lignin				15		
Allylated lignin					15	
Allylated-acetylated lignin						15
Stearic acid		2	2	2	2	2
Zinc oxide		3	3	3	3	3
Aromatic oil		10	10	10	10	10
6PPD		2	2	2	2	2
Soluble sulfur		1.5	1.5	1.5	1.5	1.5
TBBS		0.8	0.8	0.8	0.8	0.8
MDR 20 min 170°C	ML[dN m]	2.12	1.58	1.64	1.50	1.43
	MH[dN m]	12.46	10.61	10.35	7.99	9.35
	tS2[min]	2.12	2.13	2.44	2.06	1.82
	t90[min]	6.49	6.24	7.59	6.41	6.18
	t100[min]	11.65	11.00	14.72	19.96	19.46
	%RET[%]	2.61	6.76	1.26	0.15	0.25
<b>Curing</b>	<b>10 min 170°C</b>					
DENSITY	Density[g/cm <sup>3</sup> ]	1.140	1.108	1.122	1.118	1.118
RING TENSILE TEST 23°C	M50[MPa]	1.01	0.85	0.88	0.83	0.92
	M100[MPa]	1.60	1.33	1.36	1.20	1.37
	M300[MPa]	8.57	6.90	5.50	4.28	6.03
	TS[MPa]	16.58	18.42	13.40	12.29	16.20
	Eb[%]	533.09	622.76	593.65	684.64	670.59
	Energy[J/cm <sup>3</sup> ]	37.19	45.76	32.94	35.78	46.48
REBOUND 23°C	R.E.[%]	43.1	46.9	47.4	45.2	46.9
HARDNESS23°C	Hardness[IRHD]	61.5	50.4	55.6	51.1	63.1
HARDNESS100°C	Hardness[IRHD]	51.3	47.9	46.3	41.2	49.2
DISPERGRADER ANALYSIS	Average (X)[-]	5.2	5.6	0.5	0.5	7.1
	Average (Y)[-]	9.4	9.3	2.6	3.8	9.8

**Table 13.** Curing characteristics and mechanical properties of compound with carbon black, purified lignin, allylated lignin and allylated-acetylated lignin.

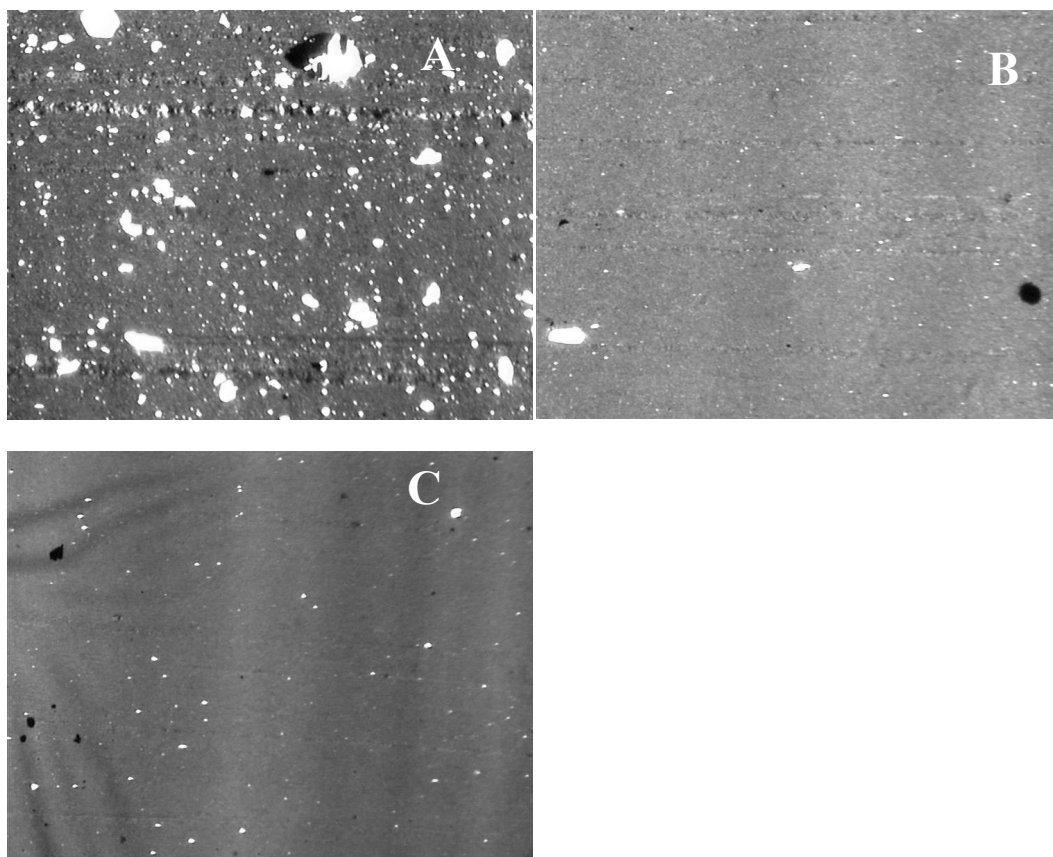


**Figure 44.** Optical microscope images of dispersion purified lignin (A), allylated-acetylated lignin (B) and Carbon black (C) in the compounds.

In order to have a good adhesion between filler and polymer, the fillers need to have precise properties like small particle size and high surface area.

Carbon black has high affinity for rubber. The high surface area of carbon black ensures an intimate contact between filler and elastomers. The available carbon black surface area for polymer adsorption decreases when other filler is added in the compound. This is could be due to the adsorption or the interaction of the filler with carbon black.

When acetylated and allylated-acetylated lignins have been utilized as filler, they have not demonstrated a good dispersion, but in combinations with carbon

black, probably due to carbon black-lignin interactions, a better dispersion has been observed. For acetylated lignin lower dispergrader analysis values, in comparison to allylated-acetylated lignin, are probably due to the presence of free carboxylic acid; whereas the presence of allylated-acetylated lignin might induce a better dispersion of carbon black.

The possible interactions between acetylated lignin and carbon black, however have reduced the carbon black active sites for polymer adsorption decreasing filler-polymer interaction and thus the mechanical properties of the compound. The presence of allylated-acetylated lignin has reduced the carbon black active sites but the introduction of allyl groups has probably facilitated the formation of filler-polymer network during the vulcanization stage that ensures good mechanical properties.

In order to evaluate the dynamic behavior of the compound the complex shear modulus  $G^*$  has been reported depending on the dynamic shear deformation (*figure 45*). The polymer free of filler has a lower  $G^*$  value than the filled compounds. In general, high modulus is caused by the formation of filler–filler interactions.

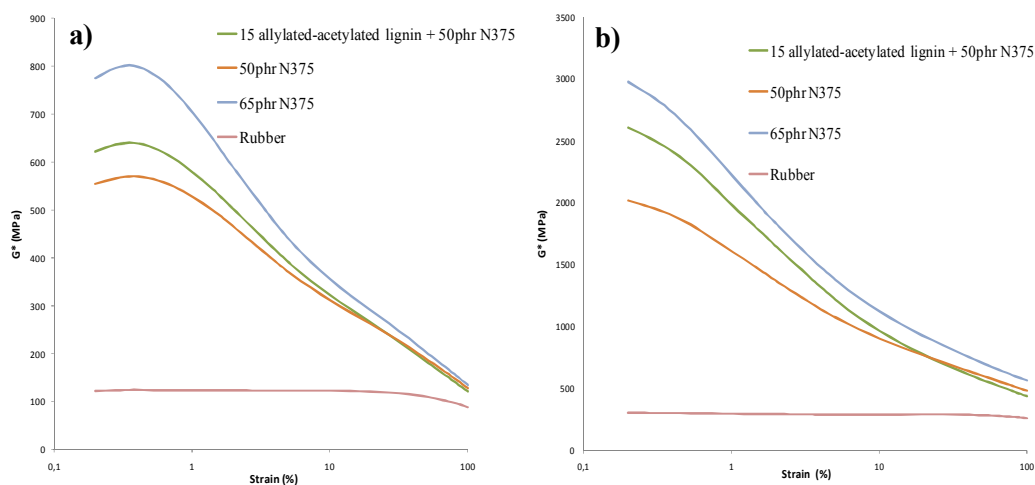


**Figure 45.** Strain amplitude dependence of  $G^*$  of the green compound (a) and vulcanized one (b).

The filler loading affects the Payne effect: the higher the loading, the higher the number of filler-filler interactions because the amount of particles in the same volume unit increases, the distance between them decreases and it is easier for them to aggregate strengthening the filler network. As demonstrated in *figure 45*, a compound with a lower carbon black loading (50 phr) had a lower Payne effect than the reference (65 phr).

The partial replacement of carbon black with lignin caused a decrease of the Payne effect. The well structured filler-filler network in presence of carbon black decreases due to the presence of lignin that could occupy a position between two CB-CB particles; this could lead a lower overall filler-filler network. This phenomenon is more accentuated in the compound with allylated-acetylated lignin due to the better interaction between lignin and polymer that decreases the probability to the formation of filler-filler networks. An increase of the Payne effect is observed from the comparison between the green and vulcanized compound: the crosslink, occurred in the vulcanization

process, caused a shift along the  $G^*$  axis. The reason of this phenomenon is that increasing the temperature the low viscosity of the polymer allows to the re-agglomeration of the filler aggregates.

In conclusion, allylated-acetylated lignin can be used as partial replacement of carbon black without loss of mechanical properties. In relation to the obtained results a patent application has been required (Patent pending N°MI2012A002167). For more extensive trials with allylated-acetylated lignin, it was necessary the production of a unique batch of 250gr with which realize additional tests. A scale up of the method has been developed starting from 200 gr of purified lignin (*figure 46*).

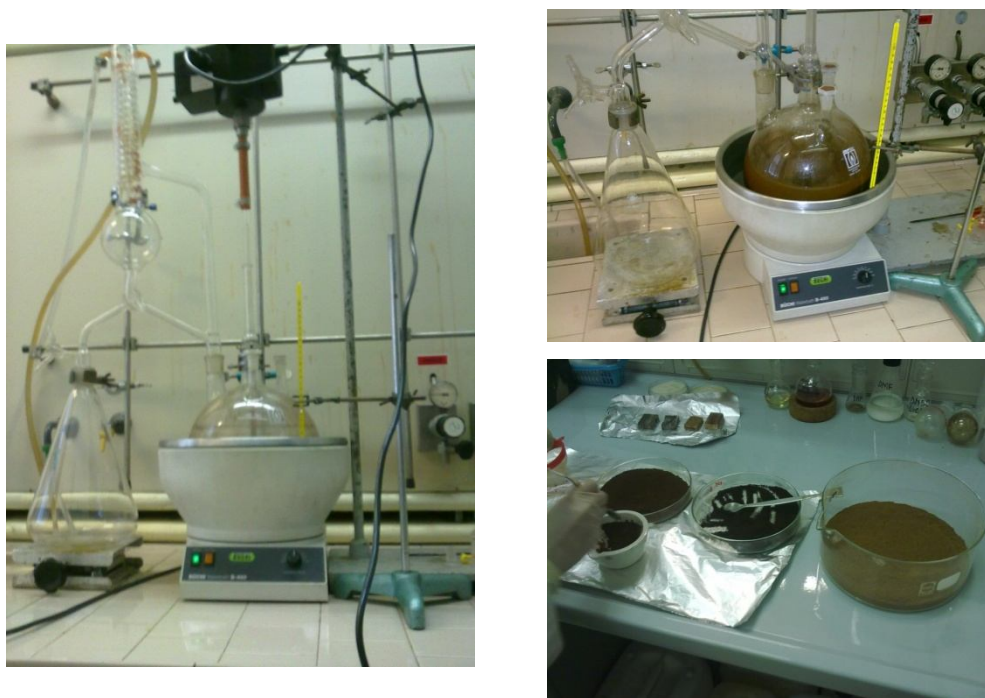


**Figure 46.** Scale up of the allylation and acetylation of purified lignin. Modification and recovery of lignin.



As previously discussed the lower MH value for a compound with allylated lignin could be due to the consumption of part of sulfur by allyl groups, reducing the total density of cross-linking. In order to evaluate the variation of the crosslink degree in presence of allyl groups, several modifications on the vulcanization system have been done increasing the amount of accelerator, the amount of sulfur or both of them.

Keeping constant the tyre recipe of allylated-acetylated compound, the vulcanization systems has been modified as follows: 0.8 phr of accelerator and 1.5 of sulfur (B), 0.8 phr of accelerator and 1.75 phr of sulfur (C), 0.8 phr of accelerator and 2 phr of sulfur (D) and 1 phr of accelerator and 2 phr of sulfur (E). These compounds are compared to a carbon black reference with 0.8 phr of accelerator and 1.5 of sulfur (A).

Increasing the amount of curing agents, as expected, the MH value increases from around 8 to 11 dNm, increasing the total density of cross-linking.

The modulus values (M50, M100 and M300) are reported in the *figure 47*. It was possible to observe that all modulus of rubber composites raised, achieving the best result with 2 phr of sulfur and 1 phr of accelerator (E).

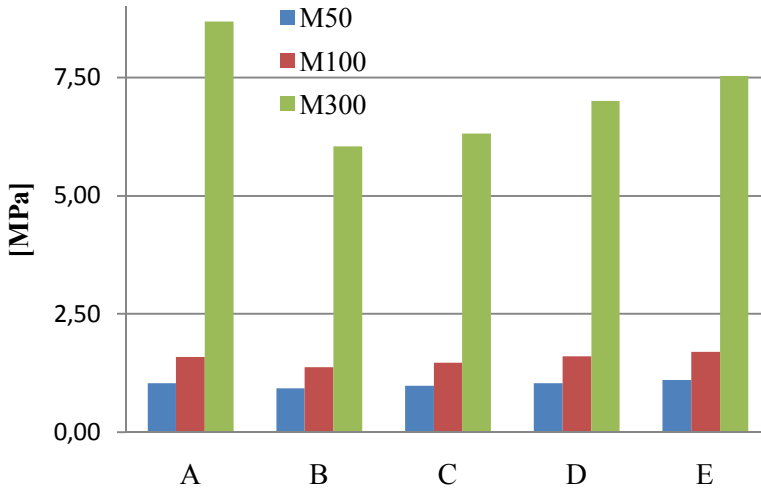


**Figure 47.** Modulus of compounds according to the change of the vulcanization system.

Also for the tensile strength and hardness, increasing the quantity of curing agents from 1.5 phr to 2 phr for the sulfur and from 0.8 phr to 1 phr for accelerator, resulted in a better performance.

The elongation at break reported in *figure 48*, decreased according to the vulcanization system's change in the sequence B > C > D > E. This expected behavior is related to the increase of crosslink density.

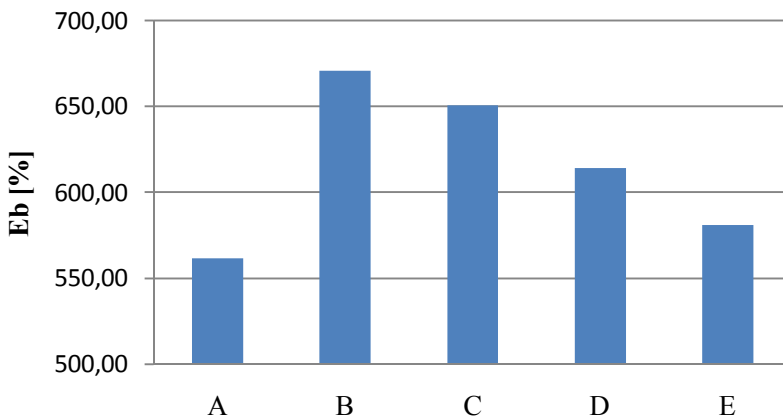


**Figure 48.** Elongation at break (%) of compounds according to the change of the vulcanization system

An unexpected behavior has been observed in the rebound (although the values remained higher than the reference with carbon black): a slight decrease has been observed in the sequence  $B > C > D > E$ . The reduction of rebound values is related to an increase of hysteresis that could be due to a different type of crosslink in the polymer matrix. Indeed, the lignin could occupy a position between two polymer chains and take part, by means of allyl groups, to the crosslink during the vulcanization. The presence of lignin influences the distance between two chains and thus part of the energy is dissipated when the compounds are stressed.

From a practical point of view the partial replacement of carbon black with allylated-acetylated lignin, with the vulcanization system E allowed to obtain mechanical performances close to the one obtained for reference with 65 phr of carbon black N375 (A).

### ***3.3.1.3 Use of coupling agent***

The reaction of silica with silane makes it more compatible with the elastomers. The silanol groups of silica react with alkoxy groups of silane in two different mechanisms: direct condensation or hydrolysis followed by condensation.

The reaction between silica and coupling agent can occur either directly during the mixing stage, or before the mixing stage through a pre-reaction (Cochet *et al.*, 1995) or with sol-gel method (Ikeda *et al.*, 2004). The addition of silica and coupling agent directly in the mixing stage is less efficient than the pre-reaction between them. Furthermore in-situ reaction needs some attentions about mixing condition and temperature. The pre-reaction of silica and coupling agent facilitates the mixing of silica with the rubber matrix.

Since the reaction takes place between silanols groups (Si-OH) of silica and alkoxy groups of silane, the presence of high amount of hydroxyl groups in

lignin suggests that the same reaction could work with lignin and thus improving its compatibility with the rubbers.

The introduction of lignin and coupling agent directly in the mixer has not worked and lignin has not been made more compatible with elastomers.

A pre-reaction of lignin with Bis-[ $\gamma$ -(triethoxysilyl)-propyl]-tetrasulfide (Si69) has been done; the occurred reaction was detected with the development of ethanol by GC-MS. The ethanol is obtained both as by-product of the reaction between silica and silane and as by-product of the reaction between two molecules of silane as shown by the mechanism of the reaction in the *figure 49*.

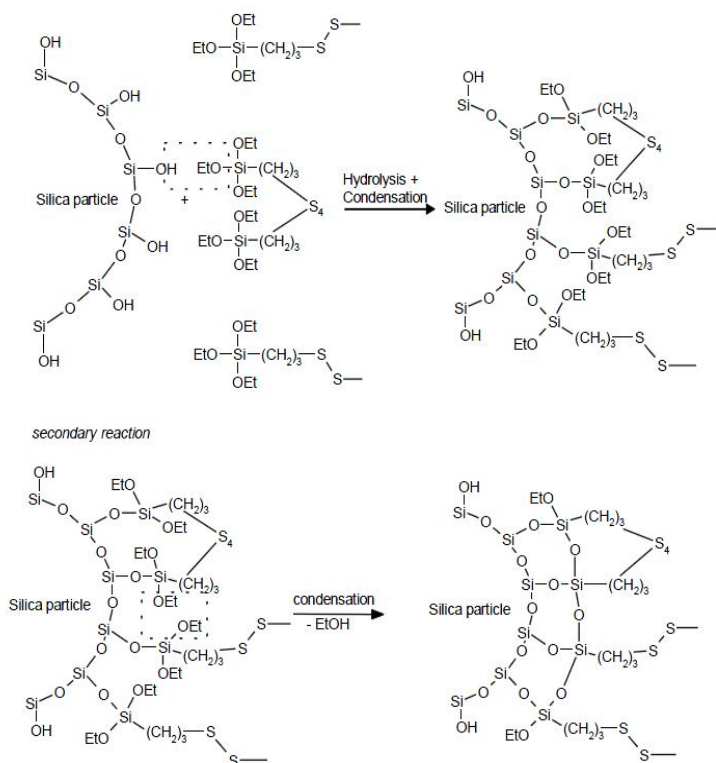


**Figure 49.** The reaction mechanism between silica and silane

In order to exclude the development of ethanol by reaction between two molecules of silane, a reference with only Si69 in the same conditions has been tested. The amount of ethanol for the reaction of lignin with Si69 was less than

the same reaction with silica but more than the only silane as showed by the histogram (figure 50); so the reaction between lignin and silane has taken place but with a very low yield.

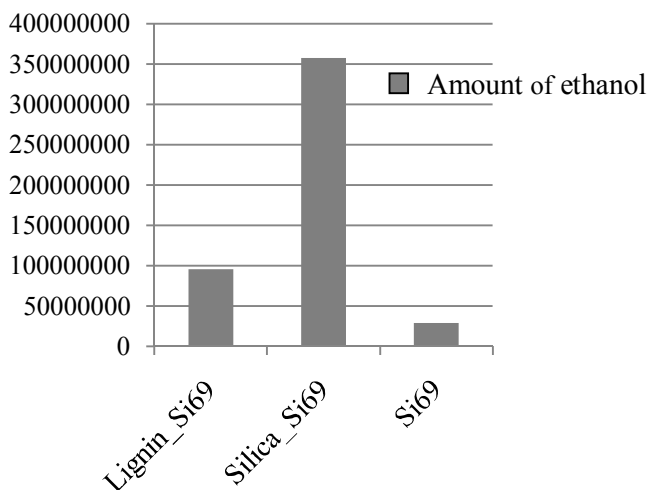


**Figure 50.** The amount of ethanol developed after the reaction with lignin (left), silica (centre) and the black (right).

The occurred reaction between lignin and Si69 has been also demonstrated by the presence of Si-O-C groups at  $1038\text{ cm}^{-1}$  in the IR spectra (figure 51).

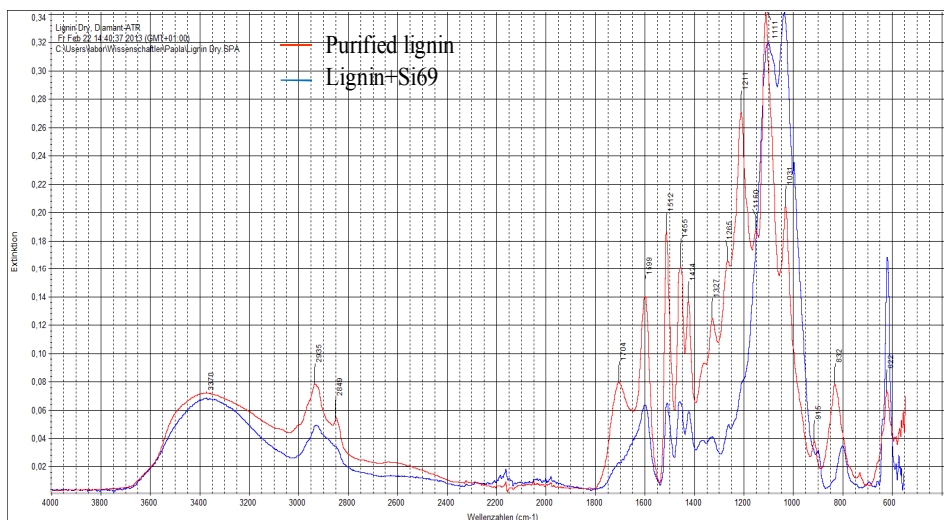


**Figure 51.** Overlapped of IR spectra of purified lignin (red) and Lignin with Si69 (blue)

The lignin reacted with Si69 has been tested in two compounds with NR and SBR.

		NR	NR_lignin	NR_lignin Si69	SBR	SBR_ lignin	SBR_ ligninSi69
		phr	phr	phr	phr	Phr	phr
STR 20		100	100	100			
SBR 1500					100	100	100
Lignin			1.25			1.25	
Lignin_Si69				1.25			1.25
Zinc oxide		3	3	3	3	3	3
Stearic Acid		2	2	2	2	2	2
TBBS		0.8	0.8	0.8	0.8	0.8	0.8
Sulfur		1.5	1.5	1.5	1.5	1.5	1.5
VISCOSITY ML (1+4) 100°C	Mooney ML(1+4) [Mooney Unit]	36.7	22.6	24.6	30.3	31.3	31.9
MDR 30min 170°C	ML[dN m]	0.69	0.77	0.71	0.43	0.59	0.63
	MH[dN m]	7.88	7.28	7.31	5.63	6.36	6.16
	t90[min]	14.74	12.47	11.25	13.81	15.08	14.15
<b>Curing 150°C</b>		<b>17 min</b>	<b>15 min</b>	<b>14 min</b>	<b>16 min</b>	<b>17 min</b>	<b>16 min</b>
TENSILE TEST 23°C	M50 [MPa]	0.6	0.5	0.6	0.5	0.6	0.5
	M100 [MPa]	0.9	0.8	0.8	0.8	0.8	0.7
	M200 [MPa]	1.4	1.2	1.3	1.3	1.0	1.0
	M300 [MPa]	2.0	1.8	1.8	1.8	1.2	1.3
	M500 [MPa]	5.6	5.0	5.5	-	2.0	2.1
	TS [MPa]	10.0	12.7	14.3	2.5	2.1	2.0
	Eb [%]	555.9	604.3	605.1	410.7	504.6	469.5
HARDNESS Shore A	Hardness [shore A]	42.3	39.6	38.9	35.0	40.0	38.2

**Table 14.** Curing characteristics and mechanical properties of pure NR, pure SBR and their composites with lignin and with lignin and silane.

The use of lignin reacted with Si69 slightly reduced the optimum cure time and slightly increased the tensile strength in natural rubber but it has not improved the mechanical properties of the compounds as reported in *table 14*. The reaction of lignin with Si69 has a very low yield and does not seem to improve lignin-elastomer compatibility.

### **3.4 COMMERCIAL SULFUR FREE LIGNINS**

As previously discussed, the purification process of the starting material is the first step that needs to be done for study the possibility to use lignins as biofiller. The method described above, if the goal is to obtaining a big amount of purified material, is very difficult for a laboratory scale and it showed also a low yield: for these reasons we have investigated the availability of commercial sulfur free lignins either with high level of purity or chemical modified.

Lignin Protobind 1000<sup>®</sup>, Protobind 2000<sup>®</sup> and Protobind 3000<sup>®</sup> have been purchased from Green Value Spa and they have been obtained by soda pulping process of herbaceous plants.

The differences in the various lignins are due to the different techniques used during lignin manufacturing, as well as some added compounds for making them compatible with different polymeric systems.

The Protobind 2000<sup>®</sup> contains a small percentage of diethylene glycol while the Protobind 3000<sup>®</sup> contains a small amount of hexamethylenetetramine.

The klason lignin is 92% for Protobind 1000<sup>®</sup>, while for Protobind 2000<sup>®</sup> and 3000<sup>®</sup> is about 80%. The materials have been characterized by GPC analyses and by means of quantitative <sup>31</sup>P-NMR spectroscopy to determine the amount of hydroxyls groups (*table 15*).

The most hydroxyl groups of lignin Protobind 1000<sup>®</sup> and Protobind 3000<sup>®</sup> are represented by phenolic hydroxyl groups while the 30% is given by aliphatic

hydroxyl groups. An important amount of carboxylic acids has been detected. In the Protobind 2000<sup>®</sup> the amount of aliphatic hydroxyl is very high due to the presence of diethylene glycol.

	<i>Protobind 1000</i> <sup>®</sup>	<i>Protobind 2000</i> <sup>®</sup>	<i>Protobind 3000</i> <sup>®</sup>
Water (%)	2.6	1.1	1.5
Ashes (%)	2.8	1.8	0.9
Klason lignin (%)	91.8	80.0	81.5
Polysaccharides (%)	2.8	17.1	16.1
<b>GPC</b>			
M <sub>n</sub> (g/mol)	3200	5600	3200
M <sub>w</sub> (g/mol)	7600	37600	8600
I	2.4	6.7	2.7
<b><sup>31</sup>P NMR</b>			
Aliphatic OH (mmol/g)	1.69	3.04	1.88
Condensed PhOH + S-OH (mmol/g)	2.02	1.41	1.51
G-OH (mmol/g)	1.00	0.93	0.87
P-OH (mmol/g)	0.44	0.28	0.28
COOH (mmol/g)	1.07	0.74	0.86
<b>Elemental analysis *</b>			
C (%)	65.3	60.9	60.7
N (%)	1.05	0.66	4.22
S (%)	0.45	0.41	0.46

**Table 15.** Compositional evaluation, GPC, and <sup>31</sup>P-NMR data for Protobind 1000, Protobind 2000 and Protobind 3000. The data indicated with \* are reported by Sahoo *et al.* (2011).

Lignin Protobind 1000<sup>®</sup> has characteristic similar to purified lignin except a superior amount of condensed phenolic and acid units due to the isolation method, so it could be used as starting material for further functionalization.

These lignins have been used as a partial replacement of carbon black in the compounds with different results: Protobind 1000<sup>®</sup> and 2000<sup>®</sup> has showed a behavior similar to the purified lignin while with lignin Protobind 3000<sup>®</sup> a higher ability to reinforce has been observed (*table 16*).



		Carbon black reference	Protobind 1000 <sup>®</sup>	Protobind 2000 <sup>®</sup>	Protobind 3000 <sup>®</sup>
		phr	phr	phr	Phr
NR		50	50	50	50
SBR		50	50	50	50
Carbon black N375		65	50	50	50
Protobind 1000 <sup>®</sup>			15		
Protobind 2000 <sup>®</sup>				15	
Protobind 3000 <sup>®</sup>					15
Stearic acid		2	2	2	2
Zinc oxide		3	3	3	3
Aromatic oil		10	10	10	10
6PPD		2	2	2	2
Soluble sulfur		1.5	1.5	1.5	1.5
TBBS		0.8	0.8	0.8	0.8
MDR 20min 170° C	ML[dN m]	2.12	1.97	1.29	1.57
	MH[dN m]	12.46	9.53	7.66	11.59
	tS2[min]	2.12	2.53	2.63	1.75
	t90[min]	6.27	11.26	8.32	4.73
	t95[min]	7.32	13.89	9.85	5.10
	t100[min]	11.68	19.98	17.33	8.16
	%RET[%]	3.39	0.13	0.63	6.47
<b>Curing</b>	<b>10 min 170°C</b>				
DENSITY	Density[g/cm <sup>3</sup> ]	1.146	1.120	1.122	1.124
RING TENSILE TEST 23°C	M50[MPa]	1.01	0.77	0.74	1.07
	M100[MPa]	1.60	1.11	1.06	1.74
	M300[MPa]	8.57	3.98	3.93	7.09
	TS[MPa]	16.58	12.42	12.25	16.03
	Eb[%]	533.09	694.00	735.98	580.19
	Energy[J/cm <sup>3</sup> ]	36.45	35.99	38.70	41.59
HARDNESS 23°C	Hardness[IRHD]	61.5	52.9	50.0	58.0
HARDNESS 100°C	Hardness[IRHD]	51.3	41.6	38.4	50.8
DISPERGRADER ANALYSIS	Average (X)[-]	5.2	0.5	2.0	0.5
	Average (Y)[-]	9.4	2.1	4.9	2.2

**Table 16.** Curing characteristics and mechanical properties of compound with carbon black, Protobind 1000<sup>®</sup>, Protobind 2000<sup>®</sup> and Protobind 3000<sup>®</sup>.

As demonstrated by the data reported in *table 16* the addition of Protobind 3000<sup>®</sup> led to the reinforcement of the compound. The Protobind 3000<sup>®</sup> is a commercial lignin that was obtained by a pre-blend step with HMT and treated in a pilot extruder (Bono *et al.*, 2008). It is evident that the addition of HMT is necessary for confer to the lignin ability to reinforce.

Following to the results obtained from the use of Protobind 3000<sup>®</sup>, two different strategies have been investigated for evaluate the influence of lignin and HMT in the rubber compound: the addition of purified lignin and HMT directly during the mixing step and the pre-reaction of lignin with HMT. This last modification can help further to avoid the use of not-healthy free HMT.

		Carbon black reference	Purified lignin	Protobind 3000	Purified lignin + 6% HMT	Purified lignin + 8% HMT	HMT pre-reacted lignin
		phr	phr	phr	phr	phr	phr
NR		50	50	50	50	50	50
SBR		50	50	50	50	50	50
Carbon black N375		65	50	50	50	50	50
Purified Lignin			15		15	15	
Protobind 3000 <sup>®</sup>				15			
HMT pre-reacted Lignin							15
Rhenogran HEXA-80 <sup>®</sup> (blend of 80% of HMT)					1.125	1.5	
Stearic acid		2	2	2	2	2	2
Zinc oxide		3	3	3	3	3	3
Aromatic oil		10	10	10	10	10	10
6PPD		2	2	2	2	2	2
Soluble sulfur		1.5	1.5	1.5	1.5	1.5	1.5
TBBS		0.8	0.8	0.8	0.8	0.8	0.8
MDR 20min 170°C	ML[dN m]	2.12	1.64	1.57	1.58	1.6	1.45
	MH[dN m]	12.46	10.35	11.59	11.54	11.83	12.72
	tS2[min]	2.12	2.44	1.75	1.90	1.81	1.66
	t90[min]	6.49	7.59	4.73	5.06	4.79	4.22
	t100 [min]	13.51	14.72	8.9	10.13	9.48	7.81
	% RET [%]	1.83	1.26	5.29	5.92	6.84	7.9
<b>Curing 10 min 170°C</b>							
RING TENSILE TEST 23°C	M50[MPa]	1.01	0.88	1.07	0.98	0.99	1.07
	M100[MPa]	1.60	1.36	1.74	1.62	1.64	1.77
	M300[MPa]	8.57	5.50	7.09	6.96	7.11	7.78
	TS[MPa]	16.58	13.4	16.03	15.99	15.79	16.43
	Eb[%]	533.09	593.65	580.19	575.80	568.19	548.15
HARDNESS 23°C	Hardness [IRHD]	61.5	55.6	58.0	60.0	59.3	63.7
HARDNESS 100°C	Hardness [IRHD]	51.3	46.3	50.8	51.7	50.7	53.0
DISPERGRADER ANALYSIS	Average (X)[-]	5.2	0.5	0.5	0.7	0.5	0.5
	Average (Y)[-]	9.4	2.6	2.2	3.3	2.9	3.0

**Table 17.** Curing characteristics and mechanical properties of compound with carbon black, Purified lignin, Protobind 3000<sup>®</sup>, Purified lignin+ 6%HMT, Purified lignin+ 8%HMT and HMT pre-reacted lignin.

Lignins have shown to influence the vulcanization process: in general, the scorch time as well as the optimum of vulcanization increased for the purified lignin. This could be attributed to the lignin phenolic group's reaction with the curing system which led to the increase in the optimum cure time, due to their acidity (Kumaran and De 1978; Nando and De 1980) and the presence of free carboxylic acid. On the other hand, the presence of HMT in the Protobind 3000<sup>®</sup> reduced the optimal cure time of the rubber composite. HMT indeed is also used as primary accelerator for NR and synthetic rubbers.

Protobind 3000<sup>®</sup> can be easily recreated with purified lignin and HMT by direct addition during the mixing stage. This is confirmed by the results reported in the *table 17*. Hardness, tensile strength, and tensile modulus measured at a certain elongation are comparable. A little amount of HMT is not enough to improve mechanical properties; the optimal percentage is between 6 and 8% as reported in the patent of Bono *et al.*, 2008.

The pre-reaction of purified lignin with HMT, before adding the material in the mixing stage, has been investigated as alternative strategy. The mechanism of the reaction is still unknown: the reaction of phenols model compounds with HMT described by Dargaville *et al.* (1996) could be the most reasonable interpretation. In this paper, the authors described the formation of di-benzylamine and tri- benzylamine from the reaction between phenols and HMT. The characterization of the material in our study seems to confirm this mechanism: the elemental analysis (reported in *table 18*) showed an increased amount of nitrogen in comparison to the purified lignin, a value close to the one obtained for Protobind 3000<sup>®</sup> as reported in *table 18*.

	C (%)	H (%)	N (%)	O (%)
<b>Purified lignin</b>	59.20	5.70	1.64	33.50
<b>HMT pre-reacted lignin</b>	50.90	5.67	3.03	40.40

**Table 18.** Elemental analysis of purified lignin and HMT pre-reacted lignin.

The HMT pre-reacted lignin was not analyzed by  $^{31}\text{P}$ -NMR spectroscopy due to the sample insolubility in the analysis solvent. The GPC analysis does not show an increase in molecular weight after the treatment with HMT.

In the Protobind 3000<sup>®</sup> IR spectrum (*figure 52 C*), the peak at  $1363\text{ cm}^{-1}$  reflected the C-H in-plane deformations due to the methylene group in Hexamethylenetetramine; in the IR spectrum of HMT pre-reacted lignin (*figure 52 B*) the same peak is present.

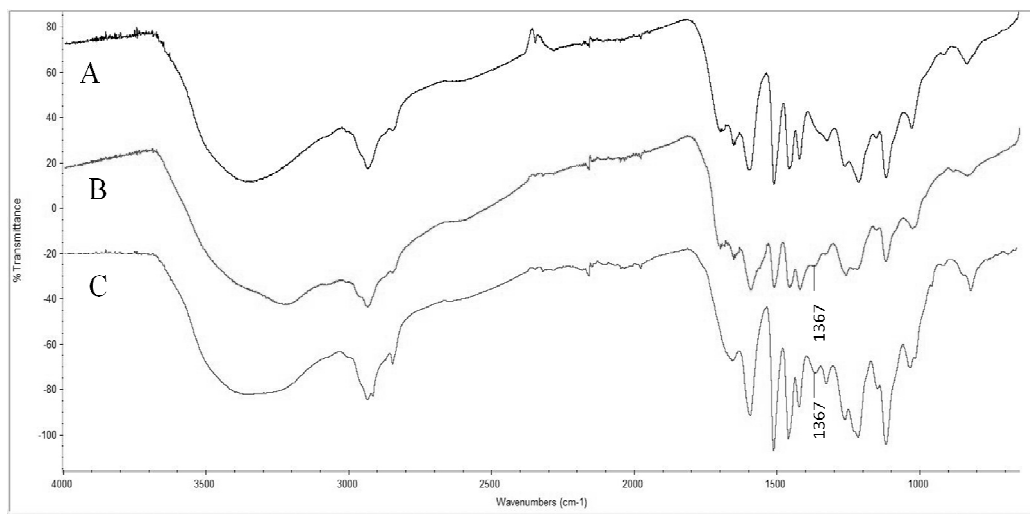


**Figure 52.** IR spectra of purified lignin (A), HMT pre-reacted lignin (B) and modified commercial lignin (C).

This material, used as a partial replacement for carbon black, has given good reinforcement results. We decided to use hardness and tensile strength as the

mechanical properties to underline and highlight the ability to reinforce the lignin in rubber composites. For clarity, the hardness at 23°C and 100°C is reported in the *figure 53*. It was possible to observe that the hardness of rubber composites with purified lignin and Protobind 3000® are lower in comparison to the reference, while HMT pre-reacted lignin leads to a higher value of hardness than the reference.

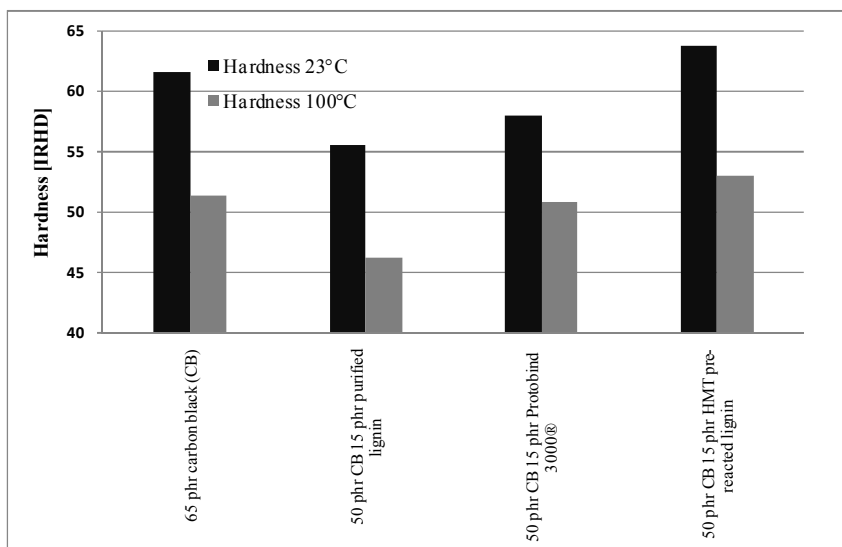


**Figure 53.** Dependence of hardness on the rubber composites.

The tensile strength for rubber composites with purified lignin strongly decreased in comparison to the carbon black reference as shown in *figure 54*. The presence of HMT increased the tensile strength in the Protobind 3000® as well as in the pre-reacted lignin, resulting in values similar to those of the carbon black reference.

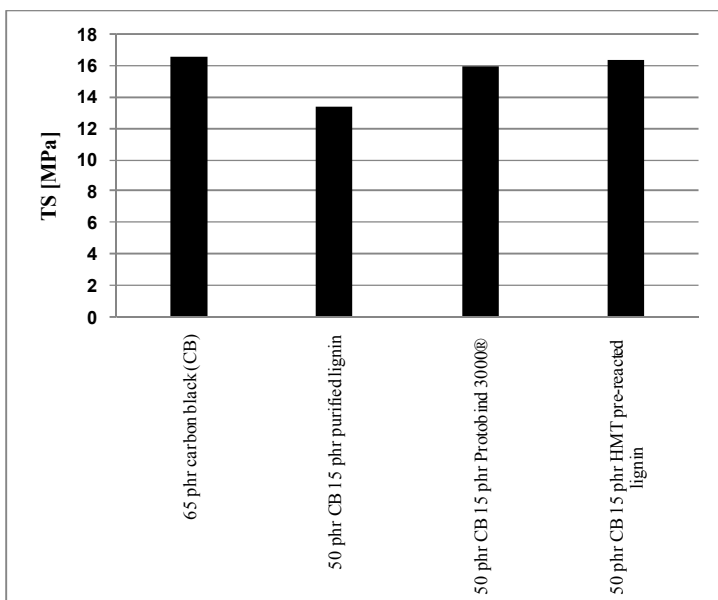


**Figure 54.** Comparison of tensile strength of the rubber composites.

The dispergrader data, reported in *table 17*, highlight a non-homogeneous dispersion of filler in the polymeric matrix in all analyzed rubber composites. The X value, that is a measure of the dispersion of filler in the polymeric matrix, is lower than the threshold limit value while the Y value indicates that agglomerates of large dimension are present in the sample.

### 3.5 REDUCTION OF PARTICLE SIZE

Another parameter that influences the filler behavior in the compound is the particle size that, together to the filler loading, determines the effective contact area between the filler and polymeric matrix.

Fillers that show a reinforcing behavior have particle size in the range from 10 nm to 100 nm. Lignin particle size is tenths of micron as shown in the *figure 55* while the average particle sizes of carbon black are in the range from 10 nm to 500 nm.

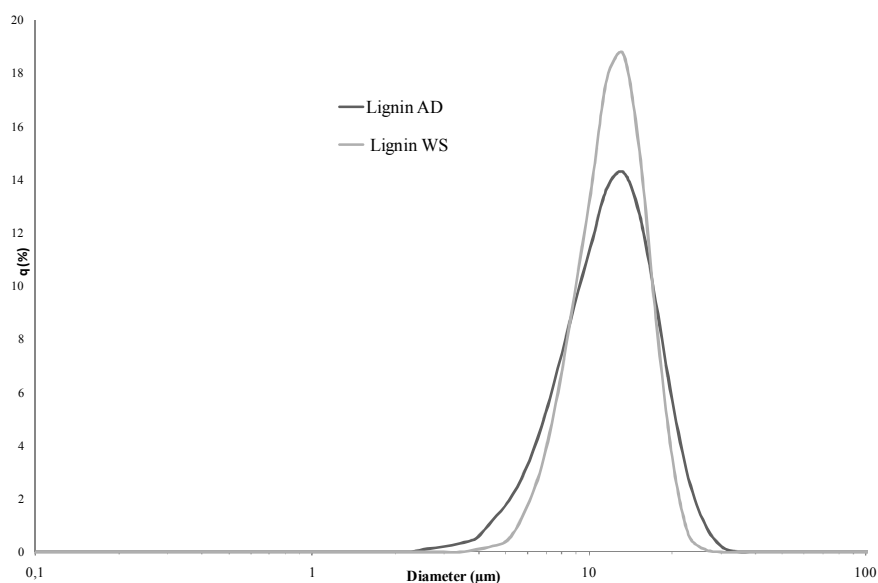


**Figure 55.** Laser scattering particle size distribution by analyzer LA-950.

In order to reduce the particle size of lignin three different approaches have been investigated: mechanical milling, the use of spray drying system and the co-precipitation of latex with lignin solution.

### **3.5.1 Milling**

The purified lignin was mechanically milled for 20 hours and then has been tested as partial replacement of carbon black and compared to the initial purified lignin.

The introduction of milled lignin has not affected the kinetics of cure. The static modulus of the compound with milled lignin were better but showed an insufficient reinforcement.

### 3.5.2 Spray drying

Lignin particles are linked to one another through hydrogen bonds, which lead to the growth of its particles, on the other hand when lignin is totally solubilized, lignin particles are smaller. The aim of the spray drying test is to convert a lignin solution into a dry powder with smaller particle size.

To achieve that a sample of acetylated lignin has been dissolved in acetone and a spray dry feasibility test has been done at the Buchi's laboratories. The particle size of the initial acetylated lignin is tenths of micron (*figure 56*).

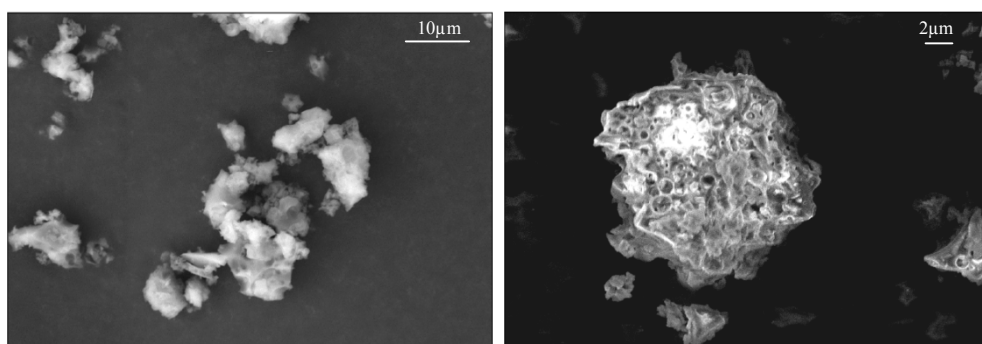


**Figure 56.** SEM images of Acetylated lignin

The sample has been successfully spray dried with the Mini Spray Dryer B-290. Spherical particles with shriveled surface have been produced. The yield has been approx. 74 % and the particle size is between 0.8 and 7 μm (*figure 57*).



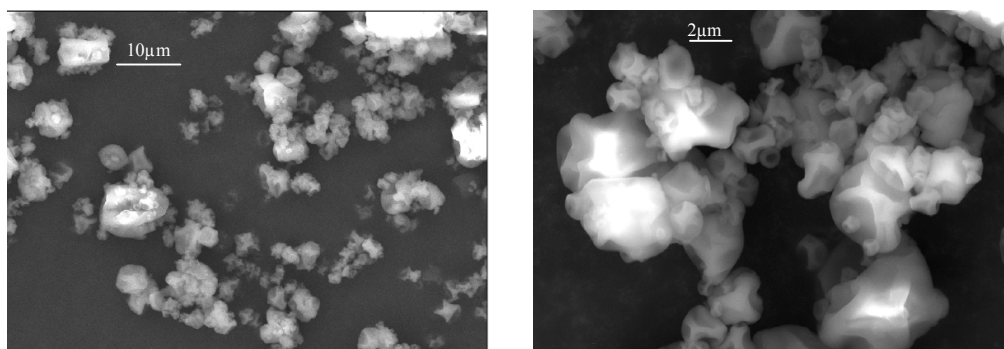


**Figure 57.** SEM images of Acetylated spray dried lignin (solution 10%)

Around 10 ml of sample was diluted 10 times with acetone to obtain a 1 % solution for the experiment with the Nano Spray Dryer B-90. The sample has been successfully spray dried. The yield has been approx. 14 % and the particle size is between 1 and 2.5 μm (*figure 58*)

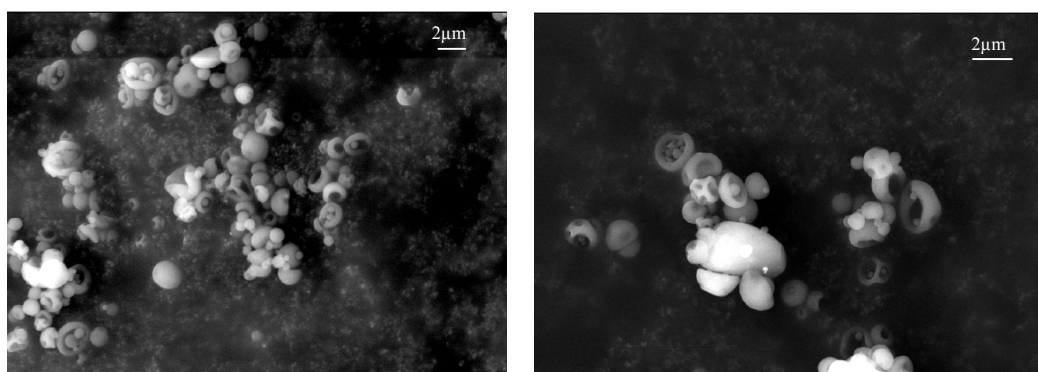


**Figure 58.** SEM images of Acetylated spray dried lignin (solution 1%)

The spray dried lignin has been tested as filler in the compound at two different concentrations (5 phr and 10 phr) and compared to the same formulation with the initial acetylated lignin. The compound compositions and properties have been summarized in the *table 19*.

		NR_reference	Acetylated lignin 5phr	Acetylated spray dried lignin 5phr	Acetylated lignin 10phr	Acetylated spray dried lignin 10phr
		phr	phr	phr	phr	phr
NR		100	100	100	100	100
Acetylated lignin			5		10	
Spray dried acetylated lignin				5		10
Zinc oxide		3	3	3	3	3
Stearic Acid		2	2	2	2	2
TBBS		0.8	0.8	0.8	0.8	0.8
Sulfur		1.5	1.5	1.5	1.5	1.5
VISCOSITY ML (1+4) 100°C	Mooney ML(1+4) [Mooney Unit]	36.7	22.5	20.6	22.6	18.4
MDR 30min 150°C	ML[dN m]	0.69	0.63	0.56	0.67	0.50
	MH[dN m]	7.88	6.75	7.01	7.57	7.25
	t90[min]	14.74	14.51	14.07	16.54	16.14
	t95[min]	17.81	17.00	16.02	19.10	18.20
	t100[min]	29.91	21.07	19.44	23.17	21.53
<b>Curing at 150°C</b>		<b>17 min</b>	<b>17 min</b>	<b>16 min</b>	<b>19 min</b>	<b>18 min</b>
TENSILE TEST 23°C	M50[MPa]	0.6	0.5	0.6	0.6	0.5
	M100[MPa]	0.9	0.8	0.8	0.9	0.8
	M200 [MPa]	1.4	1.2	1.3	1.3	1.2
	M300[MPa]	2.0	1.8	1.9	2.0	1.8
	M500[MPa]	5.6	5.4	5.9	6.1	5.1
	TS[MPa]	10.0	11.6	15.9	17.0	13.4
	Eb[%]	555.9	594.7	628.3	647.6	643.3
HARDNESS Shore A	Hardness [shore A]	42.3	30.7	30.9	40.8	38.7

**Table 19.** Curing characteristics and mechanical properties of reference compound, acetylated lignin compound (5 phr and 10 phr) and spray dried acetylated lignin compound.

The introduction of spray dried lignin has not improve the properties of compound, thus the reduction of the particle size until 1-5  $\mu\text{m}$  was not enough to improve the interaction with the natural rubber-based elastomer.

Acetylated lignin and acetylated spray dried lignin has been also used as partial replacement of carbon black in the compound. The compound compositions and properties have been summarized in the *table 20*.

		NR_CB reference	NR_CB_ Acetylated lignin	NR_CB_ Acetylated spray dried lignin (1-5 $\mu\text{m}$ )
		phr	phr	Phr
NR		100	100	100
N375		65	50	50
Acetylated lignin			15	
Acetylated spray dried lignin				15
Zinc oxide		3	3	3
Stearic Acid		2	2	2
TBBS		0.8	0.8	0.8
Sulfur		1.5	1.5	1.5
VISCOSITY ML (1+4) 100 C	Mooney ML(1+4)[Mooney Unit]	63.5	40.0	31.8
MDR 30min 150°C	ML[dN m]	3.37	1.93	1.94
	MH[dN m]	26.07	17.51	16.19
	t10[min]	2.31	3.28	3.34
	t90[min]	8.29	12.39	11.45
	t95[min]	9.56	15.36	14.09
	t100[min]	12.10	22.52	20.12
<b>Curing at 150°C</b>		<b>11 min</b>	<b>15 min</b>	<b>14 min</b>
TENSILE TEST 23°C	M50[MPa]	2.4	1.7	1.6
	M100[MPa]	4.8	2.8	2.7
	M200 [MPa]	13.1	6.0	6.1
	M300[MPa]	21.6	11.3	11.6
	M500[MPa]	-	23.5	23.2
	TS[MPa]	26.0	24.7	25.3
	Eb[%]	362.4	523.1	521.9
HARDNESS	Hardness [shore A]	75.2	69.6	68.2

**Table 20.** Curing characteristics and mechanical properties of reference compound with carbon black, acetylated lignin compound and spray dried acetylated lignin compound.

After the mixing of acetylated lignin and acetylated spray dried lignin with elastomers, no significant differences have been observed between the two lignins. Thus the reduction of particle size achieved with the spray drying test was not enough to improve the interaction filler-elastomer and therefore the mechanical properties.

### **3.5.3 Co-precipitation of latex with lignin**

In order to prepare a lignin-rubber blend two strategies can be used: dry-milling and the co-precipitation. As previously demonstrated the incorporation of purified lignin into dry rubber does not lead to a reinforcement. On the other hand lignin-rubber compound obtained after co-precipitation method has demonstrated ability to reinforcement (Asrul *et al.*, 2013).

In the method described by Jiang *et al.* (2013) the co-precipitation of sulfate lignin alkaline solution and NR latex solution at the same pH has been explored. Natural rubber latex is a stable dispersion of polymer microparticles in ammonia solution. The presence of ammonia is required for prevent the coagulation due to the development of acidity through micro-organisms and thus for long term preservation. The emulsion contains in addition to the gum, proteins, alkaloids, starches, sugars, oils, tannins and resins.

Lignin is soluble in alkali solution because of the ionization of the phenolic hydroxyl and carboxylic groups. It has been demonstrated that the parameters that influence the aggregation of lignin in alkaline solution are: temperature (Lindström and Westman., 1982), pH (Lindström, 1979 and Norgren *et al.*, 2001), concentration of lignin (Chernoberezhskii *et al.*, 2002) and surfactant (Norgren and Edlund, 2001). Lignin particle size is very sensitive to the pH, in fact at pH above 10 both phenolic hydroxyls that carboxylic acid are ionized and the particle size is in the range of 300-350 nm. At pH below 10, despite the

phenols are not ionized, lignin still has negative charge due to the carboxylic acid and the lignin particle size increase about 350 nm. Decreasing the pH the lignin particle aggregates due to the attractive forces.

The advantage of the co-precipitation method is that lignin solubilized in alkaline solution (pH 12) could be co-precipitated with rubber latex in the same pH conditions, resulting in the incorporation of lignin at small particle size.

Sulfonate Lignin-rubber composites have not demonstrated improvement in the mechanical properties. On the other hand it has been demonstrated that sulfonate lignin-natural rubber nanocomposites, obtained by co-precipitation of sulfonate lignin-cationic polyelectrolyte (PDADMAC) complexes with natural rubber latex, increased the mechanical properties. The explanation of these results is the homogenous distribution of lignin-polyelectrolyte complexes in the polymeric matrix as a consequence of the adsorption on NR latex particles (negatively charged) of the lignin-PDADMAC complexes (positively charged), avoiding the agglomeration of lignin (Jiang *et al.*, 2013).

Sulfur free lignins in solution have different behavior in comparison to sulfonate ones. The former tend to precipitate at acid pH whereas the latter prefer to remain soluble, thus during the acid coagulation the sulfonate lignins do not tend to form agglomerates. This behavior explains the necessity of the use of the polyelectrolyte PDADMAC with sulfonate lignin-NR co-precipitation experiments.

In order to evaluate the behavior of sulfur-free lignin, a preliminary test of co-precipitation of sulfur-free lignin with NR from latex has been done, introducing 2.5 phr of lignin.

		NR latex	NR latex lignin
		phr	Phr
NR coagulated from latex		100	
NR co-precipitated with lignin from latex			102.5
Zinc oxide		3	3
Stearic Acid		3	3
Sulfur		1.5	1.5
TBBS		0.8	0.8
VISCOSITY ML (1+4) 100 C	Mooney ML(1+4)[Mooney Unit]	30.2	29.0
MDR 30min 150 C	ML[dN m]	0.71	0.67
	MH[dN m]	5.81	5.35
	t05[min]	8.23	9.43
	t90[min]	20.42	23.48
	t95[min]	23.35	26.16
	T100[min]	27.53	29.04
<b>Curing</b>		<b>23 min 150°C</b>	<b>26 min 150°C</b>
TENSILE TEST 23 C	M50[MPa]	0.5	0.5
	M100[MPa]	0.7	0.6
	M200[MPa]	1.0	0.9
	M300[MPa]	1.5	1.3
	M500[MPa]	3.4	3.4
	TS[MPa]	8.2	9.6
	Eb[%]	605.9	635.7
HARDNESS Shore A	Hardness[shore A]	34.4	34.7

**Table 21.** Curing characteristics and mechanical properties of reference compound and co-precipitated lignin with latex compound.

The presence of 2.5 phr of lignin has increased the optimum of vulcanization, due to the interaction between lignin and vulcanization system and slightly improve the tensile strength and elongation at break but no improvement of hardness and static modulus at different deformation were observed (*table 21*).

Following the obtained results, further compounds with higher concentration of purified lignin (7 phr and 15 phr) and another one with 7 phr of chemically modified lignin have been tested by mixing with a Brabender mixer.

		NR coagulated from latex	NR co-precipitated with 7phr purified lignin from latex	NR co-precipitated with 15 phr purified lignin from latex	NR co-precipitated with 7 phr partially allylated lignin from latex
		phr	phr	phr	Phr
NR coagulated from latex		100			
NR co-precipitated with 7phr purified lignin from latex			107		
NR co-precipitated with 15phr purified lignin from latex				115	
NR co-precipitated with 7phr partially allylated lignin from latex					107
Stearic acid		2	2	2	2
Zinc oxide		5	5	5	5
CBS		2	2	2	2
Sulfur		2	2	2	2
MDR 60min 150°C	ML[dN m]	1.10	1.21	1.24	1.15
	MH[dN m]	9.02	9.46	8.65	8.46
	tS2[min]	7.22	10.66	10.92	11.54
	t90[min]	11.38	15.73	16.68	16.74
	t95[min]	13.39	18.09	18.79	19.34
	t100[min]	23.50	28.40	31.00	30.70
	%RET[%]	3.41	6.79	4.99	5.88
<b>Curing 30 min 150°C</b>					
HARDNESS IRHD 23°C	Hardness [IRHD]	45.6	46.6	45.9	44.2
DUMBELL TENSILE TEST 23°C	M10[MPa]	0.23*	0.23	0.22	0.20
	M50[MPa]	0.68*	0.67	0.62	0.59
	M100[MPa]	1.07*	1.05	0.97	0.90
	M300[MPa]	3.25*	3.51	3.59	2.69
	TS[MPa]	8.55*	25.07	26.22	18.39
	Eb[%]	415.15*	610.66	629.03	587.08
	ENERGY [J/cm <sup>3</sup> ]	11.27*	39.08	45.39	27.91

**Table 22.** Curing characteristics and mechanical properties of reference compound, NR co-precipitated lignin (7 phr and 15 phr) from latex compound and NR co-precipitated modified lignin from latex compound. The data indicated with \* are not reliable due to the wrong breakage of test specimen.

As demonstrated by the data reported in the *table 22*, the NR co-precipitation with 7 phr and 15 phr of purified lignin from latex has increased the tensile

strength and elongation at break of the compounds. These data cannot be compared with the reference, composed by NR latex, because the data (indicated with \*) are not reliable due to the wrong breakage of test specimen.

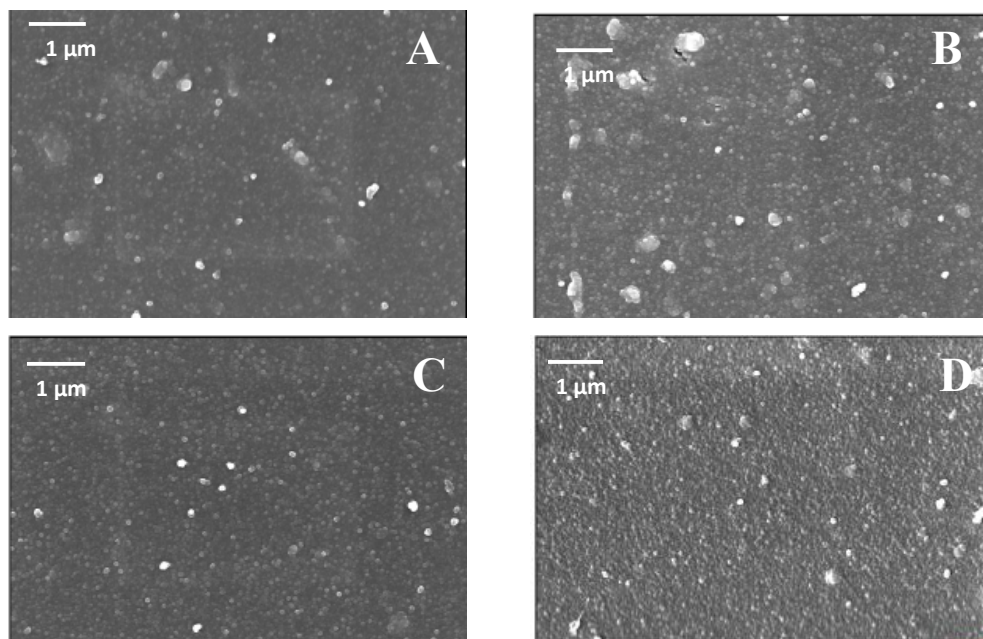


**Figure 59.** SEM images of the compounds: reference (A), NR co-precipitated with 7phr of lignin from latex (B), NR co-precipitated with 15phr of lignin from latex (C) and NR co-precipitated with 7phr of modified lignin from latex (D).

The SEM images of the compounds in which has been introduced lignin are very close to the reference (*figure 59*). All compounds have highlighted the granulometric nature of the matrix. The visible particles have been individuated as sulfur, probably not completely mixed.

In order to confirm the previously results another compound with 7 phr of co-precipitated lignin has been done, but it has not been compared with only a reference composed by NR-latex. The comparison has been done with four compounds in which to NR coagulated from latex were added, directly in the



mixing stage, 7 phr of carbon black, 7 phr of purified lignin, 7 phr of purified milled lignin and 7 phr of acetylated lignin.

		NR coagulated from latex	NR coagulated +7phr of CB	Co-precipitated NR and 7phr of purified lignin	NR coagulated +7phr of purified lignin	NR coagulated +7phr of milled purified lignin	NR coagulated +7phr of acetylated lignin
NR coagulated from latex		100	100		100	100	100
NR co-precipitated with 7phr purified lignin from latex				107			
Purified lignin					7		
N375			7				
Acetylated lignin							7
Milled purified lignin						7	
Stearic acid		2	2	2	2	2	2
Zinc oxide		5	5	5	5	5	5
CBS		2	2	2	2	2	2
Sulfur		2	2	2	2	2	2
MDR 60min 150 C	ML[dN m]	0.65	0.75	0.79	0.68	0.54	0.54
	MH[dN m]	8.98	11.29	8.87	8.94	9.14	8.41
	tS2[min]	7.58	6.16	11.54	8.82	8.82	10.33
	t90[min]	12.68	11.38	17.17	14.59	15.01	17.26
	t95[min]	15.08	13.88	19.77	17.36	17.89	20.82
	t100[min]	26.07	24.74	33.24	29.83	31.90	37.67
%RET[%]		3.00	2.85	5.82	3.15	2.79	1.52
<b>Curing 30 min 150°C</b>							
RING TENSILE TEST 23°C	M50[MPa]	0.65	0.87	0.62	0.65	0.67	0.62
	M100[MPa]	1.01	1.42	0.95	1.01	1.03	0.95
	M300[MPa]	2.73	5.86	2.83	2.86	2.74	2.44
	CR[MPa]	11.72	6.42	20.35	14.65	11.63	12.8
	AR[%]	543.74	339.09	646.73	582.07	554.71	594.50
	Energy[J/cm <sup>3</sup> ]	16.37	8.55	33.07	21.59	17.35	19.40
HARDNESS 23°C	Hardness [IRHD]	48.7	54.5	47.3	48.4	49.0	47.7
HARDNESS 100°C	Hardness [IRHD]	45.7	51.5	45.5	47.0	47.5	46.4

**Table 23.** Curing characteristics and mechanical properties of reference compound, NR coagulated+CB, co-precipitated NR with lignin from latex, NR coagulated+ purified lignin, NR coagulated + milled purified lignin and NR coagulated +acetylated lignin.

The NR co-precipitated with 7 phr purified lignin from latex has not shown an improvement in the reinforcement of the compound but has increased the tensile strength and elongation at break (*table 23*). The introduction of lignin

seems to reduce the vulcanization rate and this phenomenon could reduce the crosslink density and thus a higher elongation of break has been obtained.

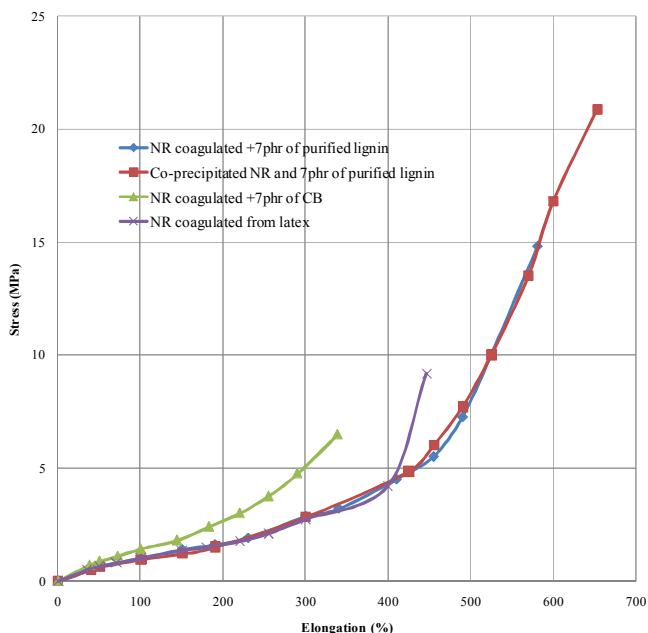


**Figure 60.** Stress-strain curve for unfilled NR, carbon black filled NR, lignin filled NR and lignin filled NR by co-precipitation.

The *figure 60* reported the stress-strain curves from tensile testing for unfilled rubber, carbon black and lignin filled rubber samples. Addition of carbon black in the NR composite increased the modulus, decreasing the elongation at break. On the other hand, the addition of lignin exhibited an increase in stress at higher deformations and in the elongation at break.

The compounds have been characterized with SEM analysis, the images are reported in the *figure 61* and a quantification of inclusion in a sample of 40mm<sup>2</sup> has been reported in the *table 24*.

	NR coagulated from latex	NR coagulated +7phr of CB	Co-precipitated NR and 7phr of purified lignin	NR coagulated +7phr of purified lignin	NR coagulated +7phr of milled lignin	NR coagulated +7phr of acetylated lignin
N° inclusion	3	0	3	10	30	7
Average diameter (µm)	8.00	0	17.00	14.32	29.24	40.93

**Table 24.** Quantification of inclusion of reference compound, NR coagulated +CB, co-precipitated lignin with latex, NR coagulated + purified lignin, NR coagulated + milled purified lignin and NR coagulated +acetylated lignin.

The reference and the compound with carbon black presented a homogenous matrix while the addition of lignin involved the formation of aggregates as demonstrated by SEM images. Furthermore, the data reported in the *table 24* showed that the compound of co-precipitated lignin had a lower amount of inclusions in comparison to the compound with lignin added to the precipitated latex. Thus the co-precipitation of lignin with latex allowed obtaining lignin well dispersed in the polymeric matrix.

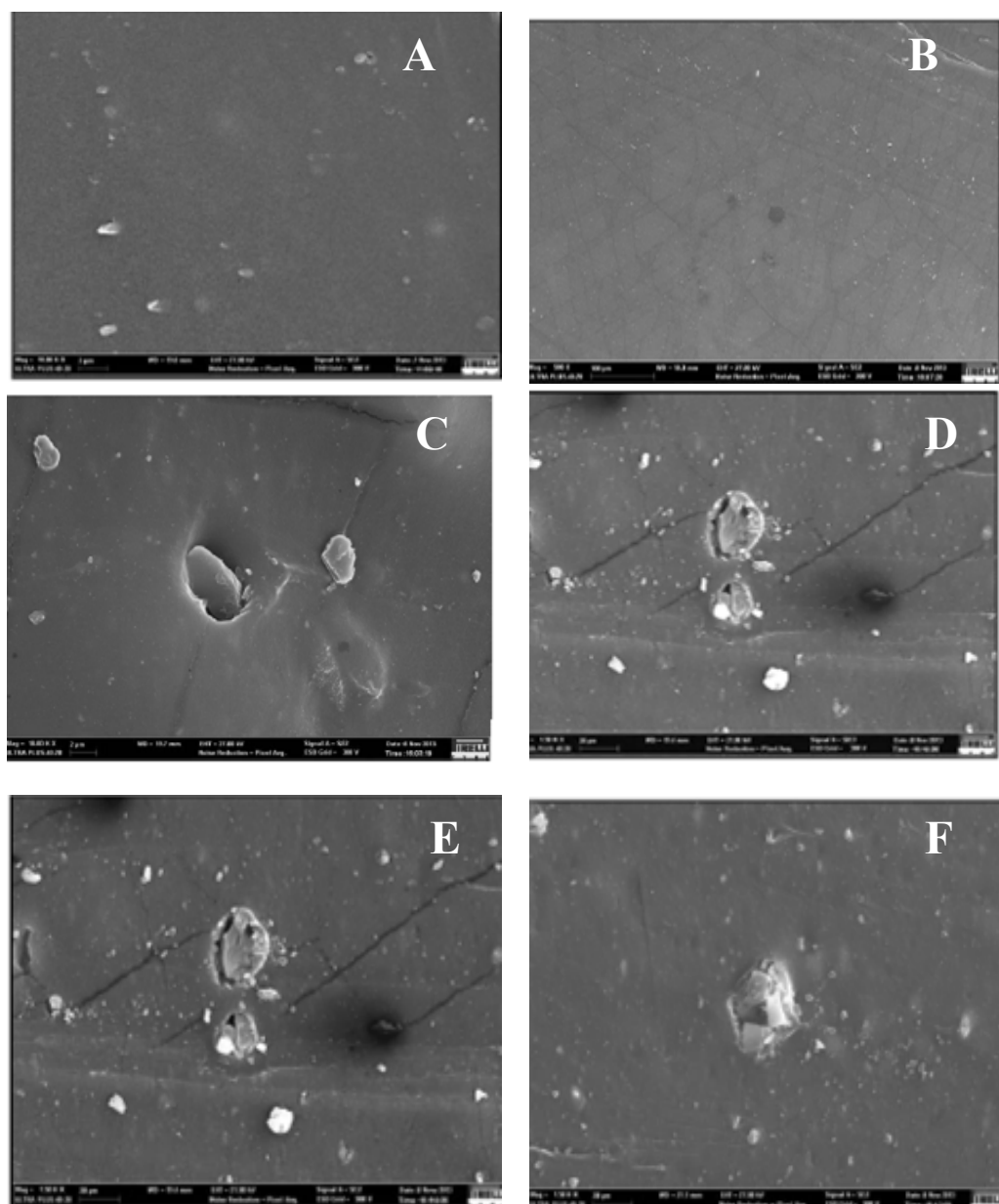


**Figure 61.** SEM images of the compounds: reference (A), NR coagulated + CB (B), coprecipitated lignin with latex (C), NR coagulated + purified lignin (D), NR coagulated + milled purified lignin (E) and NR coagulated +acetylated lignin (F).

Through a strain sweep test was possible to observe the variation in the viscoelastic properties of the compound versus strain.

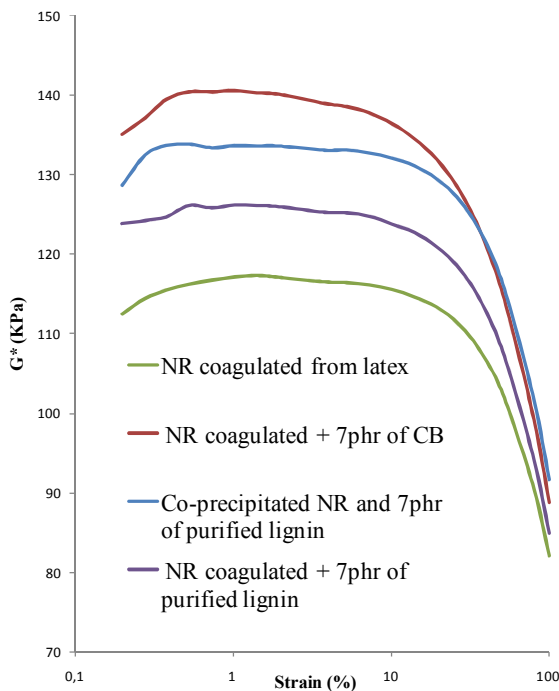


**Figure 62.** The complex modulus  $G^*$  and versus strain

Influence of filler on the complex modulus  $G^*$  has investigated and shown in the *figure 62*: the introduction of 7 phr of filler increased the modulus because for pure rubber only entanglements stretching and chain movements occurred while in filled rubber filler associations also participate. At low strain, only stretching of entanglements and linked polymer chains between filler molecules took place while the chains movement and filler-filler interaction did not suffer any deformation.

Increasing the strain, the modulus decreased rapidly due to the entanglements stretching and filler-polymer bond, but also due to the chain movements and filler-filler breakdowns. In the compound with CB the modulus was the highest,

due to more interactions of CB particles and the higher surface area that created a strong filler-filler network. In the compound with co-precipitated lignin with latex the modulus was higher in comparison to the addition of lignin to precipitated latex: smaller lignin particle size and better interaction of lignin molecules with latex advantages the formation of filler-polymer network.

The interactions between sulfur free lignin molecules and latex micelles are not clear but the hypothesis is that lignin could occupy a position between two latex micelles during the co-precipitation process.

In conclusion, NR co-precipitated with 7 phr purified lignin from latex does not show ability to reinforce but it has very good elastic properties that could suggest its use for other purpose, like belts in tyre. Furthermore, thanks to lignin antioxidant activity, the co-precipitation of lignin with NR-latex could prevent the degradation of natural rubber during the mixing at high temperature.

The co-precipitation of lignin with NR-latex is under investigations. Although the co-precipitation of sulfur free lignin with NR-latex has underlined good properties of the compounds, the introduction of polyelectrolyte could further improve the mechanical properties.

## 4 CONCLUSION

The addition of a filler to rubber is fundamental in order to improve hardness and strength properties. Nowadays, carbon black is the most commonly used reinforcing filler because its chemical and physical characteristics allow an effective enhancement of the required polymers' features.

However, also lignin has been the subject of many studies (Setua *et al.* 2000; Kumaran and De 1978; Griffith and MacGregor 1953) and patents (Benko *et al.* 2010; Boutsicaris 1984; Davidson and Wunder 1977; Doughty 1967; Doughty and Charlestion 1966) aiming at its use as a rubber filler.

Unluckily, sulfur free lignin has not shown the ability to reinforce rubber: its polar nature and complex structure prevent both a good dispersion in the polymeric matrix and a high interaction with the elastomer, so its addition as it is or as a partial replacement of carbon black strongly worsens the mechanical properties of the compound. Lignin's chemical nature and particle size are the major obstacles to its utilization in this field.

Concerning the chemical modification of sulfur free lignin, functionalization by means of acetylation makes it more hydrophobic and thus more compatible with the elastomers; nevertheless, its use as partial replacement of carbon black does not allow achieving the performances observed in carbon-black-only composites. Acetylation promotes a better dispersion of lignin in comparison to the purified one, but the composite's mechanical properties are lower than the carbon black reference. On the other hand, the introduction of HMT pre-reacted lignin as a partial replacement of carbon black improves the mechanical properties in comparison to the purified lignin, but a good enough dispersion in the polymeric matrix is not observed. Only the partial replacement of carbon black by allylated-acetylated lignin allows obtaining a compound without loss

of mechanical properties. The introduction of the allyl group probably favors the formation of a filler-polymer network during the vulcanization stage, guaranteeing a very good dispersion of the filler.

In order to improve this last feature the reduction of lignin's particle size is fundamental. In fact, while the present fillers have particle sizes in the nanometer range, lignin's ones are of the order of tenths of micron. With mechanical milling and spray drying methods, one is able to obtain a particle's diameter smaller than 10 microns, still not small enough to improve the interaction filler-elastomer. Instead, the co-precipitation of lignin with NR-latex in alkaline solution, where lignin is totally solubilized and has nanometric dimensions, is to prefer. This process has allowed understanding that the real task of lignin in rubber compounds is to confer good elastic properties. Indeed, the introduction of lignin increases the elongation and the energy at break. These properties suggest the use of lignin for other purposes than the original one of reinforcement. Furthermore, thanks to lignin's antioxidant activity, its co-precipitation with NR-latex could prevent the degradation of natural rubber during the mixing at high temperature.



## **ACKNOWLEDGMENTS**

I would like to thank Professor Marco Orlandi for his supervision to my Ph.D. project. A fundamental contribution to my work has been given by Dr. Luca Zoia, who has helped me in everything. I am very grateful for his help, his scientific advice and knowledge and many discussions and suggestions during these years.

I would like to thank Dr. Thomas Hanel and Dr. Luca Castellani for their supervision and support to my project and I have to thank as well all the people I met in Pirelli during these years, they have been very helpful with me.

I am very thankful to Prof. Dr. Jussi Sipilä and his group from University of Helsinki and Prof. Dr. Ulrich Giese from Deutsche Institut für Kautschuktechnologie (DIK) for hosting me during my period abroad and for allowing me to learn a lot and to achieve important results in my PhD project.

I have to thank all guys at DIK for helping me and for the enjoyable period that I spent there.

I would like to thank Dr. Rütli from Buchi laboratories for the spray drying feasibility tests.

I am very thankful to Anika, who shared the office with me every day, side by side for her help and her friendship.

A dear thank to all the colleagues and friends that have shared with me some experience in the laboratory and not only, during these three years.

A special thank to Annalisa, who proved to be a dear friend in every moment. I am very grateful for her support, encourage and friendship and for her helping during the writing of my thesis.

I also thank to my family for their patience, for their continuous support and for encouraging me during these three years.

Finally, a special thank to Francesco, who shared with me every moment during these years encouraging and supporting me with his affection.

## REFERENCES

- Alexy P., Feranc J., Kramárová Z., Hajšová M., Ďuračka M., Mošková D., Chodak I., S. Ilisch, (2008) KGK Januar/Februar.
- Alexy P., Košíková B., Podstránka G., (2000). *Polymer*. 41, 4901.
- Argyropoulos, D. S. and Menachem., S. B., (1998). “Lignin.” In *Biopolymers From Renewable Resources*, Kaplan, D. L Ed., Springer Verlag, , Chapter 12, pp. 292, 322.
- Argyropoulos, D.S. “Quantitative phosphorus-<sup>31</sup> NMR analysis of lignins: a new tool for the lignin chemist”, *J. Wood Chem. and Technol.* 1994. 14 (1), 45-63.
- Asrul, M., Othman, M., Zakaria, M., and Fauzi, M. S., (2013). “Lignin Filled Unvulcanised Natural Rubber Latex: Effects of Lignin on Oil Resistance, Tensile Strength and Morphology of Rubber Films”, *International Journal of Engineering Science Invention*, 2 (5), 38-43.
- ASTM C136-06, 2006 Standard Test Method for Sieve Analysis of Fine and Coarse Aggregates.
- ASTM D1646, 2004. Viscosity, stress relaxation and pre-vulcanization characteristics (Mooney viscometer).
- ASTM D2240 - 05(2010) Standard Test Method for Rubber Property—Durometer Hardness
- ASTM D6204, 2012. Standard Test Method for Rubber-Measurement of Unvulcanized Rheological Properties Using Rotorless Shear Rheometers.
- Benko, D. A., Hahn, B. R., Cohen, M. P., Dirk, S. M., and Cicotte, K. N. (2010). “Functionalized lignin, rubber containing functionalized lignin and products containing such rubber composition,” U.S. Patent 2010/0204368 A1.
- Bertini, F., Canetti, M., Cacciamani, A., Elegir, G., Orlandi, M., and Zoia, L. (2012). “Effect of ligno-derivatives on thermal properties and

- degradation behaviour of poly(3-hydroxybutyrate)-based biocomposites” *Polymer Degradation and Stability* 97(10), 1979-1987.
- Billa, E., Koukios, E.G., Monties, B., (1998). Investigation of lignins structure in cereal crops by chemical degradation methods. *Polym. Degrad. Stab.* 59, 71-75.
  - Blume A. “Kinetics of the Silica-Silane Reaction” *KGK Kautschuk Gummi Kunststoffe*, 2011, 38-43.
  - Bono P.J., Barakat A., Lepifre S., Loira J.H. (2008). “Methods for producing modified aromatic renewable materials and compositions therefore” U.S. Patent 2008/0021155 A1.
  - Boutsicaris, S. P. (1984). “Lignin reinforced synthetic rubber,” U.S. Patent 4477612.
  - Buranov, A.U., Mazza, G., (2008). “Lignin in straw of herbaceous crops”, *Ind. Crops Prod.* 28, 237-259.
  - Chernoberezhskii Y. M., Atanesyan A. A., Dyagileva A. B., Lorentsson A. V., Leshchenko T. V. (2002). “Effect of the concentration of sulfate lignin on the aggregation stability of its aqueous dispersions”, *Colloid Journal*, 64, 637-639.
  - Choi S.S., (2001). “Improvement of properties of silica-filled styrene-butadiene rubber compounds using acrylonitrile-butadiene rubber”, *J. Appl. Polym. Sci.* 79 (6), 1127-1133.
  - Choi, J. W. & Faix, O. (2011). NMR study on residual lignins isolated from chemical pulps of beech wood by enzymatic hydrolysis. *Journal of Industrial and Engineering Chemistry*, 17, 25-28.
  - Cochet P., Barriquand L., Bomal Y. and Touzet S., Paper No. 74 *presented at a meeting of the Rubber Division.*
  - Crestini, C., Argyropoulos, D.S., (1997). “Structural analysis of wheat straw lignin by quantitative  $^{31}\text{P}$  and 2D NMR spectroscopy. The occurrence of ester bonds and  $\beta\text{-O-4}$  substructures”, *J. Agric. Food Chem.* 45, 1212–1219.

- Dargaville Timothy R., De Bruyn Pauline J., Lim Audrey S. C., Looney Mark G., Potter Alan C., Solomon David H., Zhang Xiaoqing, (1996). Chemistry of Novolac Resins. II. Reaction of Model Phenols with Hexamethylenetetramine. 1389-1398.
- Davidson, M. J. G., and Wunder, R. H. (1977). "Latex coagulation process using lignin compound," U.S. Patent 4025711.
- Donnet J.B. and Voet A., (1976). "Carbon black, Physics, Chemistry and elastomer reinforcement", Marcell Dekker, 9-11.
- Doughty, J. B. (1967). "Method of dry-milling carboxylic elastomers and alkali lignins," U.S. Patent 3325427.
- Doughty, J. B., and Charleston, S. C. (1966). "Lignin reinforced rubber and method of preparation thereof," U.S. Patent 3247135.
- Faix, O., Argyropoulos, D. S., Robert, D. & Neirinck, V. (1994). "Determination of hydroxyl groups in lignins evaluation of  $^1\text{H}$ -,  $^{13}\text{C}$ -,  $^{31}\text{P}$ -NMR, FTIR and wet chemical methods". *Holzforschung*, 48, 387-394.
- Falkehag S. I. (1972). "Hexamethylene tetramine derivates of alkali lignins," U.S. Patent 3697497.
- Feldman, D., Banu, D., Campanelli, J., Zhu, H., (2001). "Blends of vinylic copolymer with plasticized lignin: thermal and mechanical properties". *J. Appl. Polym. Sci.*, 81 (4), 861-874.
- Ford, C.W., (1990). "Borohydride-soluble lignin-carbohydrate complex esters of *p*-coumaric acid from the cell walls of a tropical grass", *Carbohydr. Res.* 201, 299-310
- Fort, D. A., Remsing, R. C., Swatloski, R. P., Moyna, P., Moyna, G., Rogers, R. D., (2007). "Can ionic liquids dissolve wood? Processing and analysis of lignocellulosic materials with 1-n-butyl-3-methylimidazolium chloride", *Green Chem.* 9, 63-69.
- Fox and McDonald, (2010). "Lignin characterization", *BioResources* 2010, 5(2), 990-1009

- Furlan L.T., Rodrigues M.A. & De Paoli M-A., (1985). "Sugar Cane Bagasse Lignin as Stabilizer for Rubbers: Part III--Styrene/Butadiene Rubber and Natural Rubber". *Polymer Degradation and Stability* 13, 337-350.
- Gargulak, J.D., Lebo, S.E., (2000). "Commercial use of lignin-based materials". *ACS Symp. Ser.*, 742, 304.
- Gellerstedt G. and Henriksson G., (2008) "Lignins - Major sources structure and properties", *Monomers, polymers and composites from renewable resource*, pp. 200-224, Elsevier.
- Ghosh, I., Jain, R.K., Glasser, W.G., (2000). "Multiphase materials with lignin. Part 16. Blends of biodegradable thermoplastics with lignin esters". *ACS Symp. Ser.*, 742 (Lignin: Historical, Biological, and Materials Perspectives), 331.
- Glasser W. Lignin, in: *Pulp and Paper*, (Casey J. P., ed.). 3rd ed., p. 39 (1981).
- Gregorová, A., Košíková, B., Moravčík, R., (2006). "Stabilization effect of lignin in natural rubber. *Polymer Degradation and Stability*" 91, 229-233.
- Griffith, T. R., and MacGregor, D. W. (1953). "Aids in vulcanization of lignin-natural rubber coprecipitates," *Industrial and Engineering Chemistry* 45(2), 380-386.
- Herd, C. R.; Mc Donald, G. C.; Hess, W. M., (1991). "Morphology of carbon-black aggregates: fractal versus euclidean geometry", *Rubber chem. Technol.* 65, 1.
- Hess W. M., Ayala J. A., Vegvari P. C., and Kistler F. D., *Kautsch. Gummi Kunstst.* (1988). 41, 1215.
- Himmelsbach, D.S., (1993). Structure of forage cell walls (session synopsis). In: Jung, H.G., Buxton, D.R., Hartfield, R.D., Ralph, J. (Eds.), *Forage Cell Wall Structure and Digestibility*. Am. Soc. Agronomy Inc., Madison, WI, pp. 271-283.
- Ikeda Y., Katoh A., Shimanuki J. and Kohjiya S. (2004), *Macromol. Rapid Commun.*, 25 (12), 1186-1190.

- ISO 11345, 2006 Assessment of carbon black and carbon black/silica dispersion.
- ISO 2781, 1988, Cor 1, 1996. Determination of density
- ISO 4662:2009 Rubber, vulcanized or thermoplastic - Determination of rebound resilience
- ISO 48:1994 AMD 1, (1999). Rubber, vulcanized or thermoplastic Determination of Hardness (Hardness between 10 and 100 IRHD)
- ISO 6502:1999 Rubber - Guide to the use of curemeters.
- Jiang C., He H., Jiang H., Ma L., Jia D. M. (2013). “Nano-lignin filled natural rubber composites: Preparation and characterization” *eXPRESS Polymer Letters* Vol.7, No.5 480–493
- Karrabi M. and Mohammadian-Gezaz S., (2011). “The Effects of Carbon Black-based Interactions on the Linear and Non-linear Viscoelasticity of Uncured and Cured SBR Compounds”, *Iranian Polymer Journal* 20 (1), 15-27.
- Keilen J. J. and Pollak A. (1947) “Lignin for Reinforcing Rubber. *Rubber Chemistry and Technology*, 20(4), 1099-1108.
- Kilpelainen, I., Xie, H., King, A., Granstrom, M., Heikkinen, S., Argyropoulos, D. S., (2007). Dissolution of wood in ionic liquids. *J. Agric. Food Chem.* 55, 9142-9148
- Košíková, B, Gregorová, A., (2005). “Sulfur-Free Lignin as Reinforcing Component of Styrene-Butadiene Rubber”. *Journal of Applied Polymer Science*, Vol. 97(3), 924–929.
- Košíková, B, Gregorová, A., Osvald A., Krajčovičova J., (2007). “Role of Lignin Filler in Stabilization of Natural Rubber–Based Composites”. *Journal of Applied Polymer Science* Vol. 103 (2), 1226-1231.
- Košíková, B., Alexy, P., Gregorova, A., (2003). “Use of lignin products derived from wood pulping as environmentally desirable component of composite rubber materials”. *Wood Res. (Bratislava, Slovakia)* 48, 62.

- Kramarova, Z., Alexy, P., Chodak, I., Spirk, E., Hudec, I., Kosikova, B., Gregorova, A., Suri, P., Feranc, J., Bugaj, P., Duracka, M., (2007). "Biopolymers as fillers for rubber blends". *Polym. Adv. Technol.* 18, 135.
- Kumaran, M. G., and De, S. K. (1978). "Utilization of lignins in rubber compounding," *Journal of Applied Polymer Science* 22 (7), 1885-1893.
- Lapierre, C., Monties, B., (1989). Structural informations gained from the thioacidolysis of grass lignins and their relation with alkali solubility. In: *Wood and Pulping Chemistry 6. TAPPI Proceedings Annexe 3-2*, pp. 615-621.
- Lewis J. E., Deviney L. R., Jr., and McNabb C. F., (1970). *Rubber Chem. Technol.* 43, 449.
- Lindström T., (1979). "The colloidal behaviour of kraft lignin." *Colloid and Polymer Science*, 257, 277-285.
- Lindström T., Westman L. (1982). "The colloidal behaviour of kraft lignin", *Colloid and Polymer Science*, 260, 594-598.
- Lora, J., Naceur, B.M., Gandini, A. (2008). "Industrial Commercial Lignins: Sources, Properties and Applications. In: *Monomers, Polymers and Composites from Renewable Resources*", Eds. Naceur, B.M., Gandini, A. Elsevier, Amsterdam, pp. 225-241.
- Lora, J.H., Glasser, W.G. (2002). "Recent industrial applications of lignin. A sustainable alternative to nonrenewable materials". *J. Polym. Environm.* 10(1/2), 39-48.
- Lora, J.H., Trojan, M.J., Klingensmith, W.H., (1991). "Lignin derivatives as tackifiers for rubber compositions". EP 461,463.
- Medalia A. I. and Kraus G., (1994). "Reinforcement of Elastomers by Particulate Fillers", in *Science and Technology of Rubber*, 2nd ed., J. E. Mark, B. Erman, and F. R. Eirich (Eds.), Academic Press, San Diego,.
- Nando G. B., De S. K. (1980). "Effect of lignin on the network structure and properties of natural rubber mixes vulcanized by conventional, semiefficient and efficient vulcanization systems", *Journal of Applied Polymer Science*, 25, 1249–1252.

- Norgren M., Edlund H., (2001). “Stabilisation of kraft lignin solutions by surfactant additions”, *Colloids and Surfaces A: Physicochemical and Engineering Aspects*, 194, 239-248.
- Norgren M., Edlund H., Wågberg L., Lindström B., Annergren G. (2001). “Aggregation of kraft lignin derivatives under conditions relevant to the process, Part I: Phase behaviour. *Colloids and Surfaces A: Physicochemical and Engineering Aspects*, 194, 85-96.
- Piaskiewicz, M., Rajkiewicz, M., Gesiak, M., Berek, I., Kleps, T., (1998). “Use of waste lignin in rubber blends”. *Elastometry* 2, 43.
- Ragauskas, A.J., Williams, C.K., Davison, B.H., Britovsek, G., Cairney, J., Eckert, C.A., Frederick, W.J., Hallett, J.P., Leak, D.J., Liotta, C.L., Mielenz, J.R., Murphy, R., Templer, R., Tschaplinski, T. (2006) “The Path Forward for Biofuels and Biomaterials”. *Science*. 311(5760):484-489.
- Ralph, J., (1999). “Lignin structure: recent developments”. In: *Proceedings of the 6th Brazilian Symposium Chemistry of Lignins and Other Wood Components*, Guaratingueta, Brazil, October, pp. 97-112.
- Ralph, J., Brunow, G., Boerjan, W. (2007) *Lignins*. John Wiley & Sons, Ltd.
- Ralph, J., Marita, J.M., Ralph, S.A., Hatfield, R.D., Lu, F., Ede, R.M., Peng, J., Quideau, S., Helm, R.F., Grabber, J.H., Kim, H., MacKay, J.J., Sederoff, R.R., Chapple, C., Boudet, A.M., (1999a). “Solution-state NMR of lignins”. In: *Argyropoulos, D.S., Rials, T. (Eds.), Progress in Lignocellulosics Characterization*. Tappi press, Atlanta, GA, 55-108.
- Rivin D., (1963). “Use of Lithium Aluminum Hydride in the Study of Surface Chemistry of Carbon Black. *Rubber Chemistry and Technology*, 36(3), 729-739.
- Rivin D., (1971). “Surface properties of carbon black”, *Rubber Chem. Technol.* 44, 307-343.
- Rivin D., Aron J., and Medalia A. I. (1968). “Bonding of Rubber to Carbon Black by Sulfur Vulcanization”. *Rubber Chemistry and Technology*, 41(2), 330-343.



- Sahoo S., Seydibeyoglu M.O., Mohanty A.K., Misra M., (2011). “Characterization of industrial lignins for their utilization in future value added applications”, *biomass and bioenergy* 35 (10) 4230-4237.
- Salanti A., Zoia L., Tolppa E.-L., Giachi G., Orlandi M. (2010). “Characterization of Waterlogged wood by NMR and GPC techniques,” *Microchemical Journal* 95, 345-352.
- Salanti A., Zoia L., Tolppa E.-L., Orlandi M. (2012). “Chromatographic Detection of Lignin-Carbohydrate Complexes in Annual Plants by Derivatization in Ionic Liquid,” *Biomacromolecules* 13, 445-454.
- Savel’eva, M.B., Onishchenko, Z.V., Bogomolov, B.D., Tiranov, P.P., Lebed, I.G., Kadantseva, Y.A., (1983). “Technical lignins as promising ingredients for sole rubbers”. *Izv. Vyssh. Uchebn. Zaved., Tekhnol. Legk. Prom-sti.* 26, 53.
- Savel’eva, M.B., Shevtsova, K.V., Shelkovnikova, L.A., Kercha, Y.Y., Onishchenko, Z.V., (1988). “Effect of a binary system of lignin-based modifiers on the physicomechanical properties of vulcanizates”. *Kompoz. Polim. Mater.* 38, 40.
- Setua, D. K., Shukla, M. K., Nigam, V., Singh, H., and Mathur, G. N. (2000). “Lignin reinforced rubber composites,” *Polymer Composites* 21(6), 988-995.
- Shusheng L. and Xiansu C., (2010) “Application of Lignin as Antioxidant in Styrene Butadiene Rubber Composite”, *AIP Conf. Proc.* 1251, 344-347.
- Smook, G.A., (2002). *Handbook for Pulp and Paper Technologies*. 3rd Edition ed. Angus Wilde Publications, Inc., Vancouver, B.C.
- Soeda M. and Kurata Y., (1995). *Nippon Gomu Kyokaishi*, 68, 616.
- Stewart, D., (2008). “Lignin as a base material for materials applications: Chemistry, application and economics”, *Industrial Crops and Products*, 27, 202.
- Sun, Y., Cheng, J., (2002). Hydrolysis of lignocellulosic materials for ethanol production: a review. *Bioresour. Technol.* 83, 1, 1-11.

- Swatloski, R.P., Holbrey, J. D., Spear, S.K., Rogers, R. D., (2002). Ionic Liquids for the dissolution and regeneration of cellulose, in: Molten Salts XIII, Proceedings of the thirteenth international symposium on molten salts. De Long, H. C., Bradshaw, R. W., Matsunaga, M., Stafford, G. R., Truelove, P. C. (Eds.), pp. 155-165.
- UNI 6065:2001 Elastomeri - Prove su gomma vulcanizzata e termoplastica - Prova di trazione
- Voet A., Morawski J. C., and Donnet J. B., (1977). "Reinforcement of Elastomers by Silica", Rubber Chem. Technol. 50 (2), 342-355.
- Wang, D., Luo, D., Jia, L., (1992). "Microstructure and properties of high lignin-formaldehyde resin filled NBR-26 vulcanizate". Hecheng Xiangjiao Gongye, 15, 12
- Wang, H., Eastal, A., Edmonds, N., (2008). Pre-vulcanized natural rubber latex/modified lignin dispersion for water vapour barrier coatings on paperboard packaging. Adv. Mater. Res. (Zuerich, Switz.), 93, 47-50.
- Watson W. F., (1955). Ind. Eng. Chem. 47, 1281.
- Yeh, T.F.; Yamada, T.; Capanema, E.; Chang, H.M.; Chiang, V.; Kadla, J.F., (2005) Rapid screening of wood chemical component variations using transmittance near infrared spectroscopy. J. Agric. Food Chem., 53, 3328-3332.
- Zhu, S., Wua, Y., Chena, Q., Yub, Z., Wanga, C., Jina, S., Dinga, Y., Wu, G., (2006). Dissolution of cellulose with ionic liquids and its application: a mini-review. Green Chem. 8, 325-327.